Investigations on the Preparation of Visible Light-responsive TiO2 Thin Film Photocatalysts and Their Application to the Evolution of H2 from pure H2O and Aqueous Solutions Involving Organic Compounds

Investigations on the Preparation of Visible Light-responsive TiO_2 Thin Film Photocatalysts and Their Application to the Evolution of H_2 from pure H_2O and Aqueous Solutions Involving Organic Compounds

（可視光応答型の二酸化チタン薄膜光触媒の調製とその水や有機化合物を溶解した水溶液からの光触媒水素発生への応用に関する研究）

Afshin Ebrahimi

エブラヒミ アフシン

February 2010

Doctoral Thesis at Osaka Prefecture University

List of Contents

Chapter 1

General Introduction

1.1 Introduction

The efficient utilization of solar energy is one of the major goals of modern science and engineering that will have a great impact on technological applications.[1-9] Of the materials being developed for photocatalytic applications, titanium dioxide (TiO_2) remains the most promising because of its high efficiency, low cost, chemical inertness, and photostability.[10-13] However, the widespread technological use of TiO_2 is impaired by its wide band gap (3.2 eV), which requires ultraviolet irradiation for photocatalytic activation. Since UV light accounts for only a small fraction (4-5 %) of the sun's energy compared to visible light (45%), any shift in the optical response of TiO_2 from the UV to the visible spectral range will have a profound positive effect on the photocatalytic efficiency of newly developed materials.[14] An initial approach to shift the optical response of TiO_2 from the UV to the visible spectral range has been the doping of TiO_2 with transition metal elements.[15-21] However, metal doping has several drawbacks, i.e., the doped materials have been shown to suffer from thermal instability and the metal centers act as electron traps which reduce the photocatalytic efficiency. Furthermore, the preparation of transition metal-doped TiO_2 requires the use of high cost ion-implantation facilities.[23,24] Recently, it was shown that the desired band gap narrowing of TiO_2 can be better achieved by using anionic dopant species rather than metals ions.[15,25-27] Substitutional doping of nitrogen was found to be most effective because its *p* states contribute to the band gap narrowing by mixing with the O *2p* states. It has also been shown that TiO_2 films can be doped with nitrogen by sputtering methods which led to

enhanced photoactivity in the visible spectral range. [15] Considerable efforts have been undertaken to dope TiO_2 thin films and powders with nitrogen by annealing TiO_2 at elevated temperatures under a NH_3 flow for several hours. Nevertheless, the doping process on these micron-sized TiO_2 systems resulted in only small amounts (≤ 2%) of nitrogen incorporation.[15]

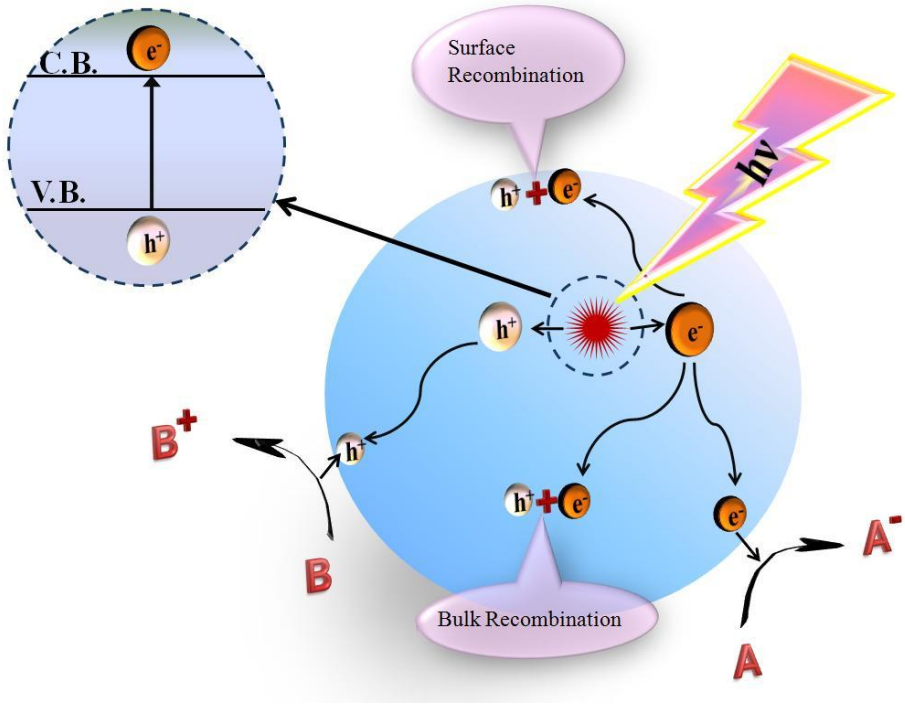

Fig. 1.1 Schematic Photocatalytic reaction on a semiconductor Surface followed by deexcitation events.

Semiconductor electronic structures are characterized by a filled valence band, VB, and an empty conduction band, CB, and can act as sensitizers for light-reduced redox processes. When a photon with energy of hv matches or exceeds the band gap energy, E_g, of the semiconductor, an electron, e^-CB, is promoted from the valence band into the conduction band, leaving a hole, h^+VB, behind. Excited state conduction-band electrons and valence-band holes can react with electron donors and electron

acceptors adsorbed on the semiconductor surface or within the surrounding electrical double layer of the charged particles or recombine and dissipate the input energy as heat, becoming entrapped in metastable surface states. The above photocatalytic process is illustrated in Figure 1.1.

Once excitation occurs across the Band gap, there should be a sufficient lifetime (in the nanosecond regime) for the created electron-hole pair to undergo charge transfer to an adsorbed species on the semiconductor surface from solution or gas phase contact. If the semiconductor remains intact and the charge transfer to the adsorbed species is continuous and exothermic, the process is termed heterogeneous photocatalysis. [28] The initial process for heterogeneous photocatalysis of organic and inorganic compounds by semiconductors is the generation of electron-hole pairs in the semiconductor particles. Upon excitation, the fate of the separated electron and hole can follow several pathways. Recombination of the separated electron and hole can occur on the surface in the volume of the semiconductor particle or with the release of heat. The photoinduced electron/hole can migrate to the semiconductor surface. At the surface, the semiconductor can donate electrons to reduce an electron acceptor (usually oxygen in an aerated solution); in turn, a hole can migrate to the surface where an electron from a donor species can combine with the surface hole oxidizing the donor species. The electron transfer process is more efficient if the species are preadsorbed on the surface. [29] The probability and rate of the charge transfer processes for electrons and holes depends on the respective positions of the band edges for the conduction and valence bands and the redox potential levels of the adsorbate species.

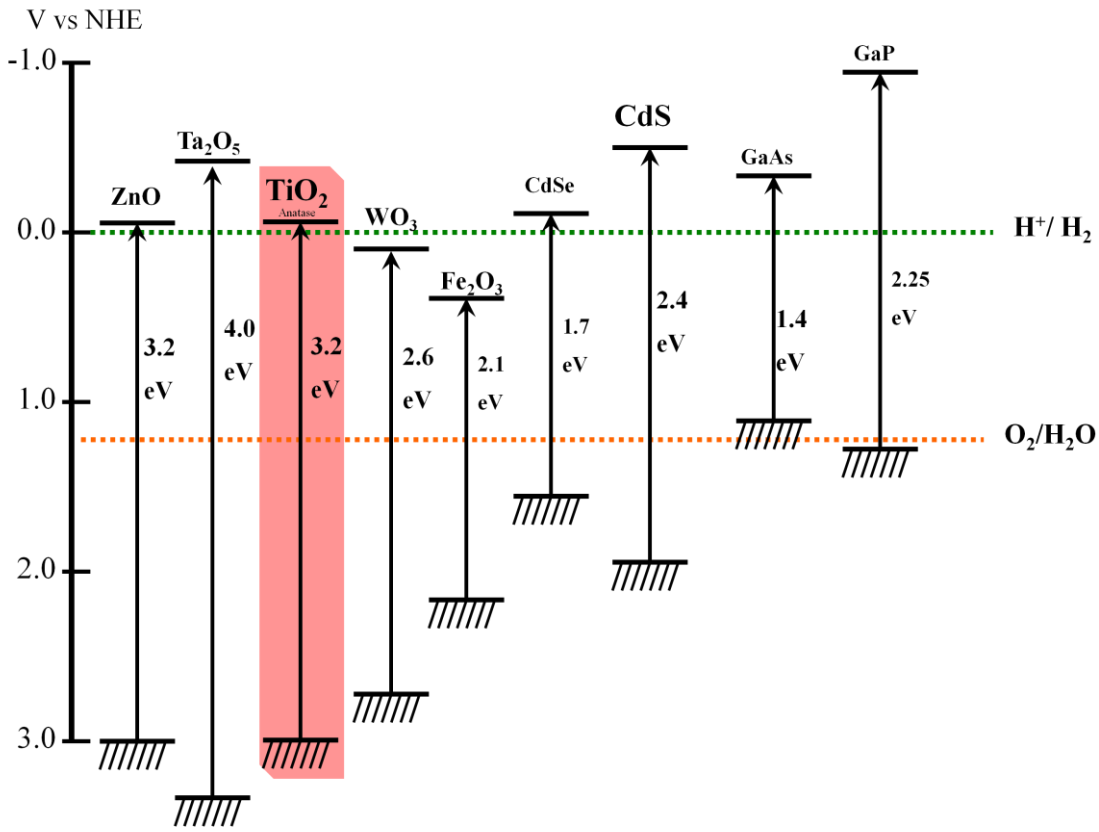

Fig. 1.2 Band gap energy position in various semiconductors and the conduction and valence band energy levels. Energy scale is indicated in electron volts (eV) using either a normal hydrogen electrode or vacuum level as reference.

$$H_2O \rightarrow 1/2O_2(g) + H_2(g);\ \Delta G = +237\ kJ/mol \qquad (1.3\ eV/e,\ \lambda_{min} = 1100\ nm)\ (1.1)$$

Reaction 1.1 is catalyzed by many inorganic semiconductors of which TiO_2 is the most widely studied metal oxide photocatalyst. Today, over 130 photocatalysts are known to either catalyze the overall splitting of water according to eq. 1.1 or cause water oxidation or reduction in the presence of external redox agents.

The three main factors in oxide semiconductor selection are band gap, band edge position and stability. In CdS, the valence band position is shallower than that of

TiO_2, therefore, H_2 production performance is better. However, the oxidizing power of CdS is milder than TiO_2 and the hole created in CdS shows weaker oxidation. Figure 1.2 shows the valence band position should shift in a more positive direction (downward) and the conduction band should shift more negative (upward) in order to prepare efficient metal oxide photocatalysts.

In terms of quantum efficiencies (QEs), NiO-modified La/$KTaO_3$ (QE=56 % utilizing pure water, UV light), [30] ZnS (QE= 90 % with aqueous Na_2S/Na_2SO_3, light with λ >300 nm), [31] and Cr/Rh-modified GaN/ZnO (QE = 2.5 %, pure water, visible light) have the highest record among the semiconductors. [32, 33] But with visible light, no material with a QE larger than 10 % has been found. [34]

Solar energy is able to meet global demand for power by several orders of magnitude: the solar flux on the surface of the Earth is some 120,000 TW and the amount of solar energy reaching the earth in one year is nearly 10,000 times greater than all energy used by humans in that same period. However, there are two principal problems preventing efficient utilization of solar power: its high cost and the form in which it can be harnassed. Presently, the most efficient method of harvesting solar power is with solid-state photovoltaic (PV) devices. While these are very efficient, an inherent limitation of PV devices is that they can only produce electricity. As a form of energy, electricity is not the most practical for many applications because it is difficult to store efficiently. While numerous methods are available for storing electricity, all incur significant efficiency losses during the charging and discharging processes, and furthermore, many are simply not able to accommodate diurnal cycling or have unacceptably short operating lifetimes.

Photoelectrochemical cells are the most efficient method known for converting

solar energy into chemical fuel. They are simple to assemble and typically involve nothing more than two electrodes immersed in an electrolyte solution and exposed to light. Furthermore, these cells are flexible in how they can be used: a regenerative photoelectrochemical cell absorbs light to generate electricity with no net chemical change; a photoelectrosynthetic cell uses light to drive a reaction and produce chemical fuel with greater energy content than the reactants. Such systems are very effective at converting sunlight into electrical and/or chemical energy. Finally, the greatest advantage of photoelectrochemical cells may be their relatively low cost.

Photoelectrochemical cells lie somewhere between photosynthesis and photovoltaics in many respects, i.e., photosynthesis is not particularly efficient but its cost is very low and photovoltaics are extremely efficient but, in many cases, prohibitively expensive. Photoelectrochemical cells are far more efficient at energy conversion than photosynthesis and much cheaper than photovoltaics. While photosynthesis is limited to the production of fuels and photovoltaics to electricity, photoelectrochemical cells can produce both. Like photovoltaic cells, they rely on the formation of the junction of a semiconductor with another material, in this case, a liquid.

In any system capable of converting light into chemical or electrical energy, four essential processes must occur: 1) the absorption of light; 2) creation of free charge carriers; 3) separation of charges; and finally 4) the collection of charges, either in the form of an electrical current or to drive a desired endothermic chemical reaction.

When a semiconductor is irradiated by photons of energy equal to or greater than that of its band gap, which it absorbs, excitation occurs and an electron moves to the conduction band leaving a hole behind in the valance band. For TiO_2 this process is

expressed as follows:

Semiconductor: $TiO_2 + h\nu \rightarrow e^- (TiO_2) + h^+ \quad (TiO_2)$ (1.2)

Water: $H_2O \rightarrow H^+ + OH^-$ (1.3)

$2e^- (TiO_2) + 2H^+ \rightarrow H_2$ (1.4)

$2h^+ (TiO_2) + 2OH^- \rightarrow 2H^+ + 1/2O_2$ (1.5)

The photogenerated electrons and holes can recombine in bulk or on the semiconductor surface, releasing energy in the form of heat or a photon. The electrons and holes that migrate to the semiconductor surface without recombination can reduce and oxidize water (or the reactant), respectively, and are the basic mechanisms of photocatalytic hydrogen production, as shown in Fig. 1.2.

The photoexcitation of TiO_2 injects electrons from its valence band into its conduction band. The electrons flow through the external circuit to the Pt cathode where water molecules are reduced to hydrogen gas while the holes remain in the TiO_2 anode where water molecules are oxidized to oxygen. The efficiency of converting light energy into hydrogen energy using suspended nanoparticle catalysts is, to date, low and the primary reason for the low efficiencies is the rapid recombination of photo-generated electron-hole pairs. Photochemical water-splitting involves at least one exthothermic reaction so that it is, thus, relatively easy for molecular hydrogen and oxygen to recombine in a backward reaction.

$H_2 (g) + 1/2O_2 (g) \rightarrow H_2O (g) + 57$ Kcal (1.6)

Another reason for the low efficiency in converting light energy to hydrogen energy is the poor visible spectrum response of corrosion resistant catalysts. TiO_2 is one of the most suitable photocatalysts with chemical stability and strong catalytic activity, however, it does not respond to visible light in its pure form.

Photocatalytic water splitting into H_2 and O_2 is an area of great interest due to the potential of hydrogen gas as a clean-energy fuel source. Since the initial work of Fujishima and Honda,[1] many different metal oxide semiconductors and metal sulfides have been reported to be active for water splitting. While initial efforts involved large band gap (E_g > 3.0 eV) semiconductors that could only utilize UV light, recent efforts have focused on using visible light as the energy source, [2-21] as the ultimate goal is to use solar energy to produce hydrogen fuel. While the overall redox potential of the reaction:

$$H_2O + h\nu \rightarrow H_2 + ½\ O_2 \qquad (1.7)$$

is only -1.23 eV (1000 nm) at pH 7, the crucial reaction for hydrogen production is believed to be the initial one-electron transfer to H^+ ion.

1.2 Outline of this thesis

Artificial photosynthesis to produce renewable energy and other green energy materials is a major challenge to mankind. Efficient use of the freely available resource of solar energy by its conversion into electricity as well as clean chemical energy will be significant in reducing our dependence on fossil fuels. TiO_2 is one of the most popular oxide materials for its many applications and potential use in a variety of technologies where surface chemistry is critical, including photocatalysis. Recently, TiO_2 has been widely studied as a key component of photocatalysis in water splitting reactions. The main objective of this study is to modify and develop new TiO_2-based photocatalysts that allow the efficient absorption of visible light, thus, enabling such modified TiO_2 to initiate various desired reactions effectively even

under visible or solar light irradiation.

Chapter 2

This chapter consist the main body of this thesis and discusses the preparation methods used to develop the TiO_2 thin films. TiO_2 thin films have been deposited by RF magnetron sputtering. The aim of this study is to investigate the effect of the deposition conditions on the structural and photocatalytic properties of the thin films. The influence of the substrate temperatures on the photocatalytic activity of the TiO_2 thin films has also been investigated. The main influence of temperature was found to affect the crystallinity of TiO_2. In this chapter, the design of optimized Vis-TiO_2 thin films for the production of H_2 and O_2 separately is also discussed. Optimizing of the photocatalytic activity of Vis-TiO_2 thin films prepared by RF-MS method by controlling the various parameters such as sputtering pressure and target-to-substrate distance D_{T-S} is investigated.

It has also been reported that chemical etching of the Vis-TiO_2 thin films with HF solution remarkably enhanced their photocatalytic activity. Moreover, it was found that the photocatalytic activity of Vis-TiO_2 for the separate evolution of H_2 and O_2 could be remarkably increased under visible light irradiation ($\lambda \geq 450$ nm) with chemical etching by HF solution. Thus, HF (60)-Vis-TiO_2/Ti/Pt thin film photocatalysts were found to be successful in realizing the stoichiometric separate evolution of H_2 and O_2.

Chapter 3

This chapter deals with post heat treatment of Vis-TiO_2 thin films to prepare visible light-responsive TiO_2 thin film photocatalysts (Vis-TiO_2) on Ti metal foil or ITO glass substrates by the radio-frequency magnetron sputtering (RF-MS) method. Calcination in ammonia was particularly effective in increasing the visible light absorption of Vis-TiO_2 as well as in enhancing its photoelectrochemical performance and photocatalytic activity. In the next step, such produced Vis-TiO_2 thin film photocatalyst utilized for separate evolution of H_2 and O_2 from H_2O. It was found that the rate of the separate evolution of H_2 and O_2 was also dramatically enhanced by calcination treatment of Vis-TiO_2 in ammonia.

Chapter 4

This chapter deals with a double-layered visible light-responsive TiO_2 thin film photocatalyst was sputtered on a Ti foil substrate. The produced DL-TiO_2/Ti consists of a UV light-responsive TiO_2 thin film (UV-TiO_2) deposited as the inner block layer on a Ti foil substrate and a visible light-responsive TiO_2 thin film (Vis-TiO_2) deposited as the outer layer. DL-TiO_2/Ti exhibited higher photoelectrochemical and photocatalytic performance under both UV and visible light irradiation than a single-layered Vis-TiO_2 thin film photocatalyst deposited on a Ti foil substrate. The separate evolution of H_2 and O_2 from H_2O was successfully achieved by using an H-type glass cell consisting of two aqueous phases separated by the DL-TiO_2/Ti/Pt and a proton-exchange membrane.

Chapter 5

The main part of this chapter investigates the photocatalytic degradation of organic

contaminants found in landfill leachate and methylene blue by utilizing our modified Vis-TiO_2 films. A novel method of water and wastewater purification is to apply the photocatalytic decomposition of water contaminants. These photocatalysts were used for the photocatalytic degradation of diluted methylene blue in water and landfill leachate under direct solar irradiation as a model reaction. In this study, COD, TOC and UV absorbance at a given wavelength (250 nm) of the leachate has been investigated. A UV/VIS spectrometer to record the spectra at 660 nm was used to determine MB concentration in order to follow the kinetics of its disappearance. The results show that the as prepared Vis-TiO_2 thin films can remarkably reduce contaminant concentrations with solar light irradiation and utilizing Vis-TiO_2 enables the breakdown of organic materials at an accelerated rate of 2 to 5 times.

Chapter 6

In this chapter the Vis-TiO_2 thin films developed in Chapter 2 are also applied in developing sandwich-type dye-sensitized solar cells (DSSC). Two kinds of sandwich-type dye-sensitized solar cells, $DSSC_{Vis}$ and $DSSC_{UV}$, were fabricated using Vis-TiO_2 and UV-TiO_2 electrodes and their photovoltaic performances were investigated. $DSSC_{Vis}$ exhibited remarkably higher incident photon-to-electron conversion efficiency (IPCE) than $DSSC_{UV.}$ Furthermore, it was found that the optimized solar-to-electric energy conversion efficiencies (η) reached 2.6 % for $DSSC_{Vis}$. UV-Vis, SEM and photoelectrochemical investigations have revealed that the unique film morphology as well as band structures of Vis-TiO_2 play an important role in realizing the high photovoltaic performance of $DSSC_{Vis}$.

Chapter 7

This chapter presents the results of the evolution of H_2 from an aqueous solution involving various light hydrogen-rich compounds for hydrogen-rich fuels or to use hydrogen for fuel cells. As NH_3 contains no carbon, it is a promising source of hydrogen. Storing hydrogen as NH_3 may solve the challenging problem of storing high-pressure hydrogen with an H_2 density of 136 Kg H_2/m^3, which is the highest in chemical compounds and makes ammonia the most hydrogen-dense chemical in existence. Investigations on photocatalytic hydrogen evolution using different concentrations of ammonia led to the development of a procedure for the production of hydrogen from water soluble ammonia (NH_3). Recent research shows that the technology of photocatalytic hydrogen production from ammonia aqueous solution is beneficial and that the photocatalytic decomposition of ammonia is a promising alternative process for low-cost, low-temperature, high-purity *in situ* hydrogen production.

Chapter 8

Finally, the results and conclusions of the core topics of Chapters 2 to 7 are summarized in the final Chapter. This chapter also presents several topics for further studies in unraveling the mechanisms behind the photocatalytic reactions as well as in the development of new photocatalysts with high performance and functionality.

1.3 References

1. Fujishima A., Honda K., Nature, 238, 37 (1972).
2. Anpo M., Takeuchi M., J. Catal., 216, 505 (2003).
3. Anpo M., Dohshi S., Kitano M., Hu Y., Takeuchi M., Matsuoka M., Ann. Rev. Mater. Res., 35, 1 (2005).
4. Matsuoka M., Kitano M., Takeuchi M., Tsujimaru K., Anpo M., Thomas J.M., Catal. Today, 122, 51-61(2007).
5. Kitano M., Takeuchi M., Matsuoka M., Thomas J.M., Anpo M., Catal. Today, 120, 133 (2007).
6. Ollis D.S., Al-Ekabi H. Eds., Photocatalytic Purification and Treatment of Water and Air, Elsevier: Amsterdam, (1993).
7. Khan S.U.M., Akikusa J., J. Phys. Chem. B, 103, 7184 (1999).
8. Licht S., Wang B., Mukerji S., Soga T., Umeno M., Tributsch H., J. Phys. Chem. B, 104, 8920 (2000).
9. Wilcoxon J.P., Photocatalysis Using Semiconductor Nanoclusters, Advanced Catalytic Materials, MRS Proc. Boston, MA, (1998).
10. Serpone N., Pelizzetti E. Eds., Photocatalysis: Fundamentals and Applications, Wiley, New York, (1989).
11. Kozhukharov V., Vitanov P., Stefchev P., Kabasanova E., Kabasanov K., Machkova M., Blaskov V., Simeonov D., Tzaneva G., J. Environ. Protec. Eco., 2, 107 (2001).
12. Schiavello M., Dordrecht H. Eds., Photoelectrochemistry, photocatalysis, and photoreactors: fundamentals and developments, Kluwer Academic: Boston, (1985).
13. Linsebigler A.L., Lu G., Yates J.T., Chem. Rev. A, 95, 735 (1995).

14. Asahi R., Morikawa T., Ohwaki K., Aoki T., Taga Y., Science, 293, 269 (2001).
15. Horishi I., Wanatabe Y., Hashimoto K., J. Phys. Chem. B, 107, 23, 5483 (2003).
16. Shah S.I., Li W., Huang C.P., Jung O., Ni C., Proc. Natl. Acad. Sci., U.S.A., 99, 6482 (2002).
17. Xu A., Zhu J., Gao Y., Liu H. Chem. Res. Chin. Univ., 17, 281(2001).
18. Wang C., Bahnemann D.W., Dohrmann J.K. Chem. Comm., 16, 1539 (2000).
19. Wang Y., Hao Y., Cheng H., Ma H., Xu B., Li W., Cai S., J. Mater. Sci., 34, 2773 (1999).
20. Coloma F., Marquez F., Rochester C.H., Anderson J.A., Phys.Chem. Chem. Phys., 2, 5320 (2000).
21. Altynnikov A.A., Zenkovets G.A., Anufrienko V.F., React. Kin. Cat. Lett., 67, 273 (1999).
22. Umebayashi T., Yamaki T., Itoh H., Asai K., J. Phys. Chem. Sol., 63, 1909 (2002).
23. Wang Y., Cheng H., Hao Y., Ma J., Li W., Cai S., Thin Solid Films, 349, 120 (1999).
24. Yamashita H., Honda M., Harada M., Ichihashi Y., Anpo M., Hirao T., Itoh N., Iwamoto N., J. Phys. Chem. B, 102, 10707 (1998).
25. Yu J.C., Yu J.G., Ho W.K., Jiang Z.T., Zhang L.Z., Chem. Mat., 14, 3808 (2002).
26. Khan S.U.M., Al-Shahry M., Ingler Jr. W.B., Science, 297, 2243(2002).
27. Weng Y., Wang Y., Asbury J.B., Ghosh H.N., Lian T., J. Phys. Chem. B, 104, 11957 (2000).
28. Linsebigler A.L., Lu G., Yates J. T. Jr., J. Chem. Rev., 95, 735 (1995).
29. Matthews R. W., J. Catal., 113, 549 (1988).
30. Kato H., Asakura K., Kudo A., J. Am. Chem. Soc., 125, 10, 3082 (2003).

31. Reber J. F., Meier K., J. Phys. Chem., 88, 24, 5903 (1984).
32. Maeda K., Teramura K., Lu D. L., Takata T., Saito N., Inoue Y., Domen K., J. Phys. Chem. B, 110, 28, 13753 (2006).
33. Maeda K., Teramura K., Lu D. L., Takata T., Saito N., Inoue Y., Domen K., Nature, 440 , 7082, 295 (2006).
34. Osterloh F.E, Chem. Mater., 20, 35 (2008).

Chapter 2

"Optimizing Novel Visible-Light responsive TiO_2 Thin Film Photocatalysts Functionality and Photocatalytic Decomposition of water with a Separate Evolution of H_2 and O_2"

2.1. Introduction

Mankind's life standards have been boosted by the use of low-cost and widely available energy resources in the last century without concern about their detrimental effect on the environment or the renewal of these resources. However, when taking a long–range view, there is great concern that an increase in energy consumption and decrease in the availability of non-renewable resources will cause energy prices to gradually escalate while energy carriers such as hydrocarbons may become a luxurious material that will not be affordable for global and widespread use. If energy consumption using fossil fuels continues in this way, we can expect living standards to decline and our living environment to be adversely affected.

Hydrogen evolution utilizing titanium dioxide using a special configuration of the TiO_2 photocatalyst electrode and platinum counter electrode immersed in aqueous electrolyte solution and applying an anodic bias has launched the novel field of photocatalysis for the production of hydrogen. Much research has been carried out since Fujishima and Honda reported these photocatalytic properties of TiO_2 for the first time in 1972. [1- 20]

Harvesting the abundant energy from sunlight and its conversion into electricity or useful chemical energy can lead to novel approaches in the direct production of hydrogen as an ultra clean energy carrier, high density light weight rechargeable batteries, safe and light weight H_2 gas containers, high density fuel cells and smart sensors for conserving precious energy. Solid state junction semiconductors, especially silicon, are the dominant devices which are used to harvest solar light. The development and improvement of new processes in manufacturing and the

characterization of these new materials, especially at the molecular and atomic level, will be essential in resolving environmental and energy issues. Novel techniques in nanoscience and technology to develop functional new photocatalysts with higher conversion efficiencies are now being widely investigated, particularly to address these issues. [17]

Nanoparticles are key components in the advancement of future energy technologies. Catalytic activities depend critically on their size-dependent properties and in order to increase the activity per unit area while decreasing the required amount of catalytic ingredients, innovative methods for the synthesis or deposition of catalysts by physical techniques such as sputtering have been studied.[6] Performance limiting factors in utilizing photocatalysts such as surface and interface area as well as band gap can be addressed by such innovative nano-scale approaches.

TiO_2 has been extensively studied in recent decades for its important photocatalytic applications, excellent functionality, long-term stability, and non-toxicity.[14-16] In terms of semiconductor photocatalysis, TiO_2 is one of the most extensively studied transition metal oxides which have a highly localized low-lying *3d* orbit of titanium atoms and *2p* orbit of oxygen atoms. The conduction band is mainly of titanium *3d* orbital character, whereas the top of the valence band essentially has an almost oxygen *2p* orbital character.[9]

It has been shown that the photocatalytic reactions of TiO_2 takes place on a crystal surface and is closely related to the band gap states. [39] As TiO_2 is a wide band gap semiconductor, only light in the UV region can excite electrons to be transmitted from the valence into the conduction band. This means pure TiO_2 is activated only by illumination with ultraviolet light of which the energy exceeds its band gap. It is, thus,

essential to find a method to narrow the optical band gap of TiO_2, a key step in enhancing its photocatalytic performance. [2, 14]

This chapter is organized as follows: In the first part, a method of producing Vis-TiO_2 is introduced along with our optimization methods and preparation procedures as well as the most influential factors affecting the TiO_2 photocatalytic activity. The second part contains the main results of HF treatment of Vis-TiO_2 and its effect on the functional activity of the modified samples. We have also discussed the influence of these surface treatments on the separate evolution of hydrogen and oxygen in our special configuration H-shape cell under sunlight irradiation. The last part consists of a brief summary and the conclusions of this study.

2.2. Experimental Section

2.2.1-Thin Film Preparation

The experiments were carried out using a RF magnetron sputtering device by O-Naru Tech Inc. with a 100 mm diameter target and RF power supply having a frequency of 13.56-MHz and maximum power of 500 W power to excite the plasma. The TiO2 thin films were prepared by RF-MS method using a TiO2 target plate (High Purity Chemicals Lab., Corp., Grade: 99.99 %) as the source material and Ar gas (99.995 %) as the sputtering gas. The calcined Ti foil and quartz substrates with dimensions of (10 mm × 20 mm) were positioned and fixed in the center of the substrate holder parallel to the target with varying target-to-substrate distances DT-S from 75 mm to 85 mm. The chamber was evacuated to less than 7.0×10^{-4} Pa before introducing the Ar sputtering gas and the chamber pressure was held at a fixed value between the range of 0.5 to 5.0 Pa as required. Before each run, the target was pre-

sputtered in argon gas for at least 10 min to clean its surface of any undesired contaminants. To maintain uniform deposition during the sputtering time, the substrate holder plate was kept rotating at 5 r min^{-1}. An induced RF power of 300 W with the substrate temperature held at a fixed value of 873 K was applied. The film thickness was adjusted to 1 μm by controlling the deposition time. The weight of the deposited TiO_2 per unit area of Ti foil was estimated to be 0.39 mg/cm^2 from the film thickness and the specific gravity of the anatase phase (3.9 g/cm^3).

These TiO_2/Ti thin films were immersed in a 0.045 vol. % HF solution at room temperature (RT) for 60 to 240 min. Thus obtained HF-treated TiO_2/Ti thin films were then referred to as HF(X)-TiO_2/Ti (X represents the treatment time). Pt was deposited on some of the TiO_2 thin films by an RF-MS method with an RF power of 70 W under a substrate temperature of 298 K for 30 sec.

2.2.2- Film characterization

The surface morphologies of the films were examined using field emission scanning electron microscopy (FE-SEM, S-4500; Hitachi). The surface areas of the films were investigated by BET surface measurements using Krypton gas as the adsorbate. The crystalline structure of the films was investigated by an X-ray diffractometer (XRD, XRD-6100, Shimadzu) equipped with Cu Kα radiation source.

The photoelectrochemical properties of the TiO_2/Ti thin films were evaluated using a potentiostat (HZ3000, Hokuto Denko) with a three-electrode cell that consists of the TiO_2/Ti film electrode, a Pt electrode and a saturated calomel electrode (SCE) as the working, counter and reference electrodes, respectively. The 0.2 cm^2 working electrode was irradiated with a 500 W Xe lamp in 0.25 M K_2ClO_4 aqueous solution

that was mechanically stirred and degassed by purging with 99.99 % pure Ar gas before and through the experiments.

Photocatalytic reactions were carried out using a quartz cell connected to a conventional vacuum system. The TiO_2 thin film photocatalyst was introduced into distilled water or an aqueous solution including a sacrificial reagent (50 % methanol or 0.05 M silver nitrate solution) in the reaction cell. The reaction cell was placed in a cooling water bath to keep its temperature constant at 288 K. The Pt-loaded HF(*X*)-TiO_2/Ti thin film photocatalyst (10 × 20 mm^2) was then introduced into the aqueous solution in the reaction cell. UV light irradiation was carried out with a 500 W high pressure Hg lamp through the quartz window of the reaction cell. The photocatalytic evolution of H_2 from a methanol aqueous solution (2 ml of a 50 % methanol solution) and the photocatalytic splitting of pure water into H_2 and O_2 were analyzed using a gas chromatograph (GC, G2800-T, Yanaco) equipped with a thermal conductivity detector (TCD).

The separate evolution of H_2 and O_2 from water was investigated by an H-shape Pyrex glass cell. The cell consisted of two aqueous phases separated by a TiO_2/Ti/Pt photocatalyst and a proton-exchange membrane, as detailed in previous publications [12]. Visible light irradiation was carried out with a 500 W Xe arc lamp through a 420 nm cut filter (L-42, Asahi Techno Glass) and sunlight irradiation was carried out using a sunlight-gathering system (Laforet Engineering, XD-50D). The evolved gases were analyzed by gas chromatography (G2800-T, Yanaco).

Optical transmittance measurements were carried out with a UV–Vis spectrophotometer (Shimadzu, UV-2200A) at room temperature in air. Secondary ion mass spectrometry (SIMS, Physical Electronics, ADEPT1010) was carried out to

obtain the depth profiles of ^{18}O and ^{48}Ti for the thin films.

2.3. Results and Discussions

Sputtering is a form of physical vapor deposition (PVD) with complex processes, often used for the production of different kinds of thin films. Sputtering involves blasting the atoms off a target with energy-charged, chemically inactive atoms called ions produced in plasma.[16] The produced ions will re-deposit onto a substrate to build up the desired thin film. The photocatalytic activities of the TiO_2 thin films are dependent on such conditions as the sputtering pressure, R.F. power input, target to substrate distance, substrate temperature, the level of vacuum reached before introduction of Ar sputtering gas and the sputtering time.[32] By changing the sputtering conditions, thin film composition and structure will change. In this laboratory, the preparation of visible light-responsive TiO_2 thin film photocatalysts by an RF magnetron sputtering deposition method is a long-term investigation with many interesting results.

During sputtering, the ejected particles from the target undergo collisions with the gas atoms in the chamber and lose a part of their energy during their transit to the substrate surface. The film growth mechanism is highly dependent on the energy of the sputtered particles, i.e., the energy flux is an advantage for the formation of mesoporous films on the substrate. The dissipation of energy by collision or "thermalization" plays an important role in the preparation of the desired metastable thin films with predefined specifications. The kinetic energy of the sputtered atoms or molecules changes to thermal energy in the gas phase. In this case, the sputtering power and pressure both play important roles.

It is known that the mobility of the atoms and clusters on the substrate, which is in proportion to their energy, will increase with an increase in the substrate temperature. Hence, the substrate temperature influences the microstructure and orientation of the TiO_2 thin film on the substrate.

The mesostructured TiO_2 film obtained by the magnetron sputtering method could be highly porous if the main parameters can be controlled, thus providing a large surface area to anchor other photoactive molecules. The ability to assemble metal nanoparticles as a three-dimensional array of clusters gives a new possibility for designing new photoactive materials such as photocatalysts, sensors and optoelectronic nanodevices. Figure 2.1 is a schematic depiction of the magnetron sputtering process and the most important parameters of the incident particles on the substrate are the energy and angular distributions. The temperature controller prevents energy accumulation from the incident atoms and maintains a stable temperature on the substrate surface. It has been reported that the incident kinetic energies of the sputtered atoms are normally distributed with an average of 3 to 5 eV per particle.[28] However, the high-energy spectrum tail may extend to energies close to the incident ion energy up to about 100 eV or more. On the other hand, there may be some sputtered atoms with energies up to a few hundred eV (less than the cathode voltage), however, the majority of atoms have energies below 10eV.[30, 31]

For stable metal oxides like TiO_2, the fraction of the multi-atomic particles is approximately 0.4, and as the strength of the oxygen-metal bond decreases, this amount may decrease. As the mass and energy of the sputtered species increases, the normal traveling distance should increase before their energies are reduced to the thermal energy of the gas. The normal travel distance decreases by increasing the

sputtering pressure. [30]

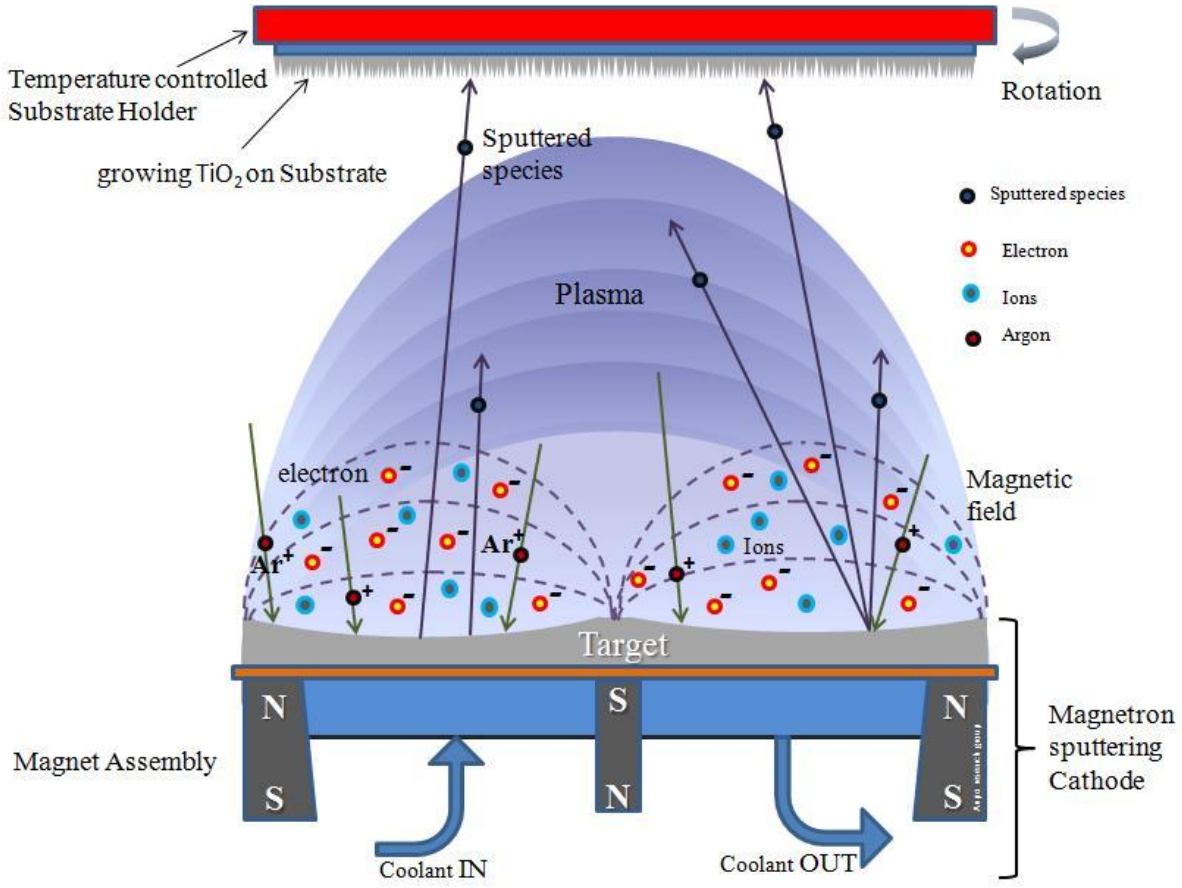

Fig. 2.1. Schematic diagram of the RF-Magnetron Sputtering Deposition Process

Figure 2.2 shows the SEM images of two distinct kinds of TiO_2 and the difference in morphologies and cross-sectional views of these two different kinds of TiO_2 thin films can clearly be observed. As is shown on the left side, a highly condensed bulk of TiO_2 can be distinguished. These kinds of thin films can be produced in moderate temperature but is only active under UV illumination and referred to as UV-TiO_2. The engineered TiO_2 thin films produced under specified conditions of sputtering are

shown on the right side of this Figure and referred to as visible-responsive TiO_2 and Vis- TiO_2. As can be seen, Vis- TiO_2 consists of large columnar TiO_2 crystals growing perpendicular to the substrate, however, in UV- TiO_2, we can see a flat smooth film formed on the substrate.

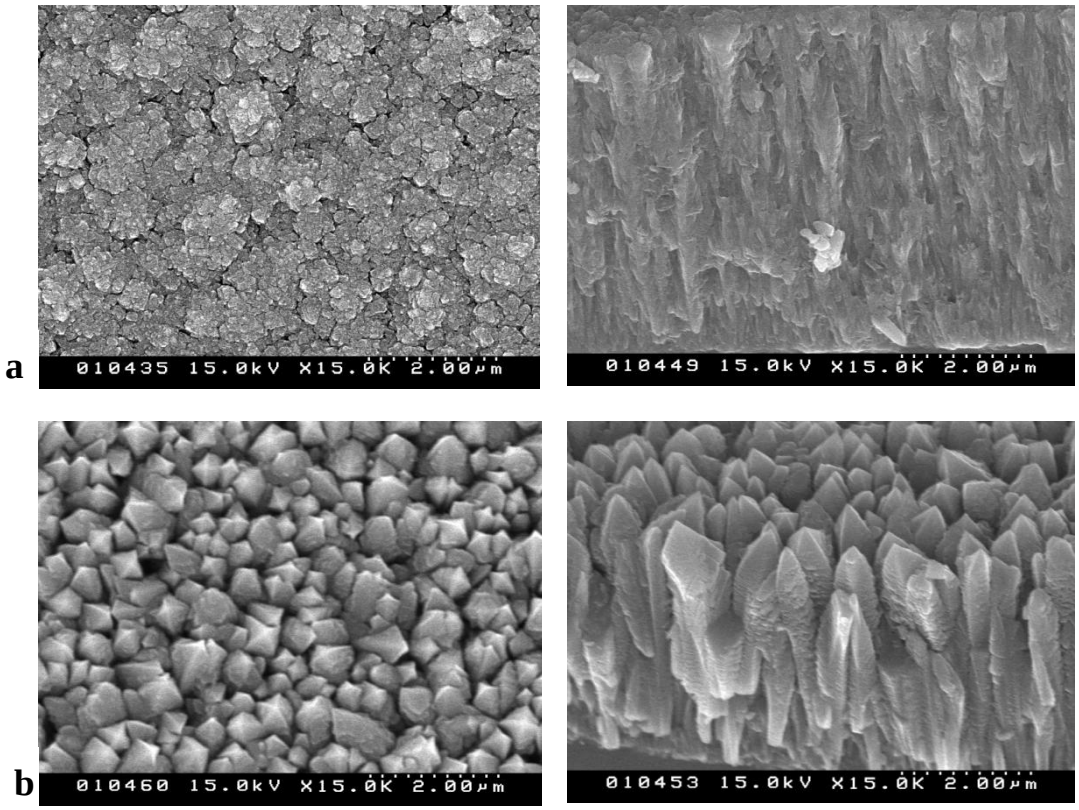

Fig. 2.2 Morphologies and cross sections of: a) UV- TiO_2 (Above), b) Vis-TiO_2

Figure 2.3 shows the UV–Vis transmission spectra of the TiO_2 thin films prepared on quartz substrates under fixed substrate temperatures and various Ar gas pressures. Unlike the UV- TiO_2 thin films which are prepared at moderate temperatures and are colorless and transparent to visible light, the TiO_2 thin films prepared at higher substrate temperatures (>673 K) were yellow-colored and exhibited considerable

absorption in wavelength regions longer than 400 nm, enabling the absorption of visible light. As can be seen for different Ar gas pressure-sputtered Vis- TiO_2, at a fixed substrate temperature of 873 K, the absorption band at visible light regions shifted toward longer wavelength regions at around 600 nm with a decrease in the Ar gas pressures from 5.0 Pa to 0.5 Pa. Among the six types of TiO_2 thin films developed, the film prepared at a sputtering pressure of 2.0 Pa showed the highest photoactivity. For TiO_2 as other metal oxide thin films, the photocatalytic activity and properties of the bulk of the materials have a more essential role than the facial properties as the optical and electrical properties of its surface.

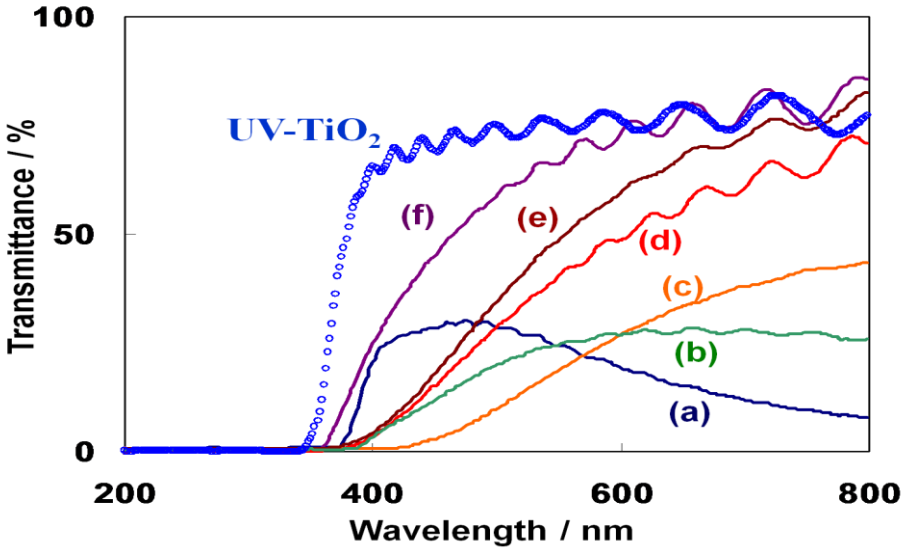

Fig. 2.3. UV-Vis transmission spectra of the TiO_2 thin films prepared under differing P_{Ar} (solid line) and the spectrum of UV-TiO_2 thin film (open circle). P_{Ar} (Pa) : (a) 0.5, (b) 1.0, (c) 1.5, (d) 2.0, (e) 3.0, (f) 5.0.

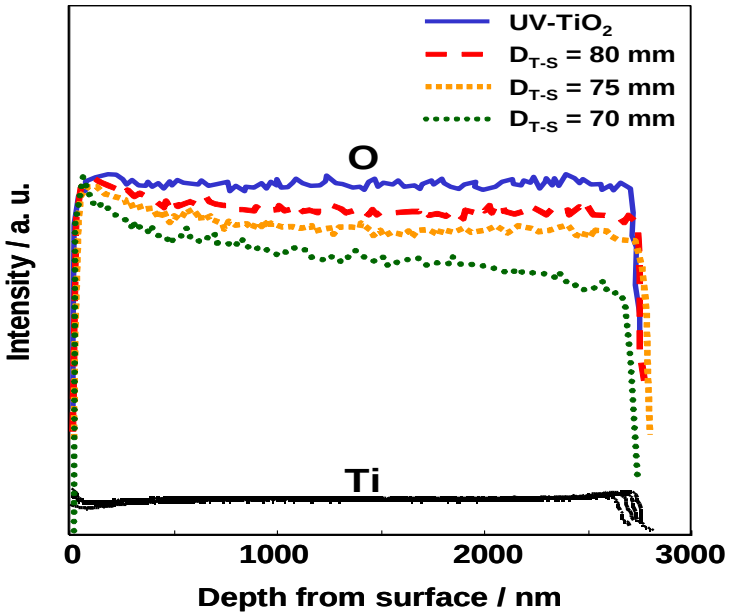

Fig.2.4 The depth distribution profiles of ^{18}O and ^{48}Ti of UV-TiO_2 and Vis-TiO_2-$D_{T\text{-}S.}$ ($D_{T\text{-}S}$ = 70, 75, 80) thin films as determined by SIMS measurements.

Figure 2.4 shows the SIMS depth profiles of UV–TiO_2 and three different targets to substrate distance Vis–TiO_2–$D_{T\text{-}S}$. This SIMS measurement has done to examine the origin, and explanation of visible light response of this kind of TiO_2. The composition, ratio of Ti and O in the direction of depth of the thin film was examined. Three different kind of visible light responsive type TiO_2 has produced for this characterization, in this case all the processing parameters in Sputtering kept fixed and just the distance between target and substrates was changed to make a survey about how it makes change on the elemental composition through the film. SIMS investigations revealed that although the concentration of O^{2-} ions for UV-TiO_2 of the bulk depth is almost fixed but the concentration of O^{2-} ions for all of Vis-TiO_2 is decreasing by distance from the film surface. Here in the figure the O^{2-} ions the concentration for Vis–TiO_2–80, Vis–TiO_2–75and Vis–TiO_2–70 is shown. As it can be seen O^{2-} ion concentration gradually decreases from the top surface (O/Ti ratio of

2.00 ± 0.01) to the inside bulk, although no significant changes were observed for UV–TiO_2 which is composed of stoichiometricTiO_2 (2.00 ± 0.01). That such a unique anisotropic structure plays a major role in the modification of the electronic properties of the Vis-TiO_2 thin films, enabling them to absorb and operate under visible light. In fact, this investigation revealed that Vis–TiO_2 exhibited a unique declined O/Ti composition from the surface to the deep inside bulk. It is obviously shown that bulk defects in these samples are different and it affects on surface phenomena and also functionality of different produced samples. As the bulk structure consist of TiO_{2-x} crystals with different amount of x in different depth and sputtering condition samples made, then the revealing the kind of defects are somehow complicated. As reported by Diebold et.al. [37] These defects might be Ti^{3+} and Ti4+ interstitials or doubly charged oxygen vacancies. As reported before calcinations of produced Vis–TiO_2 in Oxygen rich gases will decrease the photoactivity as it reduce the surface area. [20] In this case the oxygen migrates to the bulk of sample via vacancy diffusion mechanism. [36]

It has been understood that the content of oxygen, declining by decreasing the target and substrate distance D_{T-S}. In fact it cause in the smaller D_{T-S}, the Ar plasma and sputtered particles have higher kinetic energies and this energy will transfer to the substrate and produced TiO_2 thin film consequently oxygen may get loose especially in the starting of sputtering process. These results clearly indicate that the higher the kinetic energy of the sputtered atoms, the lower the O/Ti ratio of the TiO_2 thin films, accompanied by a large shift in their absorption band toward visible light regions. Such a unique anisotropic structure was seen to play an important role in the modification of the electronic properties, thus, enabling the absorption of visible

light.

Deposited metals on oxide supports such as metal–oxide interfaces play significant role in heterogeneous catalysis, small metal particles on oxide supports, may increase the activity or control the selectivity of industrial reaction processes. [21] The electronic properties of the tiny metal particles depend not only on their size but also on their shape. As using conventional electron microscopy methods specially (SEM) for finding information about nano sized deposited metal surface, particle morphology, and metal-support interface structure are not so useful. [23] Then the promising way for in this investigation is finding the effect of metal deposition on different samples with similar optimized procedure for depositing on all of produced samples and find the best photocatalytic activity.

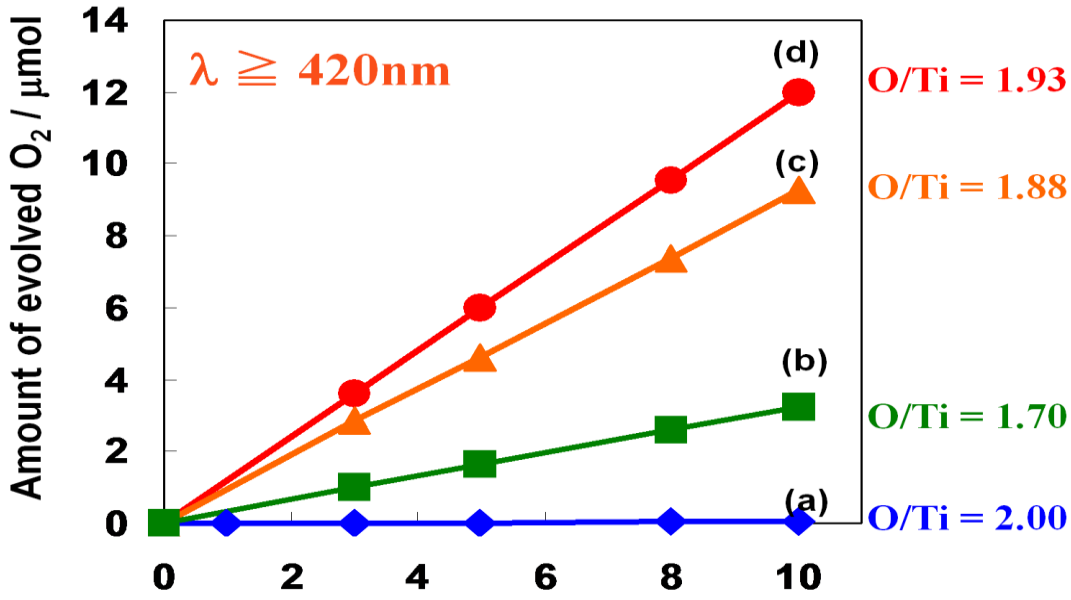

Fig.2.5 Reaction time profiles of the photocatalytic O_2 evolution from a 0.05 M $AgNO_3$ aqueous solution on Pt loaded (a) UV-TiO_2 Vis-TiO_2-$D_{T\text{-}S}$ [$D_{T\text{-}S}$: (b) 70, (c) 75, (d) 80] thin films under light irradiation of wavelengths longer than 420 nm.

Lately many papers published about the influence of metal deposition on TiO_2

photocatalyst. It was also found that Pt-loaded Vis–TiO_2 exhibited photocatalytic activity for the O_2 evolution reaction from a 0.05 M $AgNO_3$ aqueous solution even under visible light, as shown in the Figure 2.5, O_2 evolved under visible light irradiation ($\lambda \geq 420$ nm), while no gas evolution was observed in the dark under the same experimental conditions.

As it has been shown [12] only the Pt-loaded Vis-TiO_2 was found to exhibit photocatalytic activity evolution of O_2 from water involving $AgNO_3$ sacrificial reagent under visible light of wavelengths longer than 420 nm. Figure here shows the result of comparing the photocatalytic activity based on oxygen content compare to titanium in the thin films. Photocatalytic activity of Vis-TiO_2 and UV–TiO_2 based on O/Ti ratio in the bulk which measured by the SIMS measurement is shown here. It is showing the highest photocatalytic activity response at O/Ti ratio of 1.93.

To find the highest active Vis-TiO_2, thin films prepared on different sputtering pressure under fixed substrate temperature of 873 K and fixed target to surface distance. Among the five different types of produced TiO_2 thin films on different Ar^+ sputtering gas pressures from 1.0 Pa to 5.0 Pa, the film prepared at a sputtering pressure of 2.0 Pa has the highest activity. Fig. 2.5 demonstrates the dependence of photocatalytic activity of different Vis-TiO_2 based on their sputtering gas pressures P_{Ar} under visible light irradiation longer than 420 nm for overall time of 10 hours illumination.

For production of H_2 from water involving methanol sacrificial reagents had used and for evolution of O_2 water involving $AgNO_3$ sacrificial reagent had used.

As it can be see here the optimal value of P_{Ar}=2Pa is obtained. In this amount of Ar pressure the energy of sputtered particles will produce photo active catalyst, and it

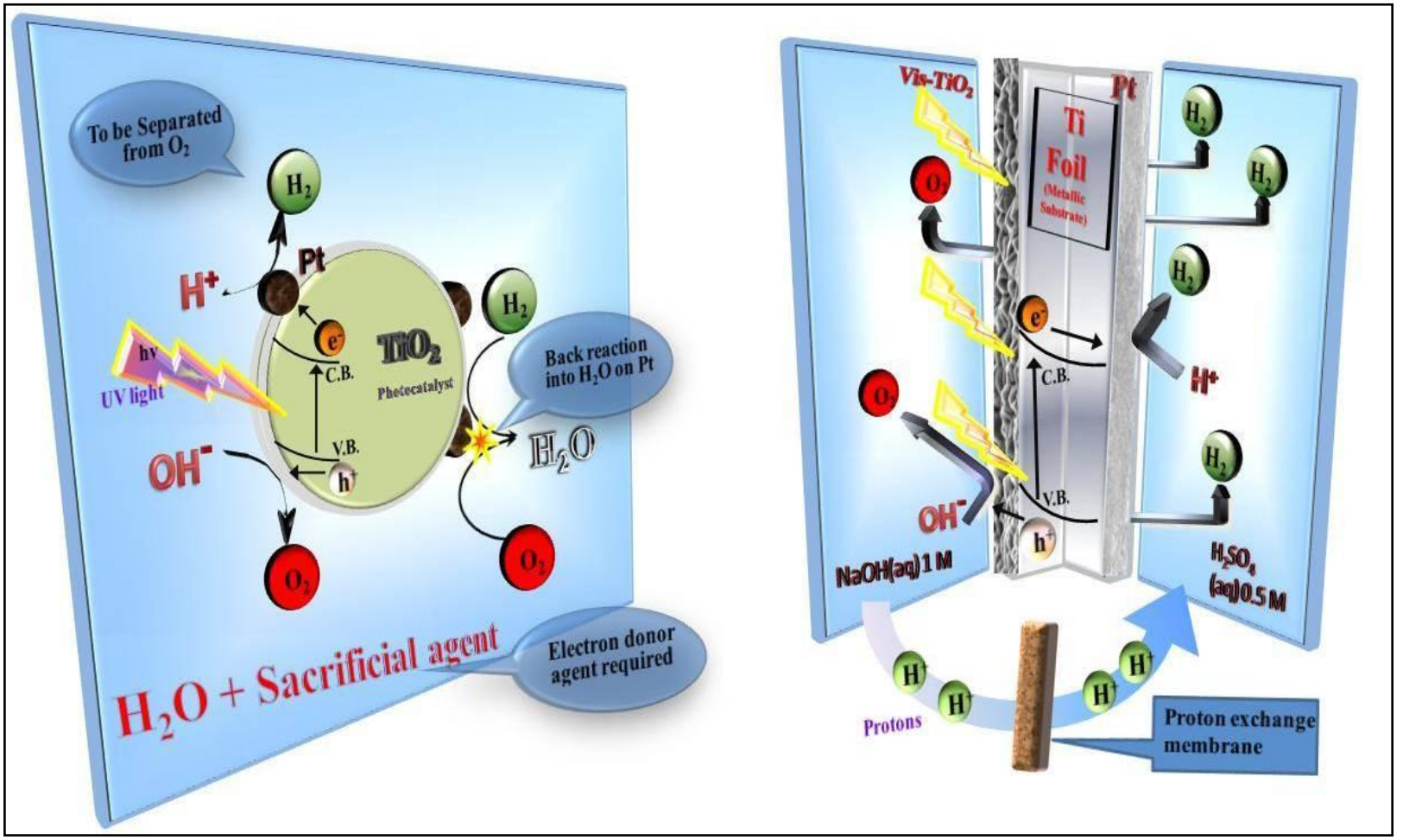

Fig.2.6 Evolution of H_2 from an aqueous solution contains of sacrificial agent (left), Separate Evolution of H_2 and O_2 from H_2O in two separate vessels which protons can transfer through a proton exchange membrane. TiO_2 side：1N NaOH aq, Pt side：0.5N H_2SO_4 aq

has been understood that in this situation Vis-TiO_2 thin film has highest potential to generate hydrogen and oxygen under a visible light irradiation.

Although the researches carried out in water splitting utilizing photocatalytical processes compare to semiconductor photocatalytic air /water purification are not widespread, but as both photocatalytic hydrogen production and photocatalytic air /water purification basically obey same rule, because photogeneration of electron / hole pairs take place in both processes despite of how these electron/hole utilize in the special process. In water splitting the conduction band (CB) level is significant but in purification processes valence band (VB) holes are important. The conduction band electrons as can be seen in the schematic Fig.2.6 reduce the existing protons in solution to H_2. [24 Ni]

In ordinary hydrogen evolution processes which takes place in a single cell and almost utilizing TiO_2 or other photocatalyst powder he total produced hydrogen depends upon the photocatalyst functionality, deposited metal dispersion and particle size and correlated with irreversibility of oxidation reactions. [22]. As it has shown in the left photo, the mentioned ordinary hydrogen evolution process have some disadvantage which the necessity to further separation of oxygen and hydrogen evolved gas and backward reactions of oxygen and hydrogen into water on Pt catalyst are main ones. In these systems using electron donor agents have essential role in effective hydrogen evolution. In these particulate systems, all reduction and oxidation reactions take place at the surface of a single particle, as can be seen in the schematic figure2.7. Utilizing a sacrificial electron donor is essential in this kind of processes and because of it this process couldn’t be considered as a commercial process for hydrogen production in future, but it is an affordable routine for

characterizing the functionality of produced catalyst and could be utilized for production of hydrogen for experimental purposes. [27]

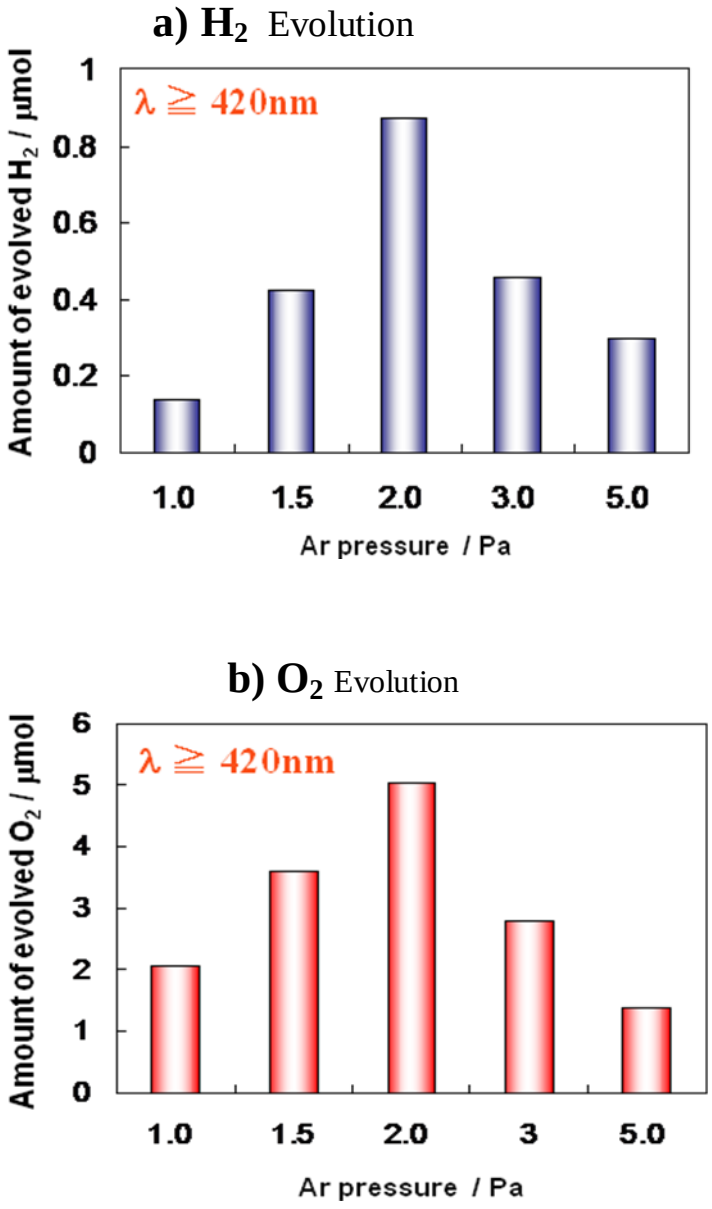

Fig.2.7 Dependence of photocatalytic activity of Vis-TiO_2-P_{Ar} thin films on P_{Ar} under visible light irradiation longer than 420 nm (Irradiation time: 10 h).

(a) H_2 evolution from aqueous methanol solution, (b) O_2 evolution from of silver nitrate aqueous solution.

In order to investigate the effect sputtering pressure on the physical properties of the TiO_2/Ti thin films, XRD, SEM and BET surface area measurements were carried out. Figure 2.8 shows the XRD patterns of the TiO_2/Ti thin films and it can be seen that their crystal structures all consist of anatase and rutile phases. The intensity of crystalline phases is weak in low sputtering pressure, as it shown in figure 6 for Ar pressure equal to 0.5 Pa; no strong peak could be finding. The intensity of the peaks due to the rutile and anatase phases increasing with rising in the sputtering pressure. Raising sputtering pressure to more than 2 Pa leads to decrease of rutile intensity and increasing of anatase phase.

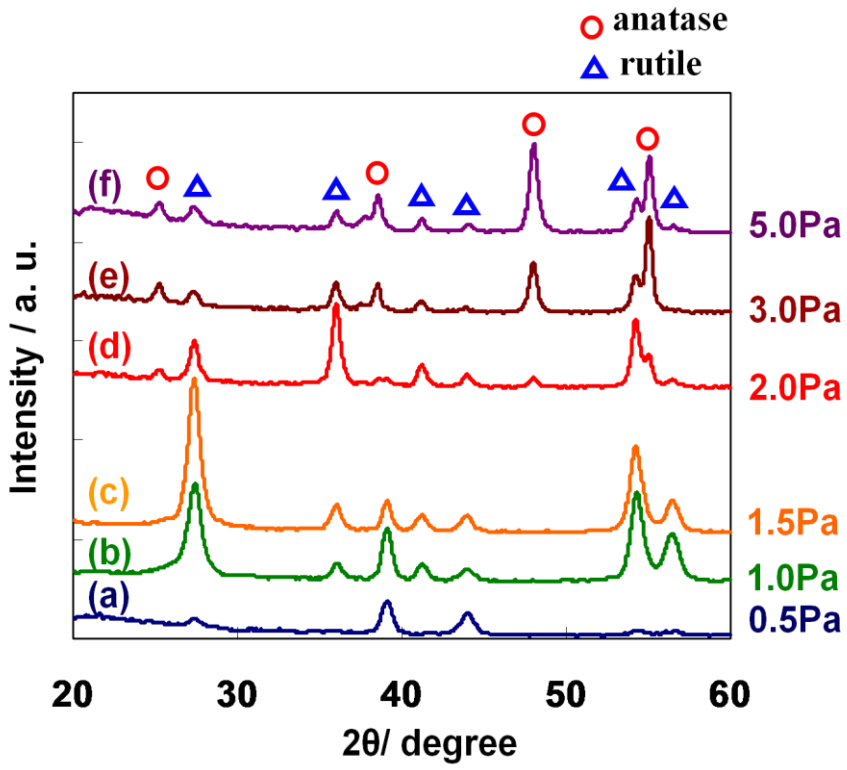

Fig. 2.8. XRD patterns of Vis-TiO_2-P_{Ar} thin films. P_{Ar} (Pa) : (a) 0.5, (b) 1.0, (c) 1.5, (d) 2.0, (e) 3.0, (f) 5.0.

An investigation for finding the highest active Vis-TiO_2, thin films prepared on different sputtering pressure under fixed substrate temperature of 873 K and fixed target to surface distance. Figure 2.9 shows that the photocurrent density for the Vis-TiO_2 film prepared at different sputtering pressure, in UV region illumination increases with increasing of sputtering pressure. With increase in surface area, the effective surface area in contact with the electrolyte increases. As a result, the charge transfer rate at the TiO_2/electrolyte interface would be greater and could more than offset the adverse effects of bulk and surface recombination. A higher photocurrent indicates that photoinduced electrons transferred more efficiently from the anode to

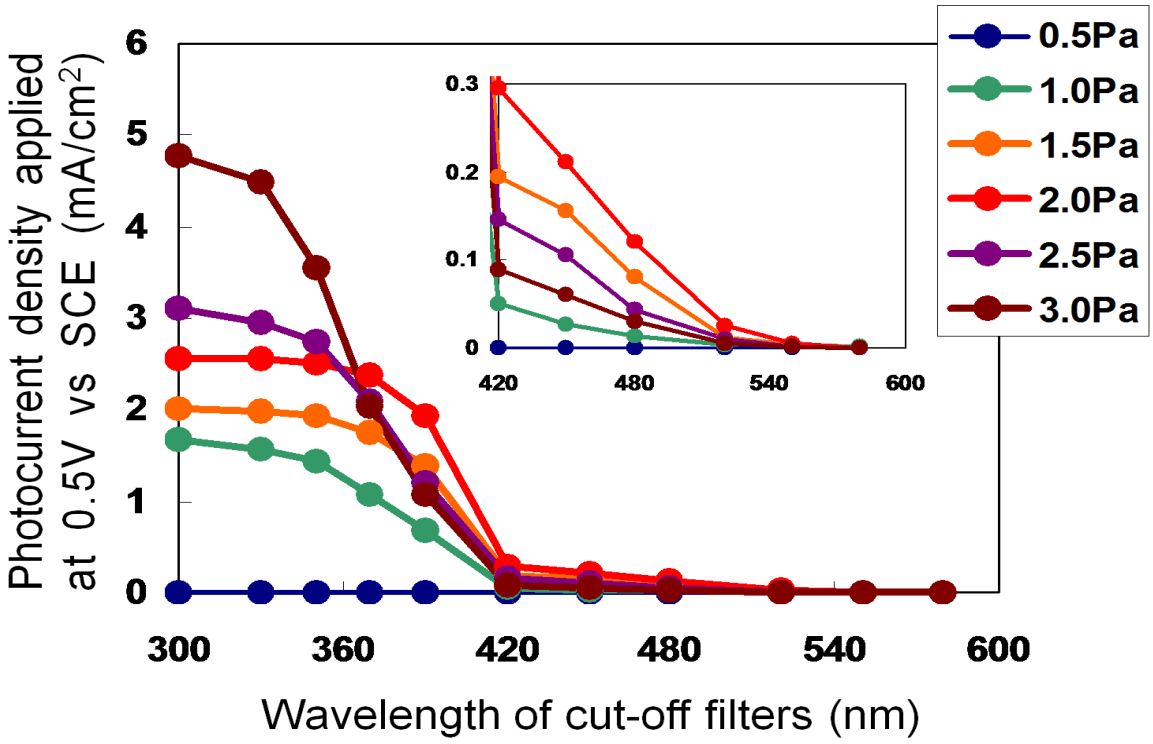

the cathode. But in the visible region this matter is a little different, as it shown in the small insider figure

Fig.2. 9. Photocurrent of Vis– TiO_2 thin film made by different sputtering gas pressure

from 0.5 to 3.0Pa.

with increasing the sputtering pressure photocurrent will increase from 0.5 to 2.0Pa, but it decreases by raising the sputtering pressure. As it is too important for us to increase the visible light response of thin films, the best choice for us is to keep sputtering pressure at 2.0 Pa.

Figure 2.10 shows the surface SEM images of the TiO_2/Ti thin films which produced under different sputtering pressures, the grain size of crystals increases by increasing the Ar sputtering gas pressure from 0.5 to 1.5Pa, but from this point increasing more Ar pressure leads to decreasing crystal grain sizes. As it is obvious, the films deposited under P_{Ar} of 1.0 and 0.5 Pa have smooth and flat surfaces.

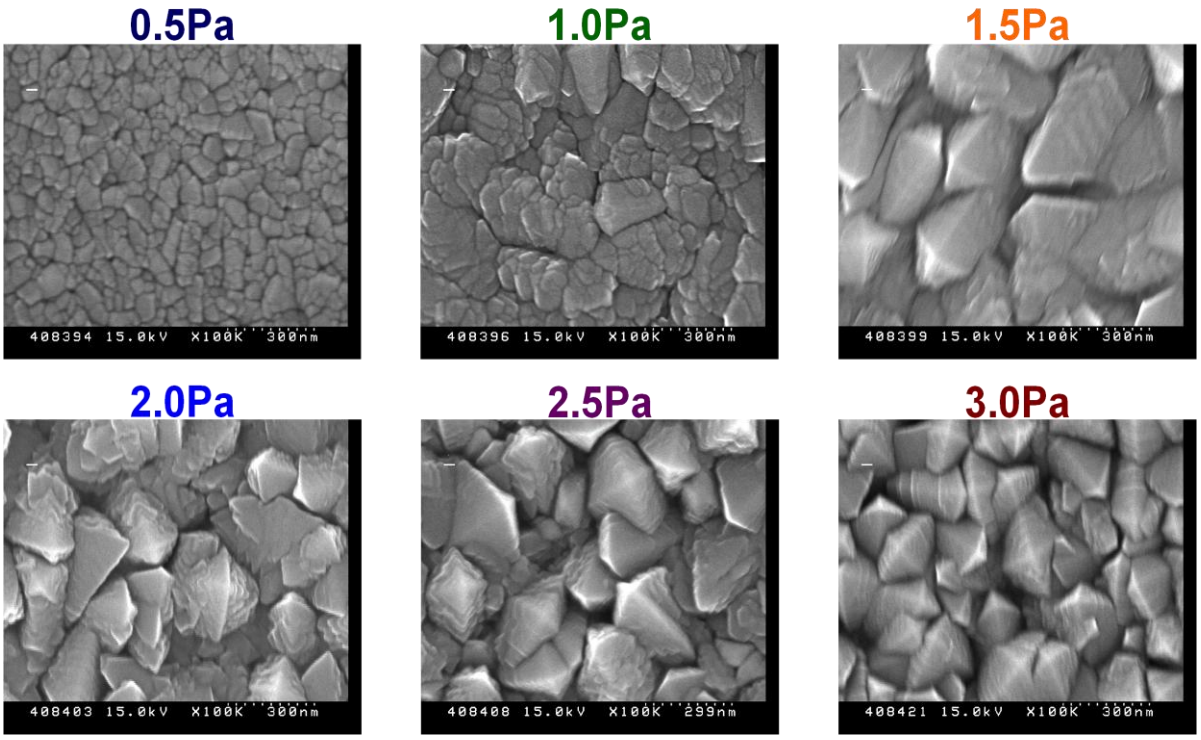

Fig. 2.10. SEM images of Vis–TiO_2 thin films based on different sputtering pressure.

It demonstrates regulating of sputtering pressure is an important parameter for control crystal structure and morphology. It is apparent that sputtered atoms from the

target material will collide with the sputtering gas in their path towards the substrate and the population and kinetic energies of the species approaching the substrate decrease with an increase in the sputtering gas pressure. [34]

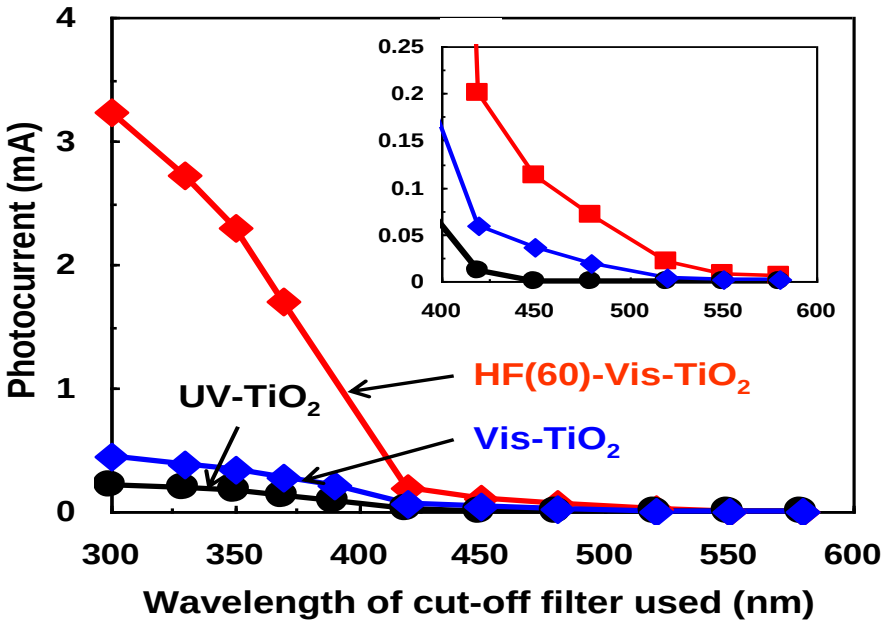

Fig. 2.11 The relative photocurrent as a function of the cut-off wavelength of incident light for HF(X)- TiO_2/Ti electrodes measured in 0.1 M HClO4 aqueous solution at +1.0 V vs SCE.

The growth of the rutile crystal becomes remarkable if the Ar gas pressure is reduced, in this case the kinetic energy will be higher and mean free paths of sputtered particles which colliding the surface become longer, it is thought that the second particles grow up too. Moreover, it is thought that the defect is caused in the thin film because the kinetic energy of sputtered particles that reach the substrate is too high and crystalline decreases when sputtering pressures reach 1.0Pa or less. The kinetic energy of sputtered atoms enhance formation of rutile phase and the crystal growth of the films of in the range of 1.5 to 5.0 Pa.

Figure 2.12 shows the photocurrent observed for the films as a function of the wavelength controlled by cut-off filters. Both Vis-TiO_2/Ti and HF (60)-Vis-TiO_2/Ti exhibited photocurrent response extending to wavelengths of around 520 nm as compared to that of UV-TiO_2/Ti at around 400 nm. Moreover, a remarkable increase in the photocurrent was observed for HF(60)-Vis-TiO_2/Ti under both UV and visible light irradiation.

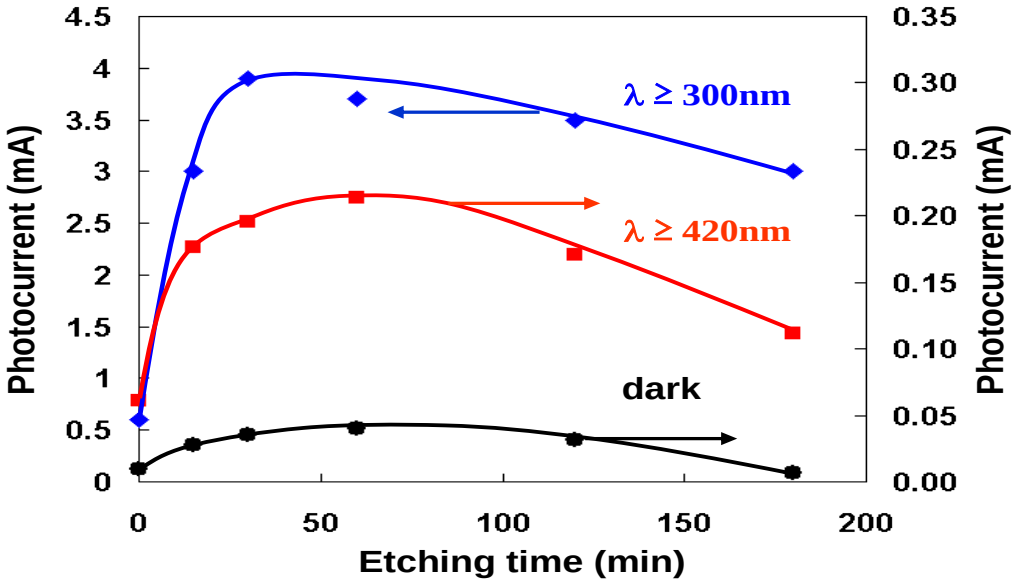

Fig. 2.12. Relationship between the photocurrents and etching times of TiO_2 thin films using UV and Visible light and dark condition.

Figure 2.12 presents relationship between the photocurrents and etching times of TiO_2 thin films using UV and Visible light and dark condition. The photocurrent observed for different kind of HF treated TiO_2 thin films, HF-TiO_2/Ti based on the treatment time as a function of the wavelength controlled by the cut-off filters. It is clearly shown with increasing of HF treatment time, the photo current will increase for UV and visible light but increasing treatment time will start to decrease after

reaching the maximum.

Vis-type TiO_2 thin films were, thus, applied for the separate evolution of H_2 and O_2 from the decomposition of water under solar light irradiation. The Vis-type TiO_2 film was prepared on one side of the Ti foil while the opposite side was deposited with small amounts of Pt. The prepared photocatalytic device was mounted on an H-type cell, as shown in Fig. 2.13. The TiO_2 side of the photocatalyst was immersed in 1.0 M NaOH solution and the Pt side was immersed in 0.5 M H_2SO_4 solution in order to add a chemical bias (ca. 0.8 V). As shown in Fig. 2.13, water could be separately decomposed into H_2 and O_2 with irradiation of natural solar light from the sunlight-gathering system, while no reaction proceeded on the UV-type TiO_2 film under the same reaction conditions. The experiment was performed on a clear sunny day in March and the changes in the relative intensity of sunlight along with the irradiation times are also shown here in this Figure. The efficiency of solar energy

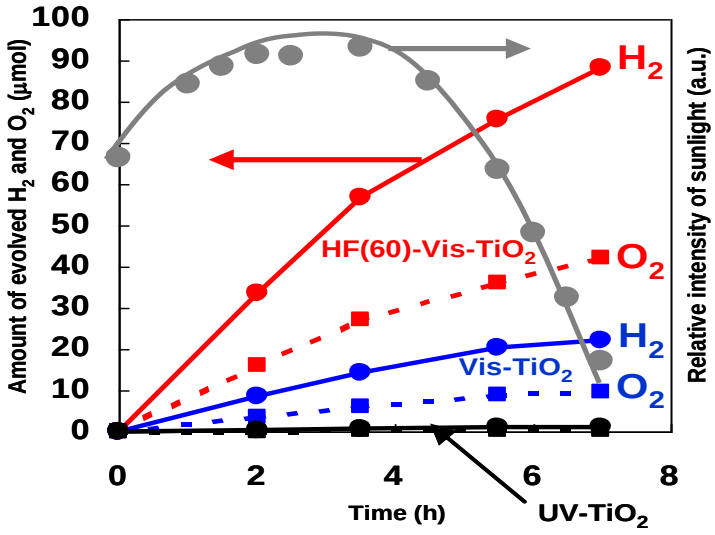

Fig. 2.13. Separate evolution of H_2 and O_2 on HF- Vis– TiO_2 thin film devices under sunlight irradiation in a H-shape glass container. (TiO_2 side, 1.0 M NaOH aq., Pt side, 0.5M H_2SO_4 aq).

conversion could be estimated at ca. 0.1% from the initial rate of H_2 evolution.

The decline observed in the evolution rates of H_2 and O_2 in the late afternoon (2:00 PM) can be attributed to a decline in sunlight intensity. A novel photocatalytic system which can produce H_2 and O_2 separately from water under solar light irradiation could, thus, be achieved with the visible light-responsive TiO_2 thin film photocatalysts we have designed and investigated.

The separate evolution of H_2 and O_2 from water under sunlight irradiation was carried out using the HF (60)-Vis-TiO_2/Ti/Pt photocatalyst. As shown in Fig. 2.13, H_2 and O_2 evolved in stoichiometric ratio under sunlight irradiation while the H_2 evolution ratio was 18μmol h-1 cm-2 in the early initial stage (up to 3 hrs) while no gas evolution was observed under dark conditions even under the same experimental conditions. Light irradiation was carried out with a sunlight-gathering system that removes the UV rays found in sunlight. In the left axis amount of evolved gases and in the right axis relative intensity of sunlight is shown.

In order to investigate the effect of HF treatment on the physical properties of the HF(*X*)-TiO_2/Ti thin films, XRD, XPS, SEM and BET surface area measurements were carried out. It is obviously can be understand from Figure 2.14 that treatment of HF will increase the porosity of the bulk of Vis-TiO_2 Fig. 2.14A is untreated Vis-TiO_2 with BET surface area of 379 cm^2 for a 1 cm^2 thin film sample. As it can be seen in the Fig. 2.14B and C, with treatment time of 60 and 120 min the surface area increased to 559 and 743 cm^2.

Figure 2.15 shows the effect of HF treatment on the UV–Vis transmission spectra of the Vis-TiO_2 thin films prepared on quartz substrates with a TiO_2 thickness of 1.5 μm. The UV–Vis spectrum of the UV-TiO_2 thin film is also shown as reference. After chemical etching by HF solution for 180 min, the surface of the film was

dramatically changed, although no noticeable change in the UV–Vis spectrum was observed before and after HF treatment. These results indicate that visible light is absorbed not at the surface of Vis-TiO_2/Ti but in the deep inside bulk while the film thickness is hardly changed after chemical etching of 180 min. The origin of visible light absorption has been described above and XPS measurements were carried out to investigate the chemical composition of the surface of HF(*X*)-Vis-TiO_2/Ti thin films.

As shown in Fig. 2.16, the HF(*X*)-Vis-TiO_2/Ti films showed a typical XPS peak at approximately 685 eV assigned to the F− ions physically adsorbed on the surface of the film [10]. The peak intensity slightly increased with an increase in the HF treatment time, while the peak position did not change even after HF treatment of 180 min.

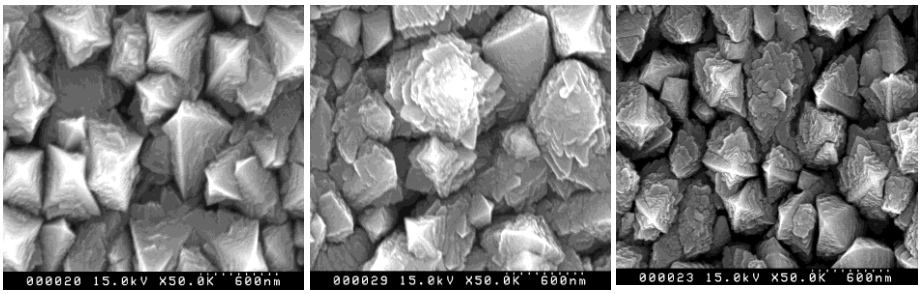

Fig. 2.14. SEM images and BET surface areas of the HF- Vis–TiO_2 thin films as a function of the treatment time in HF solution.

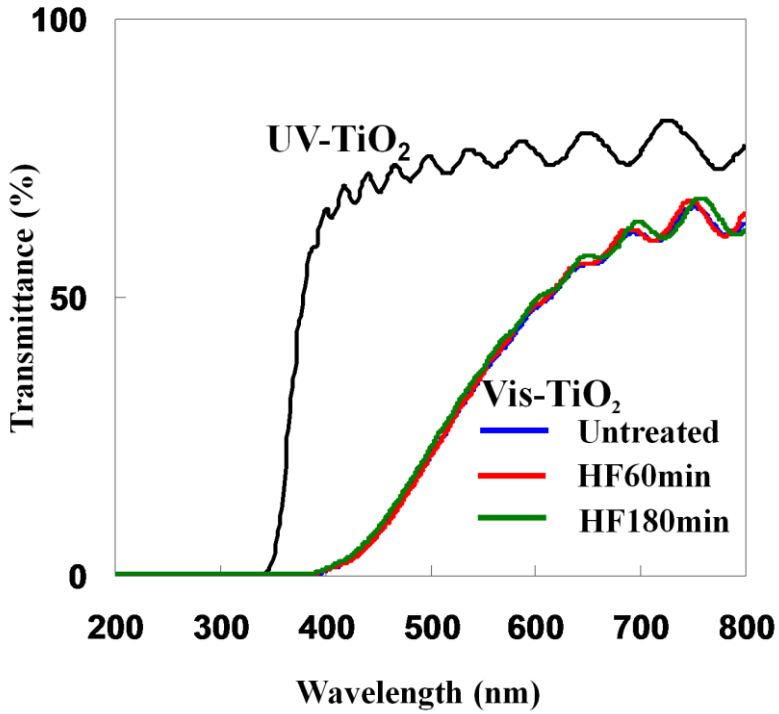

Fig.2. 15 The UV–Vis transmission spectra of: (a) UV-TiO_2, (b) Untreated Vis-TiO_2, and (c) HF(60)-Vis-TiO_2 and (d) HF(180)-Vis-TiO_2 thin films prepared on quartz substrates with a film thickness of 1.5 mm.

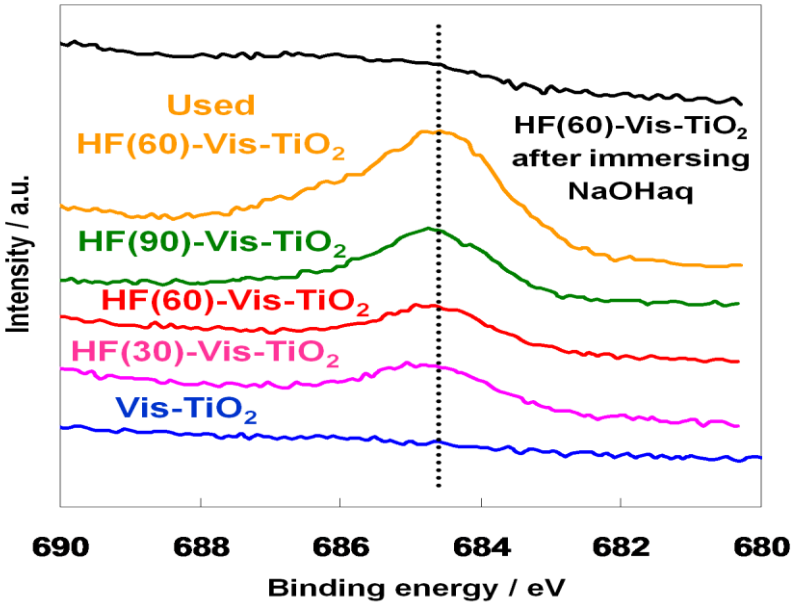

Fig.2. 16. Effect of the F^- ions physically adsorbed on the surface of Vis-TiO_2, XPS spectra of F 1s peaks.

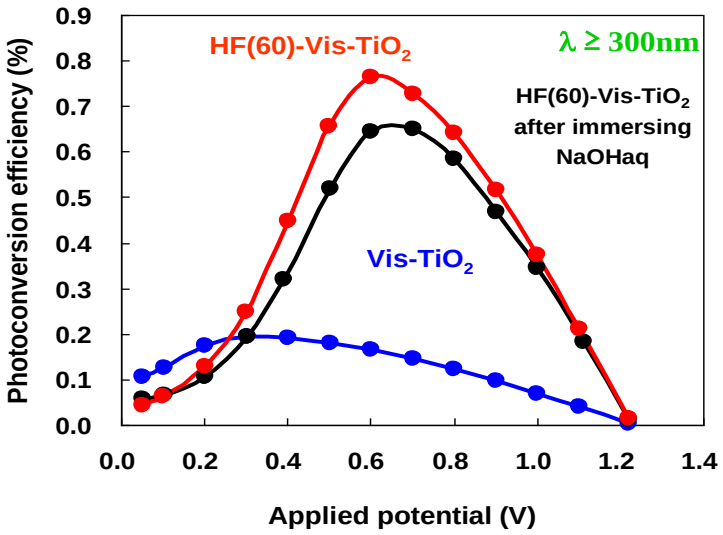

Fig. 2.17. Effect of the F^- ions on photoconversion efficiency

Yu et al. [40] have reported that the photocatalytic activity of F^- doped TiO_2 is much higher than P-25. F^- doped TiO_2 is formed by the nucleophilic substitution reaction of the F^- ions titanium alkoxide during the hydrolysis process. In fact, F^- doped TiO_2 showed a XPS peak at approximately 688 eV due to the F^- ions substituted into the TiO_2 lattice. Moreover, they have suggested that F^- doped TiO_2 exhibits stronger absorption in the UV–Vis range with a red shift in the band gap transition and playing an important role in improving the photocatalytic activity. However, no noticeable changes in the UV–Vis spectrum were observed for our samples (HF-Vis-TiO_2). Taking these results into consideration, the physisorbed F^- ions probably do not affect the photocatalytic activity of HF-Vis-TiO_2/Ti. As it is illustrated in this figure after immersing of the HF treated Vis-TiO_2 in 1M NaOH aqueous solution the peak belongs to F^- will disappear.

To understand how the F^- ions have an effect of on HF treated Vis-TiO_2 Photoactivity, photoconversion efficiency of HF(60)-Vis-TiO_2 before and after

immersion in NaOH investigated. As can be seen in Fig. 2.17, for ($\lambda \geq 300$ nm)

2.4.Conclusions

Harvesting sunlight efficiently needs novel technologies and trends to achieve a satisfactory active photocatalysts which can operate with visible light rather than UV light. In this work, the modified TiO_2 films were prepared by RF magnetron sputtering methods. Films were deposited under various process conditions. The visible light responsive TiO_2 (Vis-TiO_2) thin films which produced by RF-magnetron sputtering method, the functionality and characteristics of produced TiO_2 thin films investigated and compared with common UV-TiO_2 thin films, among different parameters which has most influence on photocatalytic activity of such produced Vis-TiO_2 thin films, the influence of sputtering pressure studied firstly.

The main tasks of this chapter focused on two aspects: optimizing the growth condition of the Vis-TiO_2 films and investigating the correlation between the microstructure and the photoelectrochemical properties of the films. Optimization of the best condition of sputtering ended up with post treatment of Vis-TiO_2 with HF to achieve highest active Vis-TiO_2.

In this chapter, we have discussed the possibility of using optimized Vis-TiO_2 thin films for producing of H_2 and O_2 separately. We select an approach to optimizing of the photocatalytic activity of Vis-TiO_2 thin films prepared by RF-MS method by controlling of different factors such as sputtering pressure and target to substrate distance $D_{T\text{-}S}$ investigated. We have shown through different characterization experiments, which the best condition for sputtering pressure is 2.0 Pa. In this

pressure the highest activity Vis-TiO_2 thin films could be attain. With fixing sputtering pressure is 2.0 Pa and changing the target to substrate distance, D_{T-S}=75mm had the best results.

As it was found previously that chemical etching with HF solution, remarkably enhance the Photocatalytic activity of Vis-TiO2 thin films, optimized produced Vis-TiO_2 thin films treated by this solution. HF-Vis-TiO_2/Ti thin film electrodes exhibited a significant increase in their photocurrent under UV and visible light irradiation as compared to untreated Vis-TiO_2/Ti. SEM and BET surface measurements revealed that the surface roughness increased and the interspace between the columnar TiO_2 crystallites were extended by HF treatment, indicating that HF-Vis-TiO_2/Ti has a shorter diffusion length for the photoformed holes to reach the solid–liquid interfaces than untreated Vis-TiO_2/Ti. The donor densities of Vis-TiO_2/Ti also increased after HF treatment, indicating that the photogenerated electrons of HF (60)-Vis-TiO_2/Ti can reach the TiO_2 substrate interface more easily than Vis-TiO_2/Ti due to its higher conductivity. Moreover, it was found that the photocatalytic activity of Vis-TiO_2 for the separate evolution of H_2 and O_2 could be remarkably increased under visible light irradiation ($\lambda \geq 450$ nm) with chemical etching by HF solution. This approach offers the advantage of stoichiometric separate evolution of H_2 and O_2 could also be successfully achieved using the HF (60)-Vis-TiO_2/Ti/Pt thin film photocatalysts while the H_2 evolution ratio was 18 $\mu mol\, h^{-1}\, cm^{-2}$ in the early initial stage, corresponding to a solar energy conversion efficiency of 0.3%. HF-Vis-TiO_2 could, thus, be considered a unique photofunctional material for applications in clean and safe H_2 production systems from water using one of the most abundant and pollution-free resources, solar energy.

2.5. References:

1. Fujishima A., Honda K., Nature, 238, 37 (1972).
2. Anpo M., Dohshi S., Kitano M., Hu Y., Takeuchi M., Matsuoka M., Annu. Rev. Mater. Res., 35, 1 (2005).
3. Anpo M., Bull. Chem. Soc. Jpn., 77, 1427 (2004).
4. Anpo M., Takeuchi M., J. Catal., 216, 505(2002).
5. Kitano M., Iyatani K., Tsujimaru K., Matsuoka M., Takeuchi M., Ueshima M., Thomas J.M., Anpo M., Top. Catal., 49, 24 (2008).
6. Kitano M., Tsujimaru K., Anpo M., Top. Catal., 49, 1 (2008).
7. Kitano M., Matsuoka M., Hosoda T., Ueshima M., Anpo M., Res. Chem. Intermed., 34, 5, 577 (2008)
8. Kitano M., Matsuoka M., Ueshima M., Anpo M., Appl. Catal. A, 325, 1(2007).
9. Matsuoka M., Kitano M., Takeuchi M., Tsujimaru K., Anpo M., Thomas J.M., Catal. Today, 122, 51, (2007).
10. Kitano M., Takeuchi M., Matsuoka M., Thomas J.M., Anpo M., Catal. Today, 120 , 133(2007).
11. Kitano M., Tsujimaru K., Anpo M., Appl. Catal. A, 314, 179 (2006).
12. Iino K., Kitano M., Takeuchi M., Matsuoka M., Anpo M., Curr. Appl. Phys., 6, 982 (2006).
13. Kikuchi H., Kitano M., Takeuchi M., Matsuoka M., Anpo M., Kamat P.V., J. Phys. Chem. B, 110, 5537(2006).
14. Matsuoka M., Kitano M., Takeuchi, M., Anpo M., Thomas J.M., Top. Catal., 35, 305 (2005).
15. Fukumoto S., Kitano M., Takeuchi M., Matsuoka M., Anpo M., Catal. Lett.,

127, 39 (2008).

16. Takeuchi M., Sakai S., Ebrahimi A., Matsuoka M., Anpo M., Top. Catal., 52, 1651(2009).
17. Grätzel M., Nature, 414, 338 (2001).
18. Raimondi F., Scherer G.G., Kotz R., Wokaun A., Angew. Chem. Int. Ed., 44, 2190 (2005).
19. Sahaym U., Norton M.G., J. Mat. Sci., 43, 5395 (2008).
20. Matsuoka M., Ebrahimi A., Nakagawa M., Kim T.-H., Kitano M., Takeuchi M., Anpo M., Res. Chem. Intermed., 35,997 (2009).
21. Bäumer M., Freund H.-J., Prog. Surf. Sci. 61, 127 (1999).
22. Ashokkumar M., Int. J. Hyd. Energy., 23, 427 (1998).
23. Henry C.R., Surf. Sci. Rep., 31, 231 (1998).
24. Ni M., Leung M.K.H., Leung D.Y.C., Sumathy K., Renew. Sustain. Energy. Rev., 11, 401(2007).
25. Oliva F.Y., Avalle L.B., Santos E., Cámara O.R., J. Photochem. Photobio. A, 146, 175 (2002).
26. Chen X., Mao S.S., Chem. Rev., 107, 2891 (2007).
27. Van De Krol R., Liang Y., Schoonman J., J. Mater. Chem., 18, 2311 (2008).
28. Beranek R., Kisch H., Photochem. Photobiol. Sci., 7, 40 (2007).
29. McCoy R.A., Deng Y., Int. J. High. Perfor. Comput. Appl., 13, 16 (1999).
30. Westwood W. D., J. Vac. Sci. Technol., 15, 1 (1978).
31. Petrov I., Barna P.B., Hultman L., Greene J.E. , J. Vac. Sci. Tech. A, 21 (2003).
32. Zhang W., Li Y., Wang F., J. Mater. Sci. Technol., 18, 101(2002).
33. Šícha J., Musil J., Meissner M., Čerstvý R., Appl. Surf. Sci., 254, 3793 (2008).

34. Heo C.H., Lee S.-B., Boo J.-H., Thin Solid Films, 475, 183 (2005).
35. Mahieu S., Ghekiere P., Depla D., De Gryse R., Thin Solid Films, 515, 1229 (2006).
36. Yamagishi M., Kuriki S., Song P.K., Shigesato Y., Thin Solid Films 442, 227 (2003).
37. Diebold U., Surf. Sci. Rep., 48, 53 (2003).
38. Diebold U., Lehman J., Mahmoud T., Kuhn M., Leonardelli G., Hebenstreit W., Schmid M., Varga P., Surf. Sci., 411, 137(1998).
39. Linsebigler A.L., Lu G., Yates Jr. J.T., Chem. Rev., 95, 735(1995).
40. Yu Y., Wu H.-H., Zhu B.-L., Wang S.-R., Huang W.-P., Wu S.-H., Zhang S.-M., Catal. Lett. 125, 168(2008).

Chapter 3

Survey on the Effect of Various Calcination Treatments on the Photocatalytic Reactivity of Vis-TiO_2 Thin Films Prepared by RF-MS method

3.1. Introduction

The photocatalytic splitting of water into H_2 and O_2 under visible or solar light irradiation has attracted much attention in terms of hydrogen production and solar energy conversion [1-10]. Recent studies have revealed that novel mixed oxides or oxynitrides such as $In_{1-x}Ni_xTaO_4$ [11] or ZnO-GaN solid solution [12,13] can induce a complete water splitting reaction even under visible light irradiation. Furthermore, it has been reported that water splitting can be achieved under visible light irradiation by a Z-scheme reaction system using two different types of photocatalysts and a redox mediator [14-16]. Pure hydrogen would be required for utilization as fuel on a large scale; however, powdered photocatalysts yield a mixture of H_2 and O_2. Recently, we have reported that a radio-frequency magnetron sputtering (RF-MS) method enables the preparation of a visible light-responsive TiO_2 thin film photocatalyst (Vis-TiO_2) by the precise control of the substrate temperature during the deposition process [5-10]. Moreover, the separate evolution of H_2 and O_2 from H_2O could be successfully achieved by using an H-type glass cell consisting of two water phases separated by a proton-exchange membrane and Vis-TiO_2 thin film photocatalyst (Vis-TiO_2/Ti/Pt), where Vis-TiO_2 was deposited on one side of the Ti metal foil substrate while nanoparticles of Pt were deposited on the other [7-9]. In the present work, we have investigated the effect of various calcination treatments such as calcination in air or NH_3 on the photoelectrochemical performance as well as photocatalytic activity of Vis-TiO_2. Special attention is focused on the effect of the calcination treatment in NH_3 on the rate of the separate evolution of H_2 and O_2 from H_2O on Vis-TiO_2/Ti/Pt.

3.2. Experimental

TiO_2 thin films were prepared by a radio-frequency magnetron sputtering (RF-MS) method using a TiO_2 plate (High Purity Chemicals Lab. Corp., Grade: 99.990%) as the source material and Ar gas (99.995%) as the sputtering gas. Ti metal foil or ITO glass substrates were fixed onto the substrate holder which was centrally positioned in parallel just above the source material with a target-to-substrate distance of 80 mm. Prior to the introduction of Ar gas, the chamber was evacuated to less than 5.0×10^{-4} Pa, followed by the introduction of Ar at 2.0 Pa. TiO_2 thin films (film thickness: 3μm) were then prepared on the Ti metal foil (TiO_2/Ti) or ITO glass (TiO_2/ITO) substrates (10 x 20 mm2) by inducing a radio-frequency power of 300 W with the substrate temperature (T_S) held at 473 or 873 K. Normal type TiO_2 thin films (UV-TiO_2/Ti, UV-TiO_2/ITO) were formed at *T*s = 473 K, while visible light-responsive TiO_2 thin films (Vis-TiO_2/Ti, Vis-TiO_2/ITO) were formed at *T*s = 873 K [5-10]. Vis-TiO_2 were then calcined in air (1.0 x 105 Pa) at 673 K for 2 h and denoted as Vis-TiO_2 (air). On the other hand, Vis-TiO_2 calcined in NH_3 (1.0×10^4 Pa) at 673 K for 2 h was denoted as Vis-TiO_2 (NH_3). TiO_2 thin film photocatalysts (UV-TiO_2/Ti/Pt, Vis-TiO_2/Ti/Pt, Vis-TiO_2 (air)/Ti/Pt and Vis-TiO_2 (NH_3)/Ti/Pt) were prepared by depositing Pt on TiO_2/Ti after various calcination treatments, where nanoparticles of Pt were deposited on the other side of the TiO_2 thin film. Pt deposition was performed by an RF-MS method with an RF power of 70 W at *T*s = 298 K. The separate evolution of H_2 and O_2 from H_2O were investigated by using an H-type Pyrex glass cell (Scheme 3.1). The glass cell consisted of two water phases, one acidic (Pt side: 0.5 M H_2SO_4) and the other alkaline (TiO_2 side: 1 M NaOH aq),

separated by a TiO_2 thin film photocatalyst (TiO_2/Ti/Pt) and a proton-exchange membrane. The evolved gasses were analyzed by gas chromatography (Yanaco, G2800-T). Light irradiation was carried out with a 500 W Xe lamp using various color glass filters through the quartz window of the reaction cell. The UV-Vis diffuse reflectance spectra were recorded with a UV-Vis spectrophotometer (Shimadzu, UV-2200A). The crystal structure of the TiO_2 thin films were determined by X-ray diffraction (XRD: Shimadzu, XRD-6100) using a CuK_α line (λ = 1.5406 Å). Secondary ion mass spectrometry (SIMS: Physical Electronics, ADEPT1010) was carried out to obtain the depth profiles of ^{18}O and ^{48}Ti for the thin films. The surface areas of the films were investigated by BET surface measurements using krypton as the adsorbate. The photoelectrochemical properties of the TiO_2 thin films were evaluated at ambient temperature using a potentiostat (Hokuto Denko, HZ3000) with a three-electrode cell that consists of a film electrode (TiO_2/Ti), Pt electrode and saturated calomel electrode (SCE) as the working, counter and reference electrodes, respectively. The 0.2 cm^2 working electrode was irradiated with a 500 W Xe lamp in 0.25 M K_2SO_4 aqueous solution that was mechanically stirred and degassed by purging with 99.99 % pure Ar gas before and during the experiments.

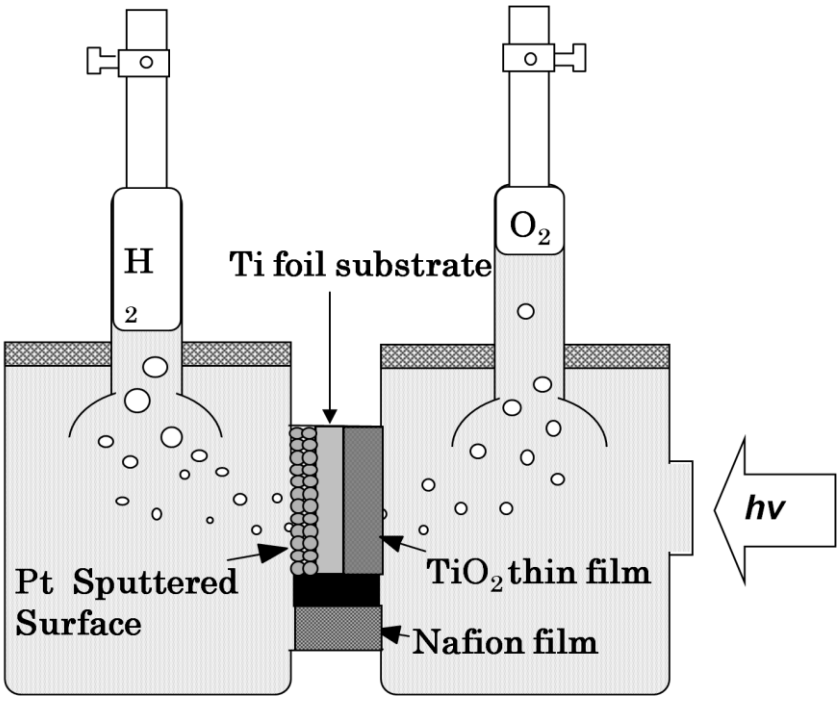

Scheme 3.1. H-type glass cell for the separate evolution of H_2 and O_2 using a TiO_2/Ti/Pt. Electrolyte: 1 M $NaOH_{aq}$ (TiO_2 side); 0.5 M H_2SO_4aq (Pt side)

3.3 Results and Discussion

Figure 3.1 (a) and (b) show the UV-Vis diffuse reflectance spectra of UV-TiO_2 and Vis-TiO_2, respectively, prepared on the ITO glass substrate. It can clearly be seen that UV-TiO_2 is transparent to visible light, thus enabling the absorption of UV light having wavelengths shorter than 400 nm, while Vis-TiO_2 can absorb visible light having wavelengths longer than 400 nm. SIMS investigations revealed that the secondary ion intensity due to ^{18}O for Vis-TiO_2 （1.6 μm thickness）gradually decreases from the top surface (O/Ti ratio = 2.00) to the inside bulk (O/Ti ratio = 1.93) although no significant change can be observed for UV-TiO_2, which exhibited the same stoichiometric O/Ti value (O/Ti ratio = 2.00) independent of the depth from the TiO_2 surface.

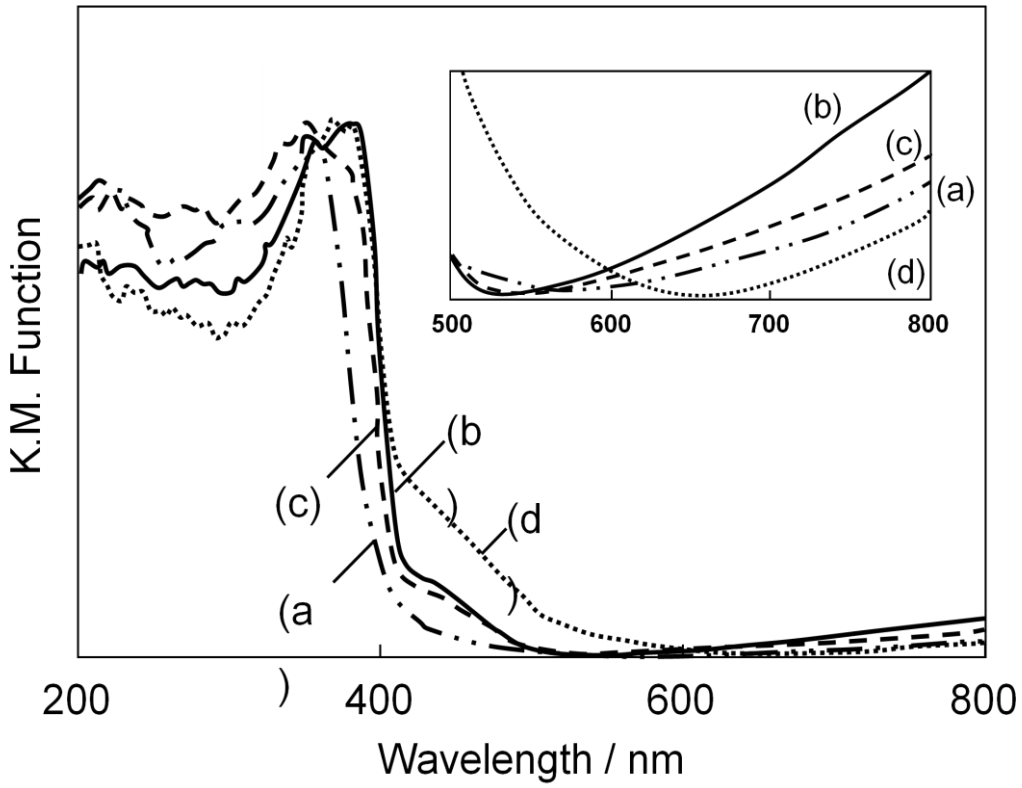

Figure 3.1. UV-Vis diffuse reflectance spectra of: (a) UV-TiO_2/ITO; (b) Vis-TiO_2/ITO; (c) Vis-TiO_2(air)/ITO; and (d) Vis-TiO_2(NH_3) /ITO. Inset shows expanded plots in wavelength regions above 500 nm.

It was, thus, suggested that the unique declined composition and anisotropic structure of Vis-TiO_2 caused a significant perturbation in the electronic structure of TiO_2, enabling the absorption of visible light [5-10]. It should be noted that Vis-TiO_2 shows a typical absorption band at wavelengths longer than 600 nm due to the existence of small amounts of the Ti^{3+} species formed under sputtering conditions [17]. Moreover, Vis-TiO_2 (air) and Vis-TiO_2 (NH_3) can absorb visible light having wavelengths longer than 400 nm while showing weak absorption bands due to the presence of the Ti^{3+} species which can act as the recombination center of the photoformed electrons and holes [18]. An increase in the intensity of the absorption

band in visible light regions (λ> 400 nm) can be observed for Vis-TiO_2 (NH_3). This increase in the visible light absorption band can be attributed to the mixing of the N 2p states with the O 2p states on the top valence band caused by nitrogen doping into Vis-TiO_2 [19, 20].

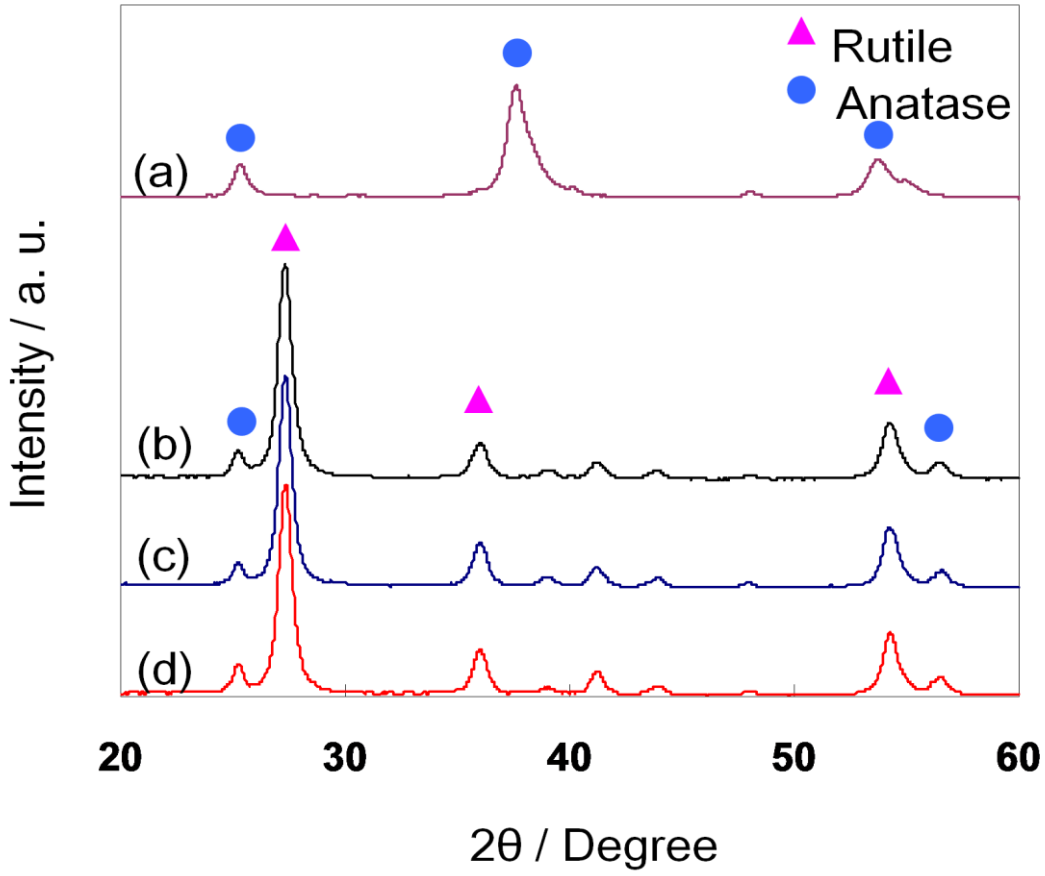

Figure 3.2. XRD patterns of: (a) UV-TiO_2/Ti; (b) Vis-TiO_2/Ti; (c) Vis-TiO_2 (air)/Ti; and (d) Vis-TiO_2 (NH_3)/Ti.

These results show that calcination in air or NH_3 leads to a decrease in the amount of Ti^{3+} species within Vis-TiO_2, while calcination in NH_3 is effective in increasing visible light absorption due to nitrogen doping into Vis-TiO_2.

Figure 3.2 shows the XRD patterns of various TiO_2 thin films prepared on the Ti metal foil substrate. UV-TiO_2 exhibited diffraction peaks due to an anatase crystalline phase. On the other hand, Vis-TiO_2 exhibited well-defined diffraction peaks due to a rutile crystalline phase as well as weak peaks due to an anatase crystalline phase. Furthermore, it was found that the crystalline phase of Vis-TiO_2 is hardly affected by treatments such as calcination in air or NH_3. Table 1 shows the BET surface areas of the various TiO_2 thin films prepared on a Ti metal foil substrate. It can clearly be observed that the surface area of Vis-TiO_2 (415 cm^2) was decreased by calcination treatment in air (Vis-TiO_2(air): 193 cm^2), while a decrease in the surface area was suppressed in the case of calcination in NH_3 (Vis-TiO_2(NH_3): 275 cm^2).

The photoelectrochemical properties of the TiO_2 thin films prepared on a Ti metal foil substrate were also investigated under light irradiation of wavelengths longer than 300 nm (Fig. 3.3).

Table 1. Effect of various calcination treatments on the BET surface area of Vis-TiO_2/Ti. (Film size: 1 cm^2)

Sample	Surface area / cm^2
Vis-TiO_2/Ti	415
Vis-TiO_2(air)/Ti	193
Vis-TiO_2(NH_3)/Ti	275

Anodic photocurrents were observed under scanning potentials of -0.5 to +1.5 V vs SCE for all TiO_2 thin films, which can be attributed to the photooxidation of water into O_2 [7-10]. UV-TiO_2 and Vis-TiO_2 (air) exhibited lower photocurrent than Vis-

TiO_2, while the photocurrent of Vis-TiO_2 (NH_3) was more than 2 times higher than that of Vis-TiO_2. These results suggest that calcination treatment in NH_3 is quite effective in improving the photoelectrochemical performance of Vis-TiO_2. The remarkable increase in the photocurrent of Vis-TiO_2(NH_3) can be attributed to the increase in visible light absorption caused by nitrogen doping as well as the decrease in the amount of Ti3+ species within Vis-TiO_2, as suggested by the UV-Vis results (Fig. 1).

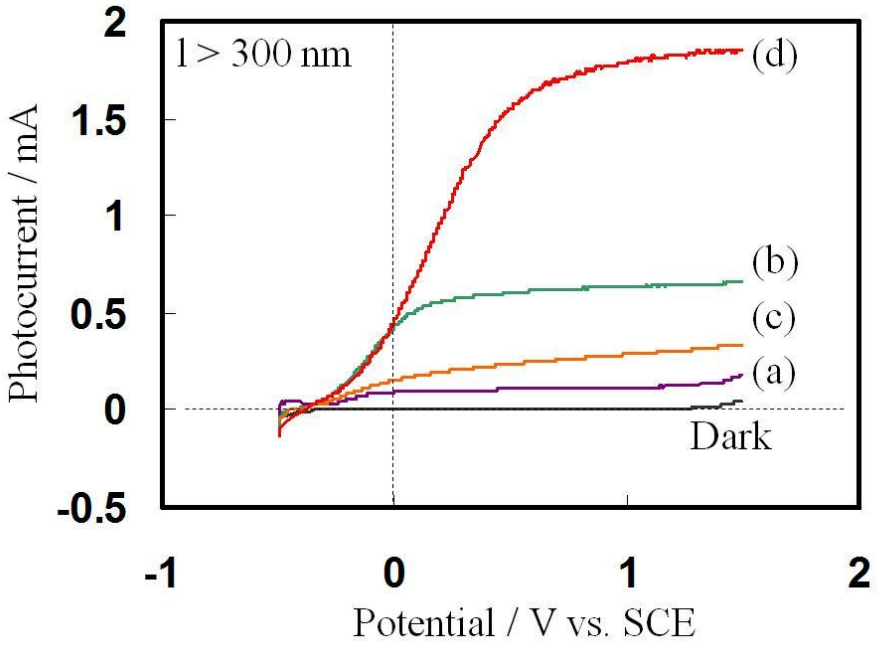

Figure 3.4. Current-potential curves of: (a) UV-TiO_2/Ti; (b) Vis-TiO_2/Ti; (c) Vis-TiO_2(air)/Ti; and (d) Vis-TiO_2(NH_3)/Ti measured under light irradiation (λ> 300 nm).

On the other hand, the decrease in the photocurrent of Vis-TiO_2 (air) can be ascribed to the drastic decrease in the surface area of Vis-TiO_2, which lessens the amount of surface reaction sites for water oxidation. Figure 4 shows the photocurrents observed for TiO_2 thin films prepared on a Ti metal foil substrate under

visible light irradiation (λ > 420 nm) at +1.0 V vs SCE. UV-TiO_2 exhibits weak photocurrent under visible light irradiation, while Vis-TiO_2 shows considerable photocurrent even after calcination treatment in air or NH_3. These results suggest that TiO_2 deposition at *T*s = 873 K is indispensable in preparing visible light-responsive TiO_2 thin films and that calcination treatment in NH_3 is effective in improving the photoelectrochemical performance of Vis-TiO_2 under visible light irradiation.

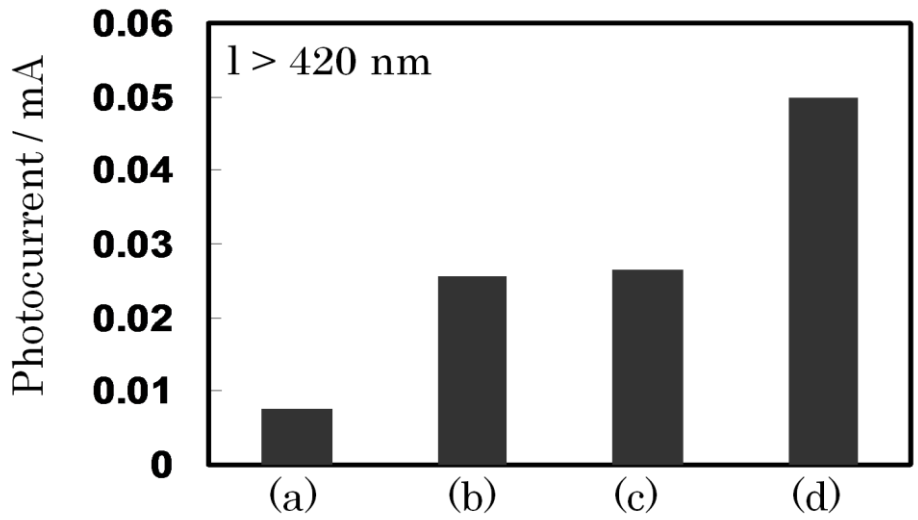

Figure 3.4. Photocurrents observed for: (a) UV-TiO_2/Ti; (b) Vis-TiO_2/Ti; (c) Vis-TiO_2(air)/Ti; and (d) Vis-TiO_2(NH_3)/Ti under visible light irradiation (λ> 420 nm) at +1.0 V vs SCE.

It should be noted that visible light can penetrate deeper into Vis-TiO_2 thin film than UV light since the absorption coefficient of Vis-TiO_2 in the visible light region is much lower than that in the UV light region. Thus, it can be considered that the photocurrent observed under visible light irradiation is less sensitive toward the surface morphology changes of TiO_2 thin film than that observed under UV light irradiation. This may be the reason that similar photocurrents were observed for Vis-

TiO_2 and Vis-TiO_2 (air) under visible light irradiation in spite of the large difference in their surface area.

Finally, the TiO_2/Ti/Pt photocatalyst was applied for the separate evolution of H_2 and O_2 from water using an H-type glass cell with two aqueous solutions, as shown in Scheme 1. Light irradiation ($\lambda > 300$ nm) of the synthesized UV-TiO_2/Ti/Pt mounted on an H-type glass cell led to the evolution of H_2 and O_2, while the separate evolution rate of H_2 and O_2 was around 4 times enhanced by using Vis-TiO_2/Ti/Pt as the photocatalyst (Fig. 5). These results clearly suggest that the photoformed holes on TiO_2 thin film oxidize H_2O into O_2, while photoformed electrons are transferred from TiO_2 side to Pt side through Ti metal foil substrate, enabling the efficient reduction of H+ into H_2. Moreover, it was found that the separate evolution rate of H_2 and O_2 on Vis-TiO_2/Ti/Pt is enhanced by more than two times after calcination treatment in NH_3. As shown in Fig. 6, the yields of H_2 and O_2 on Vis-TiO_2(NH_3)/Ti/Pt increased with good linearity against the light irradiation time ($\lambda > 300$ nm), indicating clearly that the reaction proceeds photocatalytically. It should be noted that the ratio of H_2 to O_2 (H_2/O_2) is smaller than the stoichiometric value of 2 for these reactions, which may be due to the oxidation of residual organic compounds on TiO_2 layer or the formation of adsorbed O_2- species on TiO_2 layer. Thus, it has been demonstrated that Vis-TiO_2/Ti/Pt can be applied for oxygen-free H_2 production from water, while the reaction rate can be dramatically enhanced by calcination treatment of Vis-TiO_2 in NH_3.

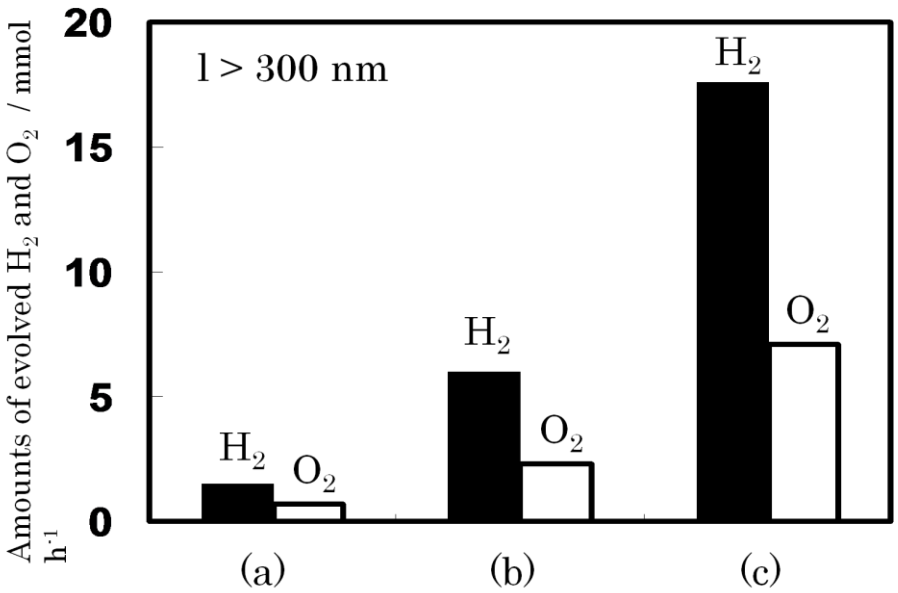

Figure 3.5. Yields of products in the separate evolution of H_2 and O_2 from H_2O on: (a) UV-TiO_2/Ti/Pt; (b) Vis-TiO_2/Ti/Pt; and (c) Vis-TiO_2(NH_3)/Ti/Pt under light irradiation (λ> 300 nm). Electrolyte: 1 M NaOHaq (TiO_2 side); 0.5 M H_2SO_4aq (Pt side)

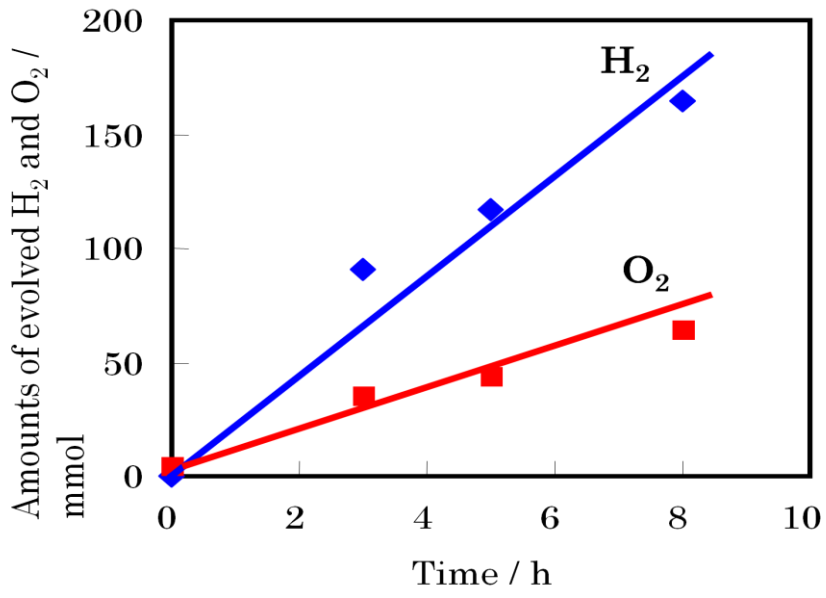

Figure 3.6. Time profiles of the separate evolution of H_2 and O_2 from H_2O on Vis-TiO_2 (NH_3)/Ti/Pt under light irradiation (λ> 300 nm). Electrolyte: 1 M $NaOH_{aq}$ (TiO_2 side); 0.5 M H_2SO_4aq (Pt side)

3.4 Conclusions

TiO_2 thin film photocatalysts were prepared on a Ti metal foil or ITO glass substrates by an RF-MS method under two different substrate temperatures. UV-TiO_2 which absorbs only UV light was formed under a substrate temperature of 473 K. On the other hand, Vis-TiO_2 prepared under a substrate temperature of 873 K exhibited an absorption band in wavelength regions above 400 nm. It was found that calcination treatment of Vis-TiO_2 in NH_3 at 673 K increases its visible light absorption capacity through nitrogen doping while decreasing the amount of Ti^{3+} species within Vis-TiO_2, leading to an enhancement of its photoelectrochemical performance. Finally, TiO_2 thin film photocatalysts (TiO_2/Ti/Pt) were prepared and applied for the separate evolution of H_2 and O_2 from H_2O by using an H-type glass cell. The separate evolution reaction of H_2 and O_2 proceeded with good linearity against the light irradiation time ($\lambda > 300$ nm) on Vis-TiO_2/Ti/Pt, while the reaction rate increased more than 2 times after calcination treatment in NH_3 at 673 K. It was, thus, demonstrated that a simple calcination treatment in NH_3 is remarkably effective in improving the photoelectrochmical performance as well as photocatalytic reactivity of Vis-TiO_2 thin film photocatalysts prepared by an RF-MS deposition method.

3.5 References

1. Hoffmann M.R., Martin S.T., Choi W.Y., Bahnemann D.W., Chem. Rev., 95, 69 (1995).
2. Pelizzetti E., Schiavello M., Eds., Kluwer Academic Publ., Dordrecht (1991).
3. Calzaferri G., Solar Energy Materials and Solar Cells, Elsevier, Amsterdam (1995).
4. Fujishima A., Honda K., Nature, 238, 37 (1972).
5. Takeuchi M., Anpo M., Hirao T., Itoh N., Iwamoto N., Hyomen Kagaku, 22, 561 (2001).
6. Anpo M., Takeuchi M., J. Catal., 216, 505 (2003).
7. Kitano M., Tsujimaru K., Anpo M., Topics Catal., 49, 4 (2008).
8. Kitano M., Takeuchi M., Matsuoka M., Thomas J.M., Anpo M., Catal. Today 120, 133 (2007).
9. Kitano M., Tsujimaru K., Anpo M., Appl. Catal. A-Gen., 314, 179 (2006).
10. Matsuoka M., Kitano M., Takeuchi M., Anpo M., Thomas J.M., Topics Catal., 35, 305 (2005).
11. Zou Z.G., Ye J.H., Sayama K., Arakawa H., Nature, 414, 6864 (2001).
12. Maeda K., Teramura K., Lu D.L., Takata T., Saito N., Inoue Y., Domen K., Nature, 440, 295 (2006).
13. Maeda K., Teramura K., Lu D.L., Takata T., Saito N., Inoue Y., Domen K., Angew. Chem. Int. Ed., 45, 7806 (2006).
14. Sasaki Y., Iwase A., Kato H., Kudo A., J. Catal., 259, 133 (2008).

15. Higashi M., Abe R., Ishikawa A., Tanaka T., Ohtani B., Domen K., Chem. Lett. 37, 138 (2008).
16. Sayama K., Mukasa K., Abe R., Abe Y., Arakawa H., J. Photochem. Photobiol. A-Chem., 148, 71 (2002).
17. Torimoto T., Fox R. J., Fox M. A., J. Electrochem. Soc., 143, 3712 (1996).
18. Ikeda S., Sugiyama N., Murakami S., Kominami H., Kera Y., Noguchi H., Uosaki K., Torimoto T., Ohtani B., Phys. Chem. Chem. Phys., 5, 778 (2003).
19. Asahi R., Morikawa T., Ohwaki T., Aoki K., Taga Y., Science, 293, 269 (2001).
20. Kitano M., Funatsu K., Matsuoka M., Ueshima M., Anpo M., J. Phys. Chem., 110, 25266 (2006).

Chapter 4

Photocatalytic Decomposition of Water on Double-layered Visible Light-responsive TiO_2 Thin Films Prepared by a Magnetron Sputtering Deposition Method

4.1 Introduction

The conversion of clean and abundant sunlight or solar energy into environmentally clean and sustainable chemical energy is the focus of much attention due to the adverse effects of global pollution and energy shortages in recent years. To address these problems, photocatalysis on semiconducting materials has been an intensive area of research since the pioneering work of Honda and Fujishima [1,2], which deals with the stoichiometric photodecomposition of water into H_2 and O_2 as eco-friendly and renewable energy. In the system reported by Honda et al, the reaction was conducted using a photoelectrochemical cell consisting of a TiO_2 and Pt electrodes with an electrochemical bias under UV light irradiation. However, because of the large band gap of TiO_2 (3.20 eV), only a small UV fraction of solar light that reaches the earth can be utilized. Therefore, the development of visible light-responsive TiO_2 photocatalysts is strongly desired. Chemical doping of TiO_2 with transition metal ions or oxides [3,4], the implantation of TiO_2 with transition metal ions under applied high voltage [5-7] and anion doping of N [8-10], S [11] and C [12] ions have been investigated to narrow the band gap of TiO_2. Most of these studies have been attempted with powdered photocatalysts. However, thin film photocatalysts have shown good results, especially for the water splitting reaction since it allows the separate evolution of pure H_2 gas that can be directly utilized as fuel. Various techniques such as sol-gel [13], spray pyrolysis [14] and chemical vapor deposition [15] methods have also been used for the fabrication of TiO_2 thin films photocatalysts. One of the most promising is the sputtering deposition method.

Previously, we have reported the successful preparation of visible light-responsive TiO_2 thin film (Vis-TiO_2) with a radio-frequency magnetron sputtering (RF-MS) deposition method, where TiO_2 deposition was carried out at a high substrate temperature (873 K) under pure Ar gas atmosphere using a TiO_2 plate as the target material [16-19]. SEM investigations have shown that Vis-TiO_2 deposited on various conductive substrates (ITO, Ti foil) consists of large columnar TiO_2 crystallites growing perpendicular to the conductive substrates. This unique film structure allows the efficient contact of the TiO_2 crystallites with the reactant molecules, thus leading to an increase in the reaction efficiency. However, at the same time, the unique film structure enables the direct and facile contact of the reactant molecules with the conductive substrate (ITO, Ti foil) under Vis-TiO_2, which can decrease the reaction rate due to the back electron transfer from the conductive substrate (ITO, Ti foil) to the reactant molecules or electrolyte. Recently, it has been reported that the introduction of a dense block layer between the conductive substrate and roughly structured TiO_2 thin film photocatalyst (such as nanocrystalline and microtube-structured TiO_2 thin films) prevents the back electron transfer process, thus enhancing the photoelectrochemical performance of TiO_2 thin films [20-22]. In the present work, we have prepared a unique double-layered visible light-responsive TiO_2 thin film on a Ti foil substrate (DL-TiO_2/Ti) upon which the UV light-responsive TiO_2 thin film (UV-TiO_2) was introduced as the block layer between the conductive Ti foil substrate and Vis-TiO_2. Dense and flat-structured UV-TiO_2 can be a suitable block layer to prevent the back electron transfer process, leading to an enhancement of the photoelectrochemical property and photocatalytic activity of TiO_2 thin films. Moreover, the thickness of the UV-TiO_2 as an inner block layer was optimized and

the relationship between the thickness of the inner layer (UV-TiO_2) and photoelectrochemical and photocatalytic properties of DL-TiO_2/Ti were also investigated.

4.2 Experimental

Various TiO_2 thin films were prepared on a Ti foil substrate (Nilaco, 50μm thickness) by the RF-MS deposition method using a TiO_2 plate (High Purity Chemicals Lab., Corp., Grade: 99.99 %) as the source material and Ar gas (99.995 %) as the sputtering gas. The base vacuum pressure and working pressure were set at 7.0×10^{-4} and 2.0 Pa, respectively. The substrate was placed parallel to the sputtering target surface with a substrate-target distance of 75 mm. Two different TiO_2 thin films were prepared by changing the substrate temperature during the deposition process. A UV light-responsive TiO_2 thin film (UV-TiO_2) which absorbs only UV light of wavelengths shorter than 380 nm was deposited on the Ti foil substrate (UV-TiO_2/Ti) at a substrate temperature (Ts) of 473 K and RF power of 300 W [18]. A visible light-responsive TiO_2 thin film (Vis-TiO_2) which absorbs visible light was prepared at a Ts of 873 K and RF power of 300 W [18]. A double-layered visible light-responsive TiO_2 thin film was prepared on a Ti foil substrate (DL-TiO_2/Ti) by sequential deposition method under different substrate temperature. DL-TiO_2/Ti consists of three components: (1) the Ti foil substrate; (2) UV-TiO_2 deposited as the inner block layer on the Ti foil substrate; and (3) the Vis-TiO_2 deposited as the outer layer. Here, the thickness of UV-TiO_2 as the inner layer was varied from 50 nm to 150 nm, while the thickness of Vis-TiO_2 as the outer layer was kept constant at 3 μm. These were denoted as DL-TiO_2(X)/Ti, where X indicates the thickness (nm) of UV-TiO_2 as the

inner layer. A single-layered Vis-TiO_2 thin film (film thickness: 3 μm) deposited directly on the Ti foil substrate was denoted as SL-TiO_2 (0)/Ti.

The cross-sectional morphologies of DL-TiO_2(X)/Ti were examined by field emission scanning electron microscopy (FE-SEM, S-4500, Hitachi). The crystal structure of the DL-TiO_2(X)/Ti and SL-TiO_2 (0)/Ti electrodes were investigated by X-ray diffraction analysis (XRD, XRD-6100, Shimadzu). The photoelectrochemical properties of the DL-TiO_2(X)/Ti and SL-TiO_2(0)/Ti electrodes were investigated with a potentiostat (HZ3000, Hokuto Denko) having a three-electrode cell that consists of the thin film electrode, a Pt electrode and saturated calomel electrode (SCE) as the working, counter, and reference electrodes, respectively. The electrolyte was a 0.25 M K_2SO_4 solution mechanically stirred and degassed by purging with 99.99 % pure Ar gas before and during the experiment. The light sources were a solar simulator (PEC-L 11, Peccell Technologies, Inc.) or a 500 W Xe arc lamp (USHIO) and their light intensities were measured at 100mW/cm2 and 950.1 mW/cm^2, respectively, using a laser power meter (OPHIR, Nova II). The incident photon to current conversion efficiency (IPCE) was defined as the number of electrons collected per incident photon using the following equation [19]:

$$IPCE = (i_{ph}/e)/(\lambda P/hc)$$

where i_{ph} (A/cm^2) is the photocurrent density, e is the elementary charge, λ (nm) is the irradiation wavelength, P (W/cm^2) is the light power density, h is the Plank's constant and c is the velocity of light. Usually IPCE is given in percent and therefore:

$$IPCE\ (\%) = 1{,}240 \times i_{ph} / (\lambda P) \times 100$$

Light irradiation was carried out using a 500 W Xe arc lamp with two types of

interference filters (k_{max} = 360 nm, half width: 22.9 nm; k_{max} = 420 nm, half width: 11.7 nm). The incident light intensity (I_{inc}) was measured by a laser power meter (I_{inc}: 378 μW/cm^2 at k = 360 nm, 787 μW/cm^2 at k = 420 nm).

The photocatalytic activities of DL-TiO_2(X)/Ti and SL-TiO_2 (0)/Ti were investigated by the separate evolution of H_2 and O_2 from water using an H-type glass cell connected to a conventional vacuum system. The back side of DL-TiO_2(X)/Ti or SL-TiO_2(0)/Ti, where the Ti foil substrate surface is exposed, was deposited with Pt by a RF-MS deposition method using a RF power of 70 W under a substrate temperature of 298 K and this device was denoted as DL-TiO_2(X)/Ti/Pt or SL-TiO_2(0)/Ti/Pt, respectively. The H-type glass cell consists of two aqueous phases (TiO_2 side: 1.0 M $NaOH_{aq}$; Pt side: 0.5 M $H_2SO_{4\ aq}$) separated by the TiO_2 thin film device and Nafion film as a proton-exchange membrane. Prior to the reactions, the reaction cell was de-aerated by purging with 99.99 % pure Ar gas for 5 h and then the Ar pressure within the reaction cell is adjusted to 98 kPa to prevent overpressure problem. Light irradiation was carried out under white light (100 mW/cm2) using a solar simulator (PEC-L 11, Peccell Technologies, Inc.) and the evolved H_2 and O_2 were analyzed by a gas chromatograph (GC, G2800-T, Yanaco) with a thermal conductivity detector (TCD).

4.3 Results and Discussion

Figure 4.1 shows the FE-SEM image of the cross-sectional morphology of DL-TiO_2 (100)/Ti. The thickness of Vis-TiO_2 and UV-TiO_2 were determined to be approximately 3 μm and 100 nm, respectively. It can be seen that UV-TiO_2 has a dense and structureless morphology, while Vis-TiO_2 has a rough morphology with a

columnar structure growing perpendicular to the substrate. The XRD patterns of DL-TiO_2(X)/Ti, SL-TiO_2 (0)/Ti and UV-TiO_2/Ti are shown in Fig.4. 2 and it can clearly be seen that UV-TiO_2/Ti with 3 μm thickness mainly consists of an anatase phase. On the other hand, SL-TiO_2 (0)/Ti mainly consists of a rutile phase, while the concentration of the anatase phase for DL-TiO_2(X)/Ti increases with an increase in the film thickness of UV-TiO_2 as the inner block layer. It should be noted that the film thickness of UV-TiO_2 (less than 150 nm) as the inner layer for DL-TiO_2(X)/Ti is too thin to be detected as well-defined XRD peaks, that is, the XRD patterns observed for DL-TiO(X)/Ti are essentially originated from Vis-TiO_2 (3 □m) which is considerably thicker than UV-TiO_2.

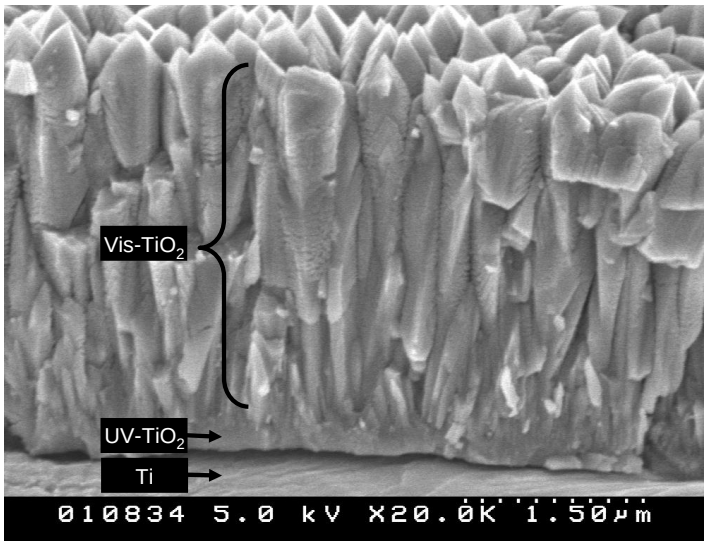

Fig.4.1. FE-SEM image of the cross-sectional morphology of DL-TiO_2(100)/Ti.

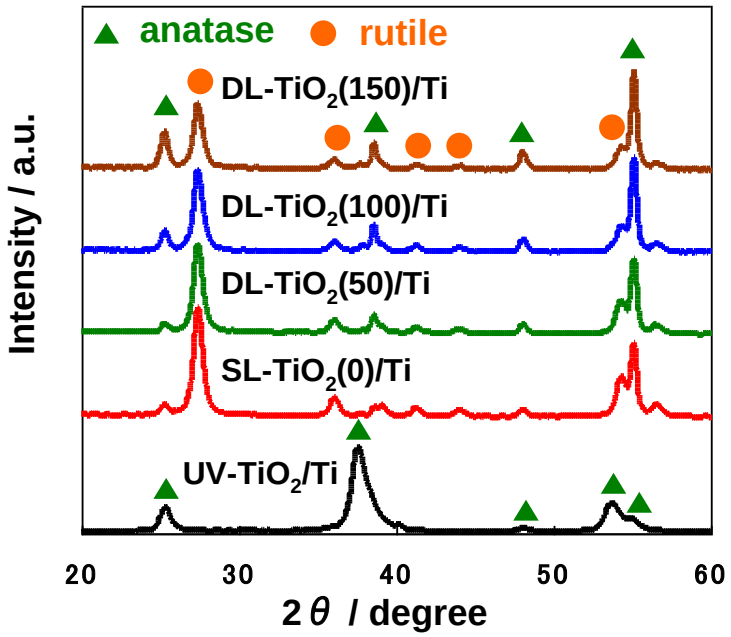

Fig. 4.2. XRD patterns of DL-TiO_2(X)/Ti (X = 50, 100, 150), SL-TiO_2 (0)/Ti and UV-TiO_2/Ti. (Film thickness of UV-TiO_2 for UV-TiO_2/Ti: 3 μm)

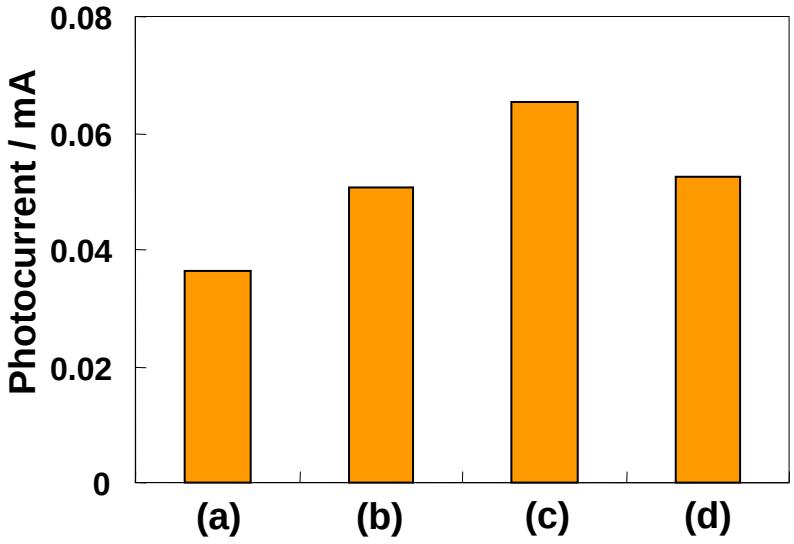

Fig. 4.3. Anodic photocurrents of various DL-TiO_2(X)/Ti and SL-TiO_2(0)/Ti electrodes under white light irradiation from a solar simulator. Measurements were performed under a bias of 1.0 V vs. SCE. (a) SL-TiO_2(0)/Ti, (b) DL-TiO_2(50)/Ti, (c) DL-TiO_2(100)/Ti, (d) DL-TiO_2(150)/Ti

These results clearly show that the phase composition of Vis-TiO_2 as the outer layer is affected by the presence of UV-TiO_2 between Vis-TiO_2 and the Ti foil substrate.

The correlation between the thickness of UV-TiO_2 as an inner block layer and the photoelectrochemical properties of the DL-TiO_2(X)/Ti electrodes were investigated. As shown in Fig. 4.3, the photoelectrochemical properties of various DL-TiO_2(X)/Ti and SL-TiO_2(0)/Ti electrodes were investigated by a three-electrode cell with a bias of 1.0 V vs. SCE in an aqueous solution of 0.25 M K_2SO_4 under white light irradiation from a solar simulator. The observed photocurrent corresponds to the anodic oxidation of water to oxygen by the photoformed holes on these electrodes. The photocurrent increased with an increase in the film thickness of UV-TiO_2 as the inner block layer and reached a maximum at 100 nm. This increase in the photocurrent can be ascribed to the fact that the dense UV-TiO_2 as the inner layer reduces the leakage current, i.e., the current due to the electron transfer from the Ti metal substrate to water or oxygen, by preventing the facile and direct contact of the conductive Ti metal substrate and water or oxygen to form the H_2 or O_2- adsorbed species, respectively [20]. Furthermore, it was found that the anodic photocurrent decreases when the film thickness of UV-TiO_2 exceeds 100 nm, suggesting that the thick UV-TiO_2 layer (about 150 nm) acts as a barrier layer to prevent efficient electron transfers from Vis-TiO_2 to the Ti metal substrate, thus increasing the charge recombination rate of the photo-formed electrons and holes [21,22]. It can be considered that the contact between anatase (UV-TiO_2) and rutile (Vis-TiO_2) phases is not the major factor to facilitate the charge separation because the conduction band of UV-TiO_2 is higher than Vis-TiO_2, i.e., anatase-rutile contact can bring negative effect

for charge separation [23]. The main origins of the visible light activity of DL-TiO_2(X)/Ti electrodes can be ascribed to Vis-TiO_2 outer layer, since the O/Ti ratio of the Vis-TiO_2 thin film gradually decreases from the top surface (O/Ti ratio of 2.00) to the inside bulk (O/Ti ratio of 1.93). Such an anisotropic morphology of Vis-TiO_2 thin film could modify the electronic properties of the thin films leading to the changes in the band gap energy [18].

The photocurrent responses of the DL-TiO_2 (100)/Ti electrode as a function of the cut-off wavelength were investigated with an applied bias of 1.0 V vs. SCE in an aqueous solution of 0.25 M K_2SO_4. A 500 W Xe arc lamp was used for the light source and the incident light wavelength was controlled using different cut-off filters.

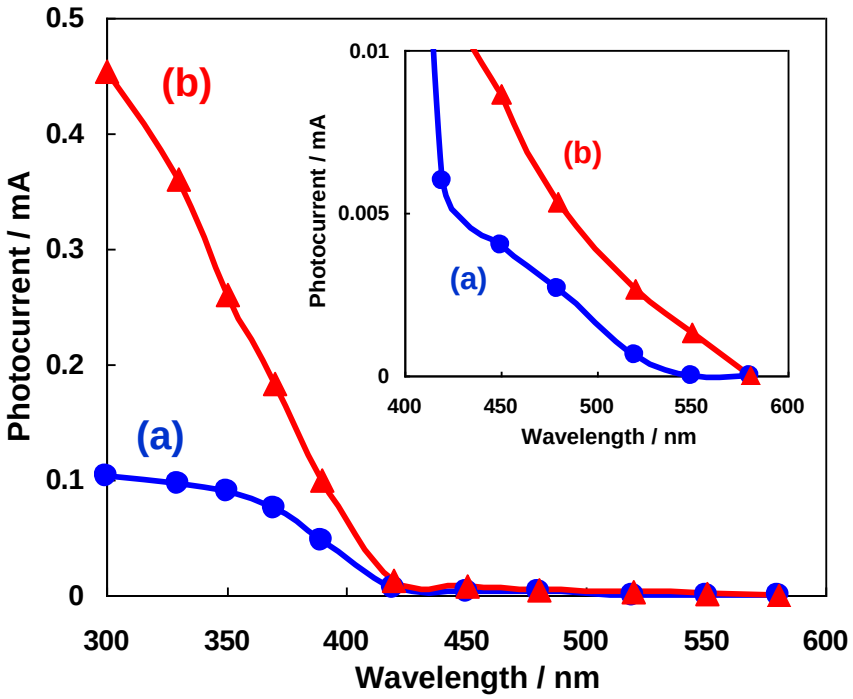

Fig. 4.4. The relative photocurrent as a function of the cut-off wavelength of the incident light for: (a) SL-TiO_2(0)/Ti electrode and (b) DL-TiO_2(100)/Ti electrode measured in 0.25 M K_2SO_4 aqueous solution at 1.0 V vs. SCE. Inset shows the expanded plots in visible regions.

Table 4.1. IPCEs of SL-TiO_2(0)/Ti and DL-TiO_2(100)/Ti electrodes measured in 0.25 M K_2SO_4 aqueous solution at 1.0 V vs. SCE.

Electrode	IPCE (%)	
	λ = 360nm	λ = 420nm
SL-TiO_2(0)/Ti	40	4.4
DL-TiO_2(100)/Ti	58	6.1

As shown in Fig. 4.4, both the SL-TiO_2(0)/Ti and DL-TiO_2(100)/Ti electrodes exhibited photocurrent responses in wavelengths regions shorter than 520 nm. Moreover, a significant increase in the photocurrent was observed for DL-TiO_2(100)/Ti under both UV and visible light irradiation as compared to SL-TiO_2(0)/Ti. The determined IPCEs at 1.0V vs. SCE are summarized in Table 4.1. It can clearly be seen that DL/TiO_2 (100)/Ti exhibits higher IPCEs than SL-TiO_2(0)/Ti under both UV (360 nm) and visible light (420 nm) irradiation.

The photocatalytic activities of two different TiO_2 thin film devices (SL-TiO_2(0)/Ti/Pt and DL-TiO_2(100)/Ti/Pt) were investigated by the separate evolution of H_2 and O_2 from water by using an H-type glass cell, as shown in Fig. 4.5. The Nafion film provides the electrical connection between the two reaction vessels while keeping the two solutions separate while also allowing electron transfers between the two vessels. The TiO_2 side of TiO_2 thin film device was immersed in 1.0 M NaOH solution and the Pt side was immersed in 0.5 M H_2SO_4 aqueous solution in order to

add a small chemical bias (0.826 V) to assist the electron transfer from the TiO_2 side to the Pt side through the Ti foil substrate. Figure 4.6 shows the reaction time profile of the separate evolution of H_2 and O_2 under white light irradiation from a solar simulator. Water was separately decomposed into H_2 and O_2 on DL-TiO_2 (100)/Ti/Pt and the H_2 evolution rate was estimated to be about 7.6 μmol h-1. The evolution rate of H_2 and O_2 slightly declined against reaction time, but the reason of the depletion is under investigation. However, the turnover number (TON = (mole of evolved H_2 during the reaction) / (mole of TiO_2 in DL-TiO_2(100)/Ti/Pt)) was calculated to be 3.29, indicating that this reaction proceeded photocatalytically. The ratio of the evolution rate of H_2 and O_2 (H_2/O_2) was higher than the stoichiometric value of 2.0. This can be ascribed to the adsorption of evolved O_2 onto the surface of TiO_2 thin film or any side reactions such as the formation of H_2O_2 at the anode side, although details are under investigation. SL-TiO_2(0)/Ti/Pt shows lower activity than DL-TiO_2(100)/Ti/Pt and the evolution rate of H_2 on SL-TiO_2(0)/Ti/Pt was determined to be at about 3.7 μmol h-1. It should be noted that DL-TiO_2(100)/Ti/Pt exhibited 2.1 times higher photocatalytic activity than SL-TiO_2(0)/Ti/Pt although DL-TiO_2(100)/Ti electrode exhibited 1.5 times (λ > 360 nm) and 1.4 times (λ > 420 nm) higher IPCE values than SL-TiO_2(0)/Ti electrode. These differences between photocatalytic activity and IPCE values can be originated from the difference in the light source and light intensity used for the each experiment. The total solar energy conversion efficiency (η) of DL-TiO_2 (100)/Ti/Pt in the presence of an external applied potential was 0.17 %, as determined by the following equation [12]:

$$\eta(\%) = \frac{100j(1.23 - E_{app})}{I_0} \qquad (4.1)$$

Where j is the current density (mA/cm^2) estimated from the H_2 evolution rate, E_{app} is the applied chemical bias (0.826 V) and I_0 is the intensity of the incident light (mW/cm^2). It was, thus, clearly demonstrated that the deposition of UV-TiO_2 as the inner block layer between the Ti metal substrate and Vis-TiO_2 as the outer layer is an effective method in improving the photocatalytic performance of the SL-TiO_2(0)/Ti/Pt thin film device. Its high performance can be ascribed to the decrease in the back electron transfer from the Ti foil substrate to water to form H_2 by the reduction of H^+, or to O_2 for form reduced oxygen, the O^{2-} species on the TiO_2 side, as suggested by the results of anodic photocurrent measurements (Fig. 4.3).

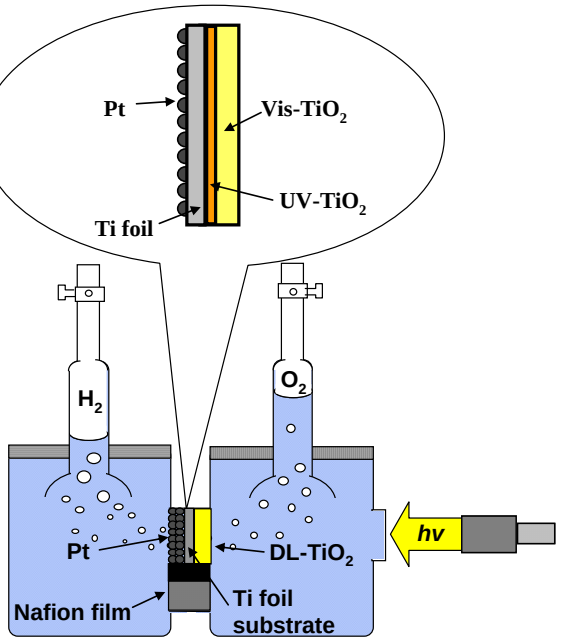

Fig. 4.5. H-type glass cell for the separate evolution of H_2 and O_2 using DL-TiO_2(X)/Ti thin films (TiO_2 side: 1.0 M NaOH aq; Pt side: 0.5 M H_2SO_4 aq).

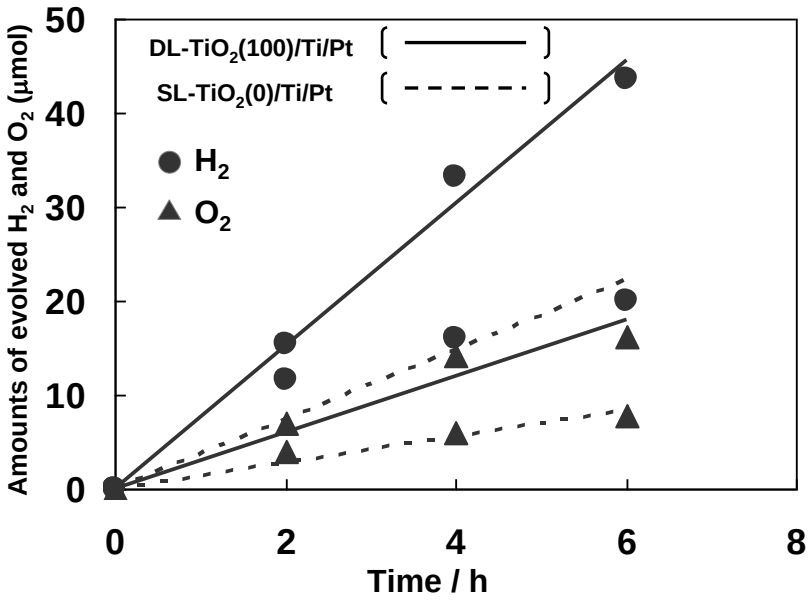

Fig. 4. 6. Reaction time profiles of the separate evolution of H_2 and O_2 under white light irradiation from solar simulator on DL-TiO_2(100)/Ti/Pt and SL-TiO_2(0)/Ti/Pt in an H-type glass cell. Irradiation area: 7 mm × 12 mm

4.4 Conclusions

A unique double-layered visible light-responsive TiO_2 thin film (DL-TiO_2/Ti) was prepared by an RF-MS method. Its photoelectrochemical performance was found to vary depending on the film thickness of UV-TiO_2 which was used as the inner block layer deposited between the Ti foil substrate and Vis-TiO_2 as the outer layer. Investigations determined the optimal film thickness of UV-TiO_2 for efficient performance to be 100 nm. Enhancement of the photoelectrochemical performance can be attributed to a decrease in the back electron transfer from the Ti foil substrate to water to form H_2 by the reduction of H^+ or to O_2 to form reduced oxygen, O^{2-}, at the TiO_2 side. In conclusion, a DL-TiO_2 thin film device (DL-TiO_2/Ti/Pt) was prepared and applied for the separate evolution of H_2 and O_2 from water using an H-type glass cell. DL-TiO_2 (100)/Pt/Ti was found to show higher performance than SL-TiO_2 (0)/Pt/Ti for the separate evolution of H_2 and O_2 from H_2O under white light irradiation from a solar simulator, suggesting that the deposition of UV-TiO_2 as an inner block layer between the Ti metal substrate and Vis-TiO_2 as the outer layer is an efficient method in improving the photocatalytic performance of SL-TiO_2 (0)/Ti/Pt.

4.5 References

1. Fujishima A., Honda K., Bull. Chem. Soc. Jpn., 44, 1148 (1971).
2. Fujishima A., Honda K., Nature, 238, 37 (1972).
3. Choi W.Y., Termin A., Hoffman M.R., J. Phys. Chem. 84, 13669 (1994).
4. Anpo M., Ichihashi Y., Takeuchi M., Yamashita H., Res. Chem. Intermed. 24,143(1998).
5. Anpo M., Takeuchi M., Kishiguchi S., Yamashita H., H. Surf. Sci. Jpn. 20, 60 (1999).
6. Yamashita H., Ichihashi Y., Takeuchi M., Kishiguchi S., Anpo M., J. Synchrotron Rad., 6,451(1999).
7. Yamashita H., Harada M., Misaka J., Takeuchi M., Ikeue K., Anpo M. J. Photochem. Photobiol. A., 148, 257(2002)
8. Asahi R., Morikawa T., Ohwaki T., Aoki K., Taga Y., Science 293, 269 (2001).
9. Irie H., Washizuka S., Yoshino N., Hashimoto K., Chem. Commun., 1298 (2003).
10. Diwald O., Thompson T.L., Goralski E.G., Walck S.D., Yates J.T., J. Phys. Chem. B, 108,52 (2004).
11. Umebayashi T., Ymaki T., Itoh H., Asai K., Appl. Phys. Lett., 81, 454 (2002).
12. Khan SUM., Al-Shahry M., Ingler WB Jr., Science 297, 2243 (2002).
13. Hardee KL, Bard A.J., J. Electrochem. Soc., 124,215 (1977).
14. Peng B., Jungmann G., Jäger C., Haarer D., Schmidt H.W., Thelakkat M., Coord. Chem. Rev., 248, 1479 (2001).
15. Yamashita H., Ichihashi Y., Harada M., Stewart G., Fox M.A., Anpo M., J.

Catal., 158, 97 (1996).

16. Song PK., Shigesato Y., Kamei M., Yasui I., Jpn. J. Appl. Phys., 38, 2921(1999).
17. Takeuchi M., Anpo M., Hirao T., Itoh N., Iwamoto N., Surf. Sci. Jpn. 22, 561(2001).
18. Kitano M., Takeuchi M., Matsuoka M., Thomas J.M., Anpo M., Chem. Lett., 34,616 (2005)
19. Long M., Cai W., Kisch H., Chem. Phys. Lett., 461, 102 (2008).
20. Lee T.Y., Alegaonkar P.S., Yoo J.B., Thin Solid Films, 515, 5131 (2007).
21. Peng B., Jungmann G., Jäger C., Haarer D., Schmidt H.W., Thelakkat M., Coord. Chem. Rev., 248, 1479 (2004).
22. Zhao Y., Zhai J., Wei T., Jianga L., Zhua D., J. Mater. Chem., 17, 5084 (2007).
23. Fukumoto S., Kitano M., Takeuchi M., Matsuoka M., Anpo M., Catal. Lett., 127, 39(2009).

Chapter 5

Photocatalytic Degradation of Organic Contaminants in Landfill Leachate Utilizing Visible Light-responsive TiO_2 Thin Film Photocatalyst Under Direct Solar Light Irradiation

5.1 Introduction

Extensive air and water pollution has caused the planet for a long time. As a response to the looming threat, the humankind has been expediting its efforts in pollution reduction. Several approaches are used: to utilize environmentally benign processes, to provide *in-situ* destruction of pollutants during the process, and to decontaminate the air or water stream emanating from the high throughput production facilities.

Water and soil contamination became a serious challenge of human being because of extending agricultural and industrial disposals and entailing advanced industrial processes which make complicated contaminating agents. Lately the planet earth is facing the biggest challenge of its whole life time, with the high rate of economical development, new ecological challenges have been introduced. Almost novel environmental pollution couldn't decompose naturally efficiently, and we face up to the fact that this pollution might endanger every aspects of life on the earth even our life.

Landfilling, which is still the most popular way for solid waste treatment in many countries, despite what are the main aims in landfiling or the nature of wastes matter, causes serious pollution of its surrounding environments. Leachate produced from landfill contains large quantities of organic and inorganic matters, and heavy metals. Heterogeneous photocatalysis could be applied for the removal of these matters. As described above, in photocatalytic process, hydroxyl radicals can be generated when the photocatalyst, such as TiO_2, is illuminated and these ultra-reactive species lead to

successful mineralization of pollutants to H_2O, CO_2, and other minerals. The studies for the elimination of non-biodegradable harmful refractory organic and inorganic components from landfill leachate by their transformation into harmless species, with heterogeneous photocatalysis on TiO_2 had been reported previously. [2].

Scientists are looking seriously to decrease the pollution with utilizing environment friendly processes and try to eliminate the pollution which entered the environment.

A novel method of wastewater disinfection tends to use photocatalytic decomposition of water contaminants. It is mainly based upon highly reactive intermediates generation utilizing photon excited photocatalysts. The treatment of industrial polluted water before discharge to prevent the quality of natural water body from deterioration and to meet regulatory requirements continues to be a significant challenge of environmental protection. In the field of wastewater treatment, many kinds of technologies in the areas of chemistry, physics, and even biochemistry have been applied under the considerations of economics and practicability. Recently, considerable interest has been shown by researchers all over the world in the application of photocatalysis assisted by titanium dioxide TiO_2 for the destruction of organic and inorganic contaminants in aqueous streams.

Many literatures have reported that a lot of toxic or hazardous industrial chemicals could be destroyed by this novel technique. However, even faster decomposition is needed to carry out the oxidation at the commercial level.

Photocatalysis is a relatively new technique of decontamination of polluted aqueous streams. For the early attempts, as described in the previous parts of this thesis, photocatalysis were developed as a possible tool for photochemical conversion

of energy. Recently, photocatalytic processes are rapidly developing in the field of degradation of pollutants. Therefore, novel methods of water and wastewater disinfection tend to use photocatalytic decomposition of contaminants. It is mainly based upon highly reactive intermediates generation as hydroxyl radicals ($^{\cdot}OH$) utilizing photon excited photocatalysts. Since then, it has drawn considerable academic interest as a very attractive, convenient process for the degradation of organic pollutants [2, 3].

However, it has found a very limited degree commercialization [4]. This trend is primarily related to the low reaction rates exhibited by commonly known photocatalysts. Recently, we have undertaken extensive studies of photocatalytic techniques assisted by Vis-TiO_2 for the removal of organic and inorganic contaminants from aqueous landfill leachate stream. As reported before, the unique kind of visible light-responsive TiO_2 (Vis-TiO_2) thin films has been developed in this research group using radio frequency magnetron sputtering (RF-MS) deposition method by optimizing operational parameters (See chapter 2). During recent years many investigations had been done to increase the photocatalytic activity of mentioned and exploiting it in better applicable processes.

Aims of this work are to investigate the photocatalytic degradation of landfill leachate treatment with our previously moderated Vis-TiO_2 photocatalyst irradiated with direct sunlight. We have considered the removal of COD and TOC, meanwhile of the toxic chemical decomposition,

Semiconductors can provide light-induced charges for redox processes, which is primarily due to their electronic configuration [2]. In particular they are characterized by a filled valence band and empty conduction band [5]. The elementary mechanism

of photocatalytic transformation includes a number of steps, which have been exhaustively described in the literature [2, 6]. All photocatalysts must possess semiconducting properties in order to be able to perform photoinduced reactions. A simplified diagram of the Photocatalytic mechanism is presented in the following chart.

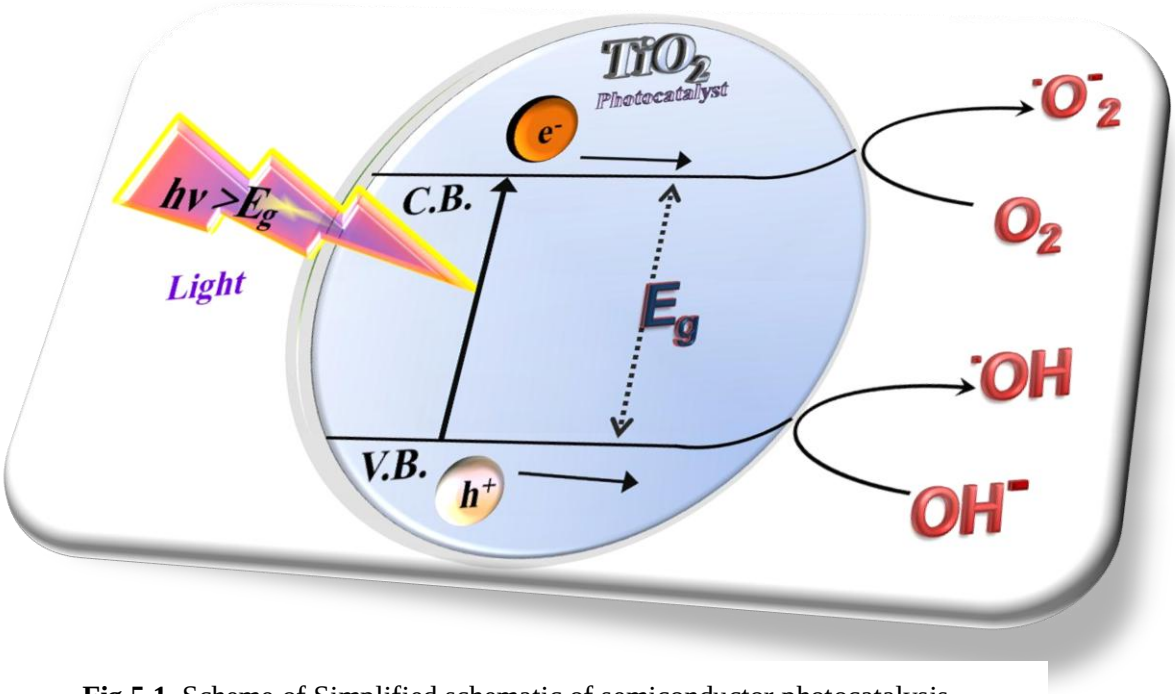

Fig.5.1. Scheme of Simplified schematic of semiconductor photocatalysis

Oxygen is crucial for photooxidation of organic compounds. [13, 14] From studies on the (110) surface of rutile, Lu et al. [15] have determined that oxygen cannot be adsorbed on a defect-free rutile surface. The O_2 hopping rate depends on the number of oxygen vacancies in TiO_2, and the latter also determines the density of conduction electrons. [16] Thus, electrons created in the interior of a rutile particle following light absorption, cannot be efficiently transferred to surface O_2 due to an insufficient concentration of active oxygen vacancies on particle surfaces. The result is a high

electron-hole recombination rate, thus limiting [11, 17-19] the activity of rutile for organic photooxidation [11, 20].

Harvesting sunlight efficiently needs novel technologies and trends to achieve a satisfactory active photocatalysts which can operate with visible light rather than UV light. Visible light responsive TiO_2 thin films produced by RF-magnetron sputtering method, the characteristics of produced TiO_2 thin films compared with common UV-TiO_2 thin films and among the parameters which has most influence on photocatalytic activity.

The main tasks of this research can be focused on two aspects: visible light responsive TiO_2 thin films production, characterization and then investigating the decomposition of organic pollutants as methylene blue and organic leached compounds in landfill for photocatalytic properties of the produced films. In this chapter, the engineered Vis-TiO_2 thin films were prepared by RF magnetron sputtering methods as described in chapter 2.

5.2 Experimental

5.2.1 Thin Film Preparation

Experiments were carried out using a RF magnetron sputtering made by O-Naru Tech Inc. with 100 mm diameter target and RF power supply with a 13.56-MHz frequency and maximum 500 W power was used to excite the plasma. The TiO_2 thin films were prepared by RF-MS method using TiO_2 target plate (High Purity Chemicals Lab., Corp., Grade: 99.99 %) as the source material and Ar gas (99.995 %) as the sputtering gas. The quartz substrates with dimensions of 45mm×45mm were positioned and fixed in the center of a substrate holder parallel with the target with

different target-to-substrate distance $D_{T\text{-}S}$ of 80 mm. The chamber was evacuated to less than 6.5×10^{-4} Pa before introducing of Ar sputtering gas, Chamber pressure held at a fixed value 2.0 Pa. Before each run, the target was pre-sputtered in argon gas for at least 10 min to clean up its surface from any unwanted contaminants. To keep uniform deposition during the sputtering time, the substrate holder plate was kept rotating at 5 r min^{-1}. The induced RF power of 300 W with the substrate temperature held at a fixed value of 873 K for Vis-TiO_2 thin films has been used. For making of UV-TiO_2 thin films substrate temperature were fixed on 473 K. The film thickness was adjusted to about 2 μm by controlling the deposition time for 200 min. The weight of deposited TiO_2 per unit area of quartz substrates was roughly estimated to be 0.78 mg/cm^2 from the film thickness and the specific gravity of anatase phase (3.9 g/cm^3).

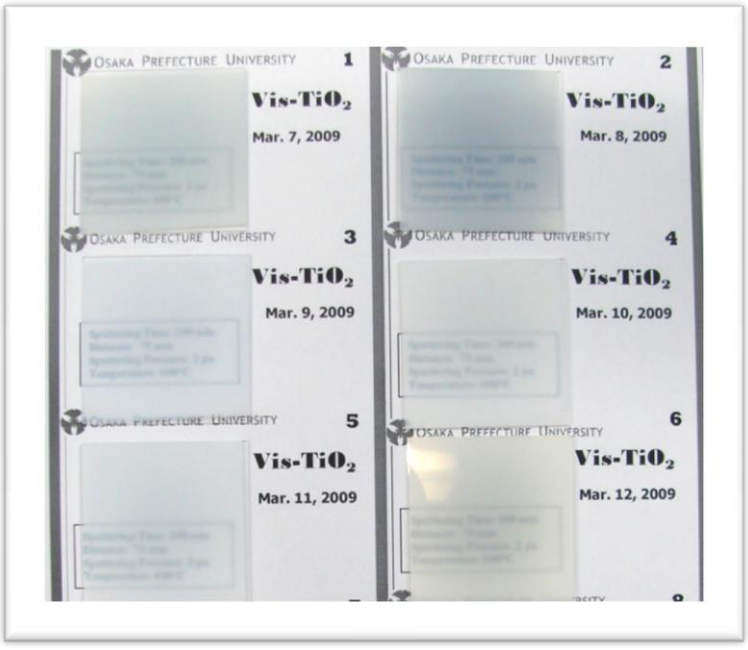

Fig. 5.2. Produced Visible light responsive TiO_2 thin films, Vis-TiO_2 on quartz substrate（4.5cm×4.5cm）

Figure 5.3 represents the X-ray diffraction pattern of the Sputtered Vis-TiO_2 thin

film on quartz. Corresponding to the peaks, it shows Vis-TiO_2 thin film on quartz almost crystal ratio of anatase (A) phase.

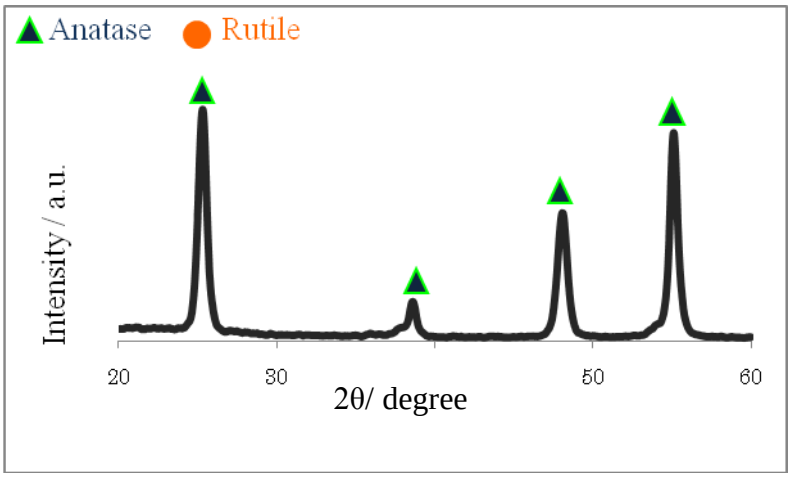

Fig.5. 3. The diffraction peaks agree with those of TiO_2 in the dominant anatase peaks at 2θ = 25.3°, 38.5°, 48° and 55°

5.2.2 Photocatalytic Activity

To assure that the Vis-TiO_2 thin films has photocatalytic activity on solar irradiation; three sets of preliminary tests have been conducted. The first sets tests utilise methylene blue as a model organic composition, while two other sets are used to test the photocatalytic activity of the synthesized Vis-TiO_2 to decompose extracted landfill leachates. The photocatalytic activity of the Vis-TiO_2 thin films is evaluated by measuring the changes in absorption of the methylene blue "MB" solution at 660 nm during photocatalytic decomposition, upon irradiation with bare direct sunlight.

Pyrex Dishes with 6.6 cm diameter were used as reaction cells for all of experiments; in each cell 25 ml of aqueous solution added, as it shown in the photos of Fig 5.4, for each reaction cell which contained a Vis-TiO_2 thin film catalyst sheet, other reaction cell which contained a UV-TiO_2 thin film catalyst sheet and a similar counterpart cell with same concentration solution but without catalyst prepared as

witness.

UV/VIS spectrometer recording the spectra of the 660nm was used for the determination of MB concentration to follow its kinetics of disappearance.

The total reaction time for the photocatalytic degradation process is 480 min (6 hrs) in all experiments, under conditions of V_0 = 25ml; methylene blue initial concentration of $[MB]_0$ = 0.001% W; all of Vis and UV-TiO_2 thin films dimensions were 4.5cm × 4.5cm, Temperature of solution were ambient temperature which recorded from 15.9 ℃ to 20.2 ℃of November 5, 2008 - April 30, 2009 .

Fig.5. 4. The outdoor configuration of Pyrex Dishes which used as reaction cells in this research.

5.3 Analytical Methods

Methylene blue (MB) is a brightly colored, blue cationic thiazine dye with maxima of absorbance at 660 (the most prominent). [12] It has often been used as a model compound to test the photocatalytic degradation of organic materials.

The concentrations of diluted samples were determined by measuring the solution absorbance using a UV/VIS spectrophotometer (HITACHI U-2000) equipped with quartz cuvettes of 1-cm light path. The wavelengths used for landfill leachate and methylene blue measured at 250 nm, and 660 nm, respectively. Necessary calibrations were done for spectrophotometric determination of these compounds. Methylene blue, with dye content above 82% and molecular weight 319.86 g/mol, was directly used without further purification.

A LI-250, LI-COR Co. Ltd illuminometer used to measure the sunlight intensity, A TOC-VCSN, Shimadzu Co. Ltd utilized to measure the TOC. And JIS-K0102-17 standard method used for measurement of COD.

Outline of experiments

Target: 0.001% Methylene blue

Solution volume: 25mL

Photocatalysis: Vis-TiO_2 thin films (4.5cm × 4.5cm)

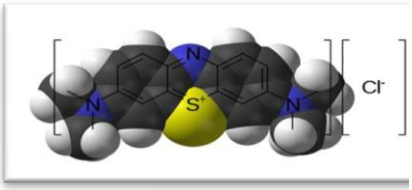

Solar Irradiation time: November 5, 2008 - April 30, 2009 (Total 11 times)

Weather: Sunny

Irradiation time: 10 am to 16 pm (6 hours)

5.3.1 Photodegradation Measurements

Decomposition of Methylene blue – Under sunlight

Like other common organic pollutants, methylene blue can be decomposed under light irradiation and eventually mineralized on visible light responsive TiO_2 thin films into CO_2, NH_4^+, NO_3^- and SO_4^{2-} . Figure 5.5 depicts a series of results where the absorbance values have been presented as a function of time, a) photocatalytic reaction cell with Vis-TiO_2 thin film and b) witness solution. It has been found that the reaction follows an overall first-order kinetics during the photodegradation process.

The visible light leads to the degradation of the dye structure. A very slow rate of degradation was observed in the witness solution which doesn't contain any TiO_2 photocatalyst. Figure 5.5 Also clearly shows that if only methylene blue is treated in the batch reactor, without using any photocatalyst the only in the presence of Vis-TiO_2 thin film, It is, therefore, obvious that catalyzes the reaction efficiently. It is interesting to note that the reaction is catalyzed to a negligible extent if don't utilize any photocatalyst.

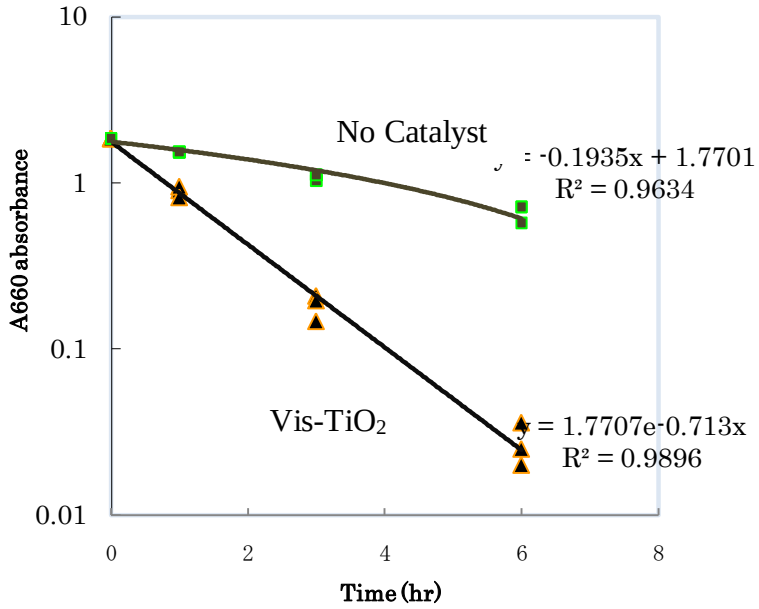

Fig. 5.5 Decomposition of methylene blue under outdoor sunlight condition, a) No catalyst, b) UV-TiO_2, c) Vis-TiO_2

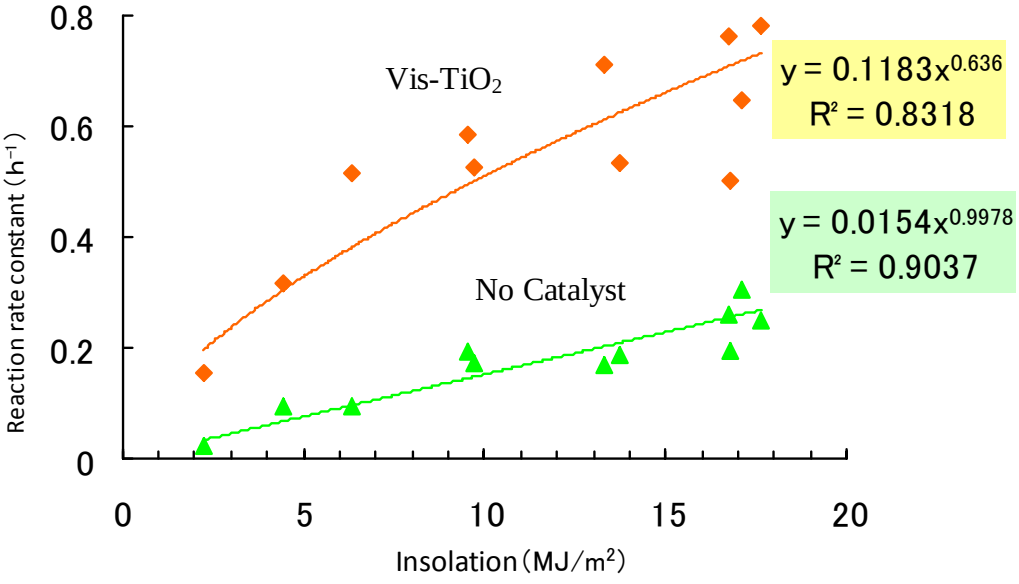

Fig. 5.6 The linear change of reaction rate constant with increasing the light insolation. a) No catalyst, b) Vis-TiO_2

Figure 5.7 shows the decomposition of methylene blue during the irradiation, as it can be see the methylene blue dye concentration decreases linearly with irradiation time.

The decoloration is very slow in the reaction cell which has no photocatalyst and decomposition is on photolysis. For films prepared on moderately temperature which we named it as UV-TiO_2 thin films degradation rate increases compare to the witness sample without any photocatalyst. But as it shown the highest rate of decomposition relates to Vis-TiO_2 thin film which is highly active under visible light.

Fig. 5.7 Decomposition of methylene blue as a function of irradiation time (t) under sunlight Irradiation: (a) Vis-TiO_2 thin film, (b) Vis-TiO_2 thin film, (c) Without catalyst

The comparison of reaction rate is shown in this Figure where the catalytic activity of Vis-TiO_2 thin film is found to play an extremely important role. Such an effect investigated in next section by using landfill leached solution.As it clearly shown about after 6 hours almost all of Methylene blue decomposed and decomposition follows a First order linear reaction. (Fig. 5.6)

Table 5.1 - Amount of organic compound decomposition by time

Processing date No.	Irradiation Amount	A250			COD(mg/L)			TOC(mg/L)		
Day	MJ/m^2	Before	Witness Sol.	Vis-TiO_2	Before	Witness Sol.	Vis-TiO_2	Before	Witness Sol.	Vis-TiO_2
1	9.0	1.199	1.172	1.128	77.2	77.2	71.4	69.0	68.9	68.4
5	34.4	1.199	0.995	0.713	77.2	54.7	45.1	69.0	52.9	42.2
5	77.9	1.059	0.918	0.179	76.8	62.7	27.5	61.6	54.4	20.5
7	76.9	0.878	0.655	0.278	78.8	60.5	33.9	61.6	48.1	26.0
10	70.9	1.199	1.063	0.264	77.2	54.4	29.0	69.0	50.0	22.8
10	167.6	0.878	0.385	0.040	78.8	48.1	14.4	61.6	30.9	5.8

A survey on decomposition of organic landfill leached solution under sunlight irradiation

Decomposition of organic matter in the landfill leached solution under outdoor sunlight condition, was the next part of this research, in this part by outdoor experiments with direct sunlight irradiation, it could be shown that COD and TOC in landfill leachate could be degraded to an significant extent in water and the low capacity of adsorption onto Vis-TiO_2. The contribution of Vis-TiO_2 thin film photocatalyst in diminution of toxics investigated by utilizing witness solution without using any photocatalyst there. As it can be seen in the Figures 5.8 to 5.10,

The reaction rate constants of COD and TOC, however, were very lower than in the presence of Vis-TiO_2 (photocatalysis), when the light source was illuminated in the absence of Vis-TiO_2 (direct photolysis). It means that Vis-TiO_2 ease the decomposition reactions.

Results shown in Table 5.1 illustrated the summary of Figures 5.8 to 5.10.

As it shows in Table 5.1, using Vis-TiO_2, accelerate 2 to 5 times more to break down organic material. Figure 5.11 shows the removal rate of organic matter in the landfill leached solution under outdoor sunlight condition utilizing Vis-TiO_2 thin film, utilizing different total irradiation in different intervals of time.

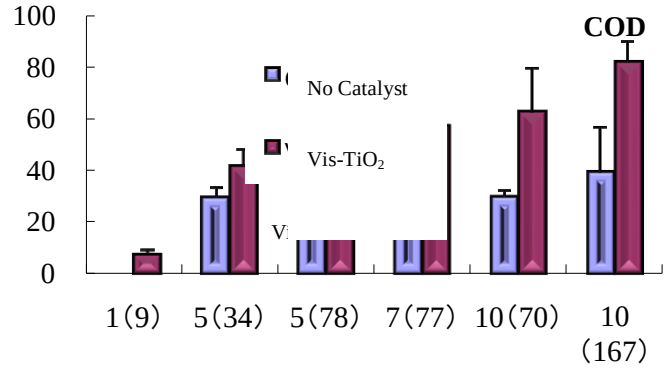

Fig. 5.8 Time-course of COD, during illumination of a landfill leachate containing Vis-TiO_2 thin film (The number in parentheses is total insolation amount) (MJ/m^2)

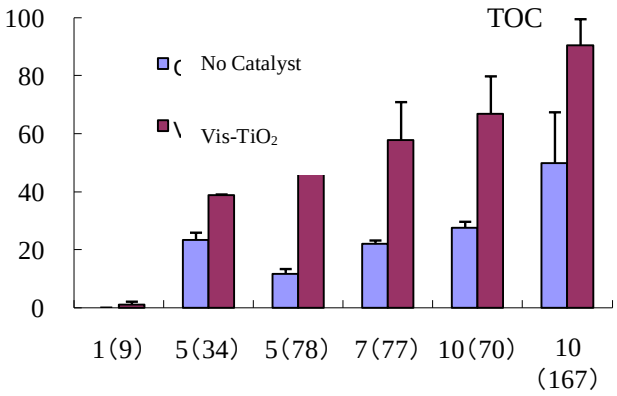

Fig. 5.9 Time-course of TOC during decomposition of organic matter in the landfill leached solution under outdoor sunlight condition, (The number in parentheses is total insolation amount) (MJ/m^2)

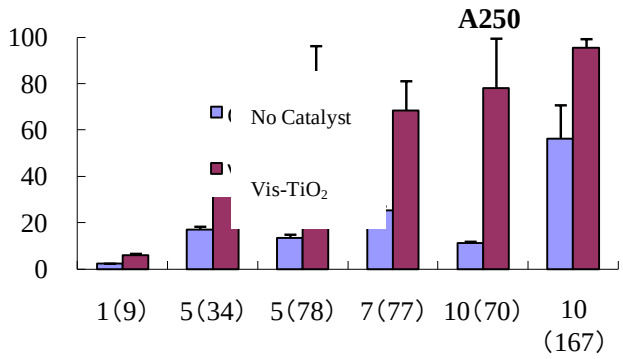

Fig. 5.10 Time-course of A250, during illumination of a landfill leachate containing Vis-TiO_2 thin film (The number in parentheses is total insolation amount) (MJ/m^2)

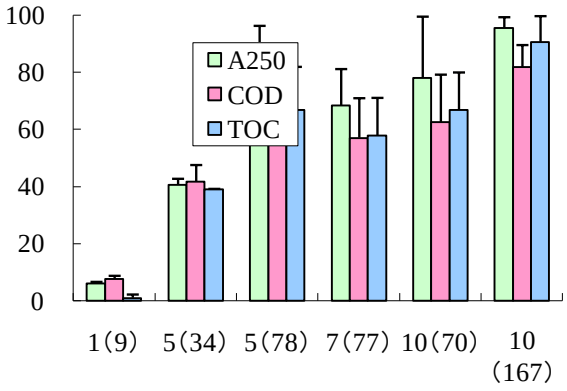

Fig. 5.11 Removal rate of organic matter in the landfill leached solution under outdoor sunlight condition utilizing Vis-TiO_2 thin film, (The number in parentheses is total insolation amount) (MJ/m^2)

5.4 Conclusion:

Design and development of TiO_2 photocatalysts which operate effectively under visible light or solar beam irradiation are required for a large-scale utilization of TiO_2 photocatalysts. However, TiO_2 photocatalysts cannot absorb visible light and only make use of 3–5% of the solar beam that can reach the earth, necessitating the utilization of an ultraviolet light source.

It is, therefore, necessary to develop a photocatalytic system which can be applied under visible and/or solar light irradiation.

In the present study, we deal with the preparation and characterization of visible light responsive TiO_2 thin films (Vis-TiO_2) utilizing RF magnetron sputtering deposition method. The mentioned photocatalysts utilized for photocatalytic degradation of diluted Methylene blue in water and landfill leachate under direct solar irradiation as a model reaction of the photocatalytic purification of landfill leachate or wastewater using solar light. In this study COD, TOC and UV absorbance at a given wavelength (250 nm) of the leachate has been investigated. The results show that as prepared Vis-TiO_2 thin films have great effect on reducing of contaminants concentration, utilizing solar light irradiation.

We have investigated the removal of COD, TOC, and the deposition of nitrogen compounds in landfill leachate. By outdoor experiments with direct sunlight irradiation, it could be shown that COD and TOC in landfill leachate could be degraded to an significant extend in water and the low capacity of adsorption onto Vis-TiO_2.

The contribution of photocatalyst in diminution of toxics investigated by utilizing

of witness solution without using any photocatalyst. The reaction rate constants of COD and TOC, however, were very lower than in the presence of Vis-TiO_2 (photocatalysis), when the light source was illuminated in the absence of Vis-TiO_2 (direct photolysis).

The photocatalytic capability of Vis-TiO_2 thin films was used in this research to treat water polluted by low concentration of methylene blue and landfill leachate for studying the Photocatalyst activity and reaction kinetics.

Experimental data fit quite well with good correlation coefficient values with first order kinetic reaction models.

5.5 References:

1. Bekbölet M., Lindner M., Weichgrebe D., Bahnemann D.W., Solar Energy, 56, 455(1996).
2. Dhananjeyan M.R., Annapoorani R., Renganathan R., J. Photochem. Photobiol. A: Chem., 109, 147(1997).
3. Cho S.P., et al., Appl. Catal. B: Environmental , 39, 125 (2002).
4. Harada M., Tanii A., Yamashita H., Anpo M., Zeitschrift fur Physikalische Chemie, 213, 59(1999).
5. Pelizzetti E., Solar water detoxification, Zeitschrift fur Physikalische Chemie, Bd. 212, S. 207,(1999).
6. Takeuchi M., Sakai S., Ebrahimi A., Matsuoka M., Anpo M., Top. Catal. 52, 1651(2009).
7. Anpo M., 12th International Congress on Catalysis, Proceedings of the 12th , ICC Volume 130, Part 1, 157 (2000).
8. Yamashita H., Harada M., Misaka J., Takeuchi M., Neppolian B., Anpo M., Catal. Today, 84, 191 (2003).
9. Cho S.P., Hong S.C., Hong S.-I., Appl. Catal. B: Environmental, 39 ,125(2002),
10. Wiszniowski J., Robert D., Surmacz-Gorska J., Miksch K., Weber J.V., Environ. Chem. Lett. 4, 51 (2006).
11. Anpo M., Shima T., Kodama S., Kubokawa Y., J. Phys. Chem., 91, 4305(1987).
12. Anpo M., Pure Appl. Chem., 72, 1265(2000).
13. Fox M. A., Dulay M. T., Chem. Rev., 93, 341(1993).

14. Wong J.C.S., Linsebigler A., Lu G., Fan J., Yates J.T., J. Phys. Chem. 99, 335(1995).
15. Lu G., Linsebigler A., Yates J.T., J. Chem. Phys., 102, 3005(1995).
16. Lu G., Yates J.T, J. Chem. Phys., 103, 9438(1995).
17. Wahlstom E., Vestergaard E.K., Schaub R., Ronnau A., Vestergaard M., Laegsgaard E., Stensgaard I., Besenbacher F., Science, 303, 511(2004).
18. Turchi C.S., Ollis D.F., J. Catal., 122, 178 (1990).
19. Davydov L., Smirniotis P.G., J. Catal., 191, 105 (2000).
20. Kormann C., Bahmemann D.W., Hoffmann M.R., Environ. Sci. Technol., 25, 494 (1991).
21. Serpone N., Pelizzetti E.,Eds., Photocatalysis: Fundamentals and Applications, 99, Wiley Interscience, (1989).

Chapter 6

Photovoltaic Performance Of a Dye-sensitized Solar Cell Using a Visible Light-responsive TiO_2 Thin Film Electrode Prepared by RF Magnetron Sputtering Deposition

6.1 Introduction

Dye-sensitized solar cells (DSSCs) offer particular promise as an efficient, lowcost alternative to single-crystal semiconductor photovoltaic devices and represent a specific type of photoelectrochemical cell. The advantages of DSSCs are that they do not rely on expensive or energy-intensive processing methods and can be printed on flexible substrates using roll-to-roll methods. Rather than using a single crystal semiconductor, DSSCs rely on a thin mesoporous film (5–15 μm thick) of nanocrystals of a metaloxide, most often TiO_2, which is sensitized to visible light with a molecular light absorber. The sensitized nanoparticles are immersed in a redox-active electrolyte solution to produce a regenerative photoelectrochemical cell (see Scheme 6.1).

The sensitized TiO_2 thin film immersed in an electrolyte solution, typically containing the iodide-triiodide redox couple. The basic sequence of events in a DSSC is as follows:

$$TiO_2 \mid Dye + h\nu \rightarrow TiO_2 \mid Dye^*$$

$$TiO_2 \mid Dye^* \rightarrow TiO_2 \mid Dye^+ + e^-_{TiO2}$$

$$2e^-_{Pt} + I^{-3} \rightarrow 3I^-$$

$$3/2\ I^- + TiO_2 \mid Dye+ \rightarrow 1/2I^{-3} + TiO_2 \mid Dye$$

Upon absorption of light, an electron is injected from a metal-to-ligand charge transfer (MLCT) excited state of the dye into the conduction band of the metal oxide. The rate of this electron injection reaction is ultrafast, typically occurring on the order

of hundreds of femtoseconds to tens of picoseconds. The injected electron percolates through the TiO_2 film, and is thought to move by a "hopping" mechanism and is driven by a chemical diffusion gradient (rather than an electric field), and is collected at a transparent conductive substrate of fluorine-doped tin oxide glass (SnO_2:F), on which the TiO_2 film is printed. After passing through an external circuit, the electron is reintroduced into the solar cell at the platinum counter electrode, where triiodide is reduced to iodide. The iodide then regenerates the oxidized dye, thereby completing the circuit with no net chemical change. Additionally, deleterious back reactions compete with these forward reactions.

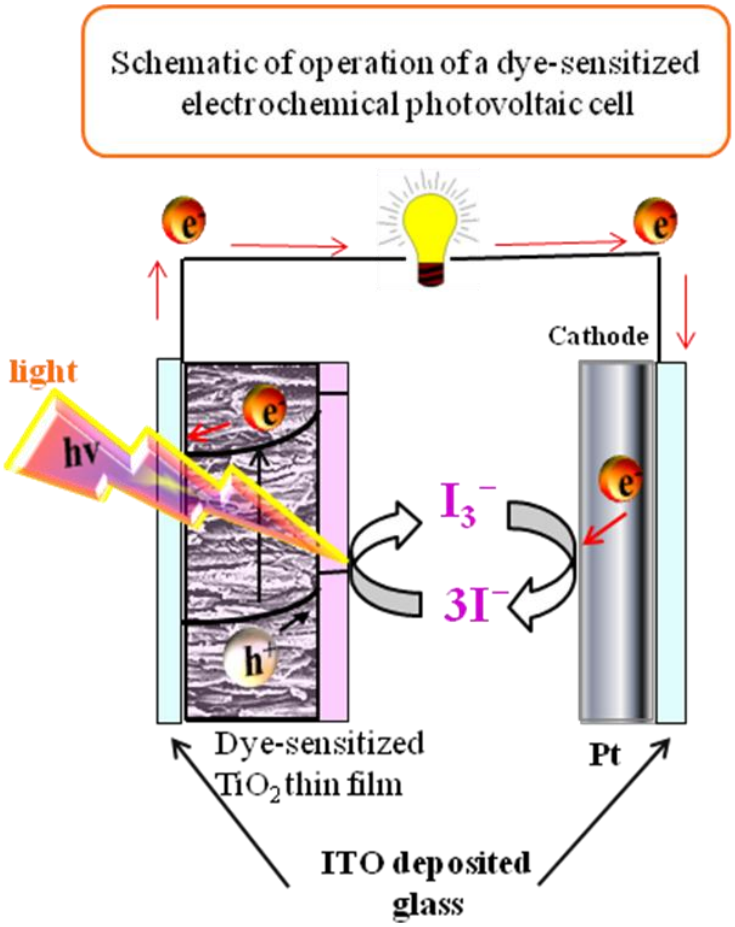

Scheme 6.1. Schematic diagram of dye-sensitized solar cells

Photoelectrochemical cells are an extremely promising technology for solar energy conversion on a large scale. Their low cost and ability to generate chemical fuels makes them a very attractive alternative to photovoltaics. However, there remain a number of challenges to overcome before such systems can be implemented on the scale required to provide a viable alternative to fossil fuels. Dye-sensitized solar cells (DSSCs) are a unique type of photoelectrical cell with great promise as an efficient, low-cost solar energy conversion device.

In recent years, dye-sensitized solar cells have attracted much attention as new types of solar cells, due to their low production cost and high solar-to-electric energy conversion efficiency. Grätzel et al. have reported on the fabrication of DSSCs using a porous TiO2 working electrode sensitized with a ruthenium complex, which shows a solar-to-electric energy conversion efficiency of up to 7-11 %.[1,2] It has also been reported that the performance of DSSCs greatly depends on their morphologies, as well as the electronic structures of the semiconducting materials used for the working electrode.[3,4] Recently, we have reported on a radio frequency magnetron sputtering (RF-MS) deposition method which enables precise control of the morphology as well as the electronic structure of TiO_2 thin films deposited on various substrates.[5-8] For example, visible light-responsive TiO_2 thin film (Vis-TiO_2) consisting of well-defined columnar TiO_2 crystallites can be prepared by RF-MS deposition method under a high substrate temperature (873 K), enabling the absorption of visible light of wavelengths up to 600 nm.[5-8] In the present study, two kinds of sandwich-type DSSCs ($DSSC_{Vis}$ and $DSSC_{UV}$) were fabricated using N719 dye sensitized Vis-TiO_2 and UV-TiO_2 electrodes, respectively, and their photovoltaic performances were investigated. Special attention has been focused on

the relationship between the photovoltaic performance of DSSCs and their morphologies as well as the electronic structures of the TiO_2 thin film electrodes.

6.2 Experimental

TiO_2 thin films were deposited on a conducting ITO-glass plate as a substrate by RF-MS method using a calcined TiO_2 plate (High Purity Chemicals Lab., Corp., Grade: 99.99 %) as the source material and Ar (99.995 %) as the sputtering gas. Conducting ITO-glass plates were cut with dimensions of 20 × 30 mm^2 and utilized as the substrate for making working electrodes. Such prepared substrates were positioned and fixed in the center of a substrate holder parallel with the target, with a constant target-to-substrate distance ($D_{T\text{-}S}$) of 75 mm. The active deposition areas of these thin films were fixed to 20×20 mm^2. Prior to the introduction of the sputtering gas, the chamber was evacuated to lower than 7.00 × 10^{-3} Pa followed by the introduction of Ar at a pressure of 2.0 Pa. For the preparation of visible light-responsive TiO_2 thin film (Vis-TiO_2) and UV light-responsive TiO_2 thin film (UV-TiO_2), the substrate temperature was held at 873 K and 473 K, respectively. The RF power of 300 W was induced and the sputtering time was adjusted to 100, 300, 700 and 1000 min to obtain different thickness for both TiO_2 thin films. These electrodes are denoted as Vis-$TiO_{2(x)}$ and UV-$TiO_{2(x),}$ where x shows the sputtering time (x = 100, 300, 700 and 1000 min).

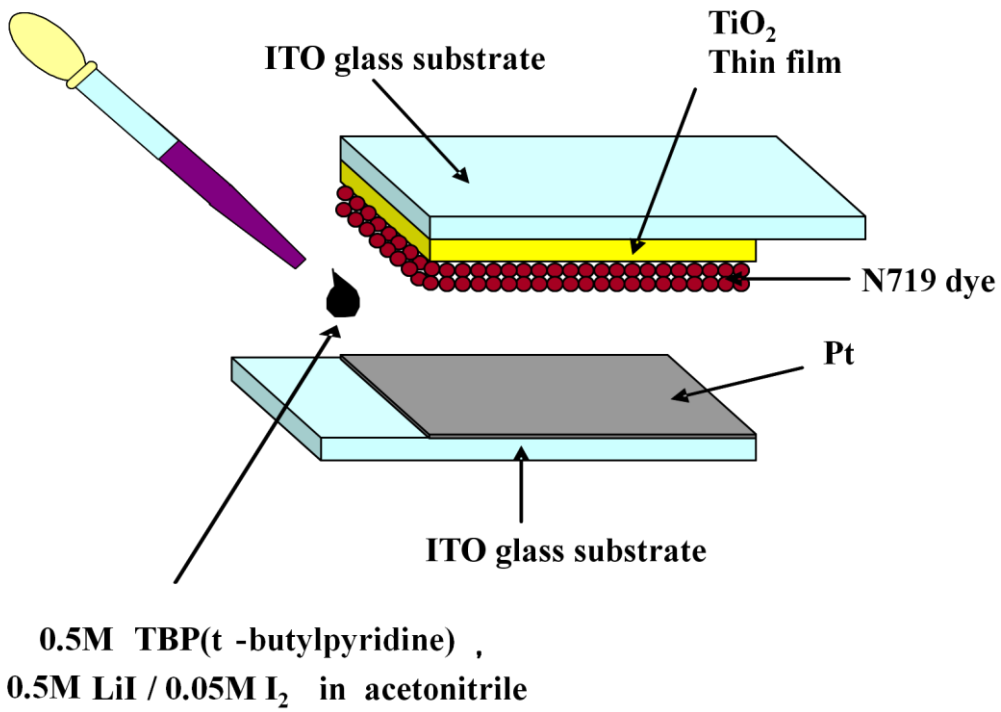

Scheme 6.2. Schematic diagram of sandwich-type dye-sensitized solar cells fabricated using N719-Vis-TiO_2 or N719-UV-TiO_2 electrodes and Pt counter electrode.

UV-Vis transmission as well as UV-Vis diffuse reflectance spectra were measured with a UV-Vis spectrophotometer (Shimadzu, UV-2200A). FE-SEM measurements (S-4500, Hitachi) were performed to observe the cross-sectional morphologies of the produced thin films. Roughness factor (rf: effective surface area per project area) were determined by a krypton adsorption apparatus (BEL Japan, BELSORP TCV). The photoelectrochemical properties of the films were investigated using a potentiostat (HZ3000, Hokuto Denko). The TiO_2 thin film as a working electrode was irradiated by a 500 W Xe arc lamp in 0.05 M NaOH (pH=12.3) solution under pure Ar gas. TiO_2 electrodes were sensitized with N719 dye (*cis*-bis(isothiocyanato)bis(2,2'-bipyridyl-4,4'-dicarboxylato)ruthenium (II) bis (tetrabutylammmonium) obtained from Solaronix). Vis-TiO_2 and UV-TiO_2 were

immersed in an ethanol solution including 5.0×10-4 M N719 for 24 hours at room temperature followed by heating at 353K under vacuum for 5 min. These UV-TiO_2 or Vis-TiO_2 electrodes sensitized with a N719 dye are denoted as N719-UV-$TiO_{2(x)}$ and N719-Vis-$TiO_{2(x)}$, respectively. The sandwich-type DSSCs were fabricated using N719-UV-$TiO_{2(x)}$ or N719-Vis-$TiO_{2(x)}$ and Pt counter electrode deposited on a conducting ITO-glass substrate. These DSSCs were denoted as $DSSC_{UV(x)}$ and $DSSC_{Vis(x)}$, respectively, where x shows the sputtering time (x = 100, 300, 700, 1000 min). An acetonitrile solution including 0.5 M LiI, 0.05 M I_2 and 0.5 M TBP (4-tertbutylpyridine) was used as the electrolyte. The incident photon-to-electron conversion efficiency (IPCE) and photocurrent-voltage measurements of the DSSCs were performed in air at room temperature under illumination with an AM-1.5 Solar Simulator lamp (100 mW cm^{-2}) using a Bunkoh-Keiki CEP-2000 system.

6.3 Results and Discussion

UV-Vis transmission spectra of TiO_2 thin films prepared on the ITO substrates with a sputtering time of 100 min are shown in Fig.6. 1. UV-$TiO_{2(100)}$ electrode prepared at

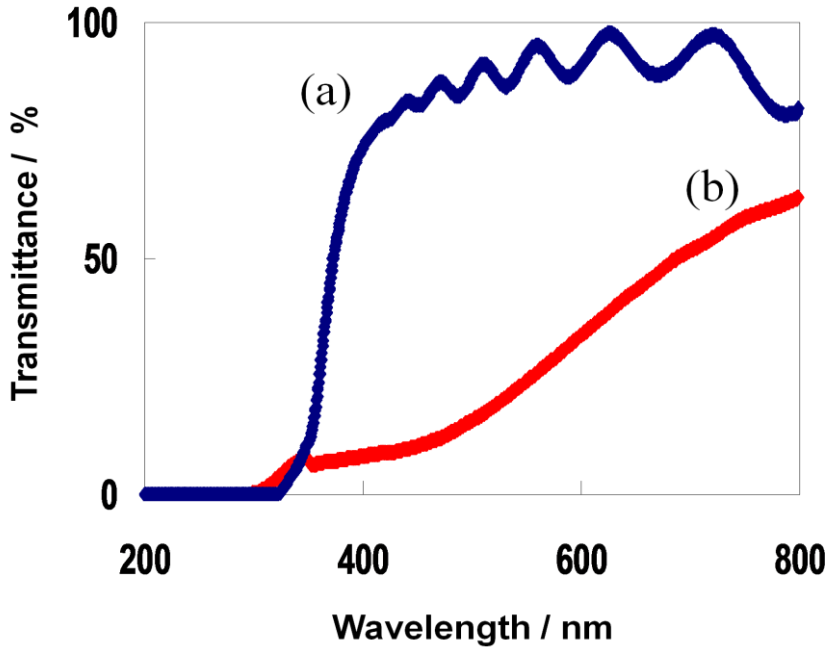

Figure 6.1. UV-Vis transmission spectra of: (a) UV-$TiO_{2(100)}$; and (b) Vis-$TiO_{2(100)}$ electrodes prepared by a RF-MS deposition method.

473K was colorless and transparent to visible light, enabling the absorption of only UV light (λ < 380 nm). The Vis-$TiO_{2(100)}$ electrode prepared at 873K were yellow-colored, thereby enabling the absorption of visible light of up to 600 nm.[5-8] As already reported, SIMS measurements revealed that the atomic ratio of oxygen to titanium (O/Ti) for Vis-TiO_2 gradually decreased from the top surface (O/Ti = 2.00) to the inside bulk (O/Ti = 1.93), a characteristic indicating the origin of the visible light reactivity.10,11 On the other hand, SIMS measurements showed that UV-TiO_2

was composed of stoichiometric TiO_2 in throughout the thin film(O/Ti = 2.00).[6,9] The anodic photocurrents were also measured under scanning of the potentials from –1.2 to +1.0 V versus SCE, in order to determine the zero current potential which is equivalent to the flat band potential (E_{FB}) of the polycrystalline TiO_2 semiconductors. The flat band potentials (E_{FB} (V): vs. SCE at pH = 12.3) of Vis-TiO_2 and UV-TiO_2 were determined to be –0.82 and –0.91, respectively. The conduction band edge (E_{CB} (V): vs. SCE at pH = 12.3) of Vis-TiO_2 and UV-TiO_2 were, therefore, estimated at –1.02 and -1.11, respectively, since the energy difference between E_{CB} and E_{FB} was assumed to be 0.2 eV for n-type semiconductors.[10-12] As reported previously,10-12 the unique declined composition of Vis-TiO_2 with an anisotropic structure causes a significant perturbation of the electronic structure of TiO_2, thus, enabling the absorption of visible light. Cross-sectional SEM images of the Vis-TiO_2 and UV-TiO_2 prepared on ITO substrates by the RF-MS deposition method with a sputtering time of 700 min are shown in Fig. 6.2. SEM observations revealed that Vis-$TiO_{2\ (700)}$ electrode consists of columnar TiO_2 crystallites growing perpendicular to the ITO substrate with huge free interspaces in the bulk, in stark contrast to UV-$TiO_{2\ (700)}$ electrode, where a rather smooth and flat film is formed on the substrate. These results suggest that the rough surface and large interspaces between the columnar TiO_2 crystallites of Vis-$TiO_{2(700)}$ electrode can provide a large number of adsorption sites for the N719 dye on the TiO_2 surface, thus realizing the ideal thin film morphology for a working electrode in DSSCs.

Electrodes prepared under different sputtering times are shown in Fig. 6.3. N719-Vis-TiO_2 electrodes show typical absorption band in the wavelength region above 400 nm due to N719 dye. N719-Vis-$TiO_{2\ (700)}$ (film thickness: 12μm) shows more intense

absorption band than N719-Vis-$TiO_{2\ (300)}$ (film thickness: 4.7 μm). These results indicate that the loading

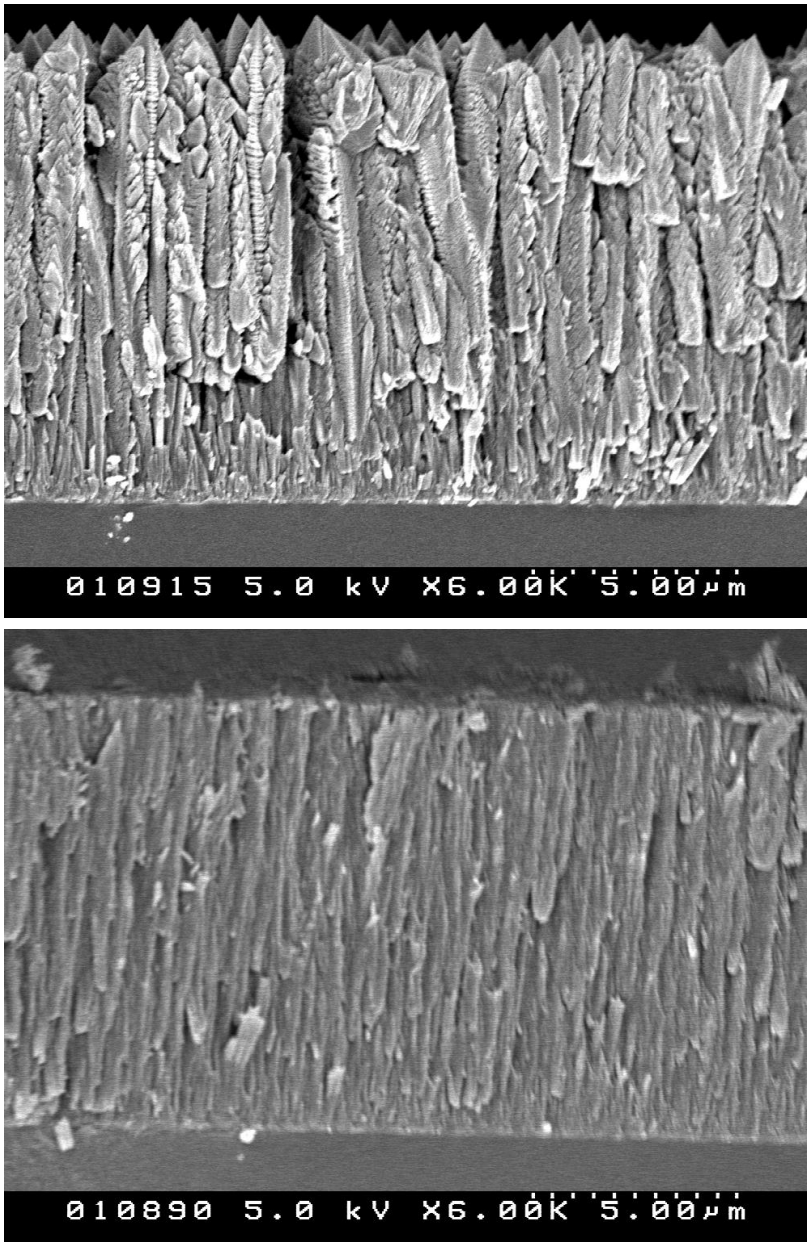

Figure6. 2. SEM images of: (a) UV-$TiO_{2(700)}$; and (b) Vis-$TiO_{2(700)}$ electrodes prepared by a RF-MS deposition method. UV-Vis diffuse reflectance spectra of N719-Vis-TiO_2

amount of N719 dye is larger for N719-Vis-$TiO_{2(700)}$ than N719-Vis-$TiO_{2(300)}$, showing that the TiO_2 film thickness is one of the key factors to control the loading

amount of N719 dye. Photocurrent action spectra of $DSSC_{Vis(700)}$ and $DSSC_{Vis(300)}$ are shown in Fig. 6.4.

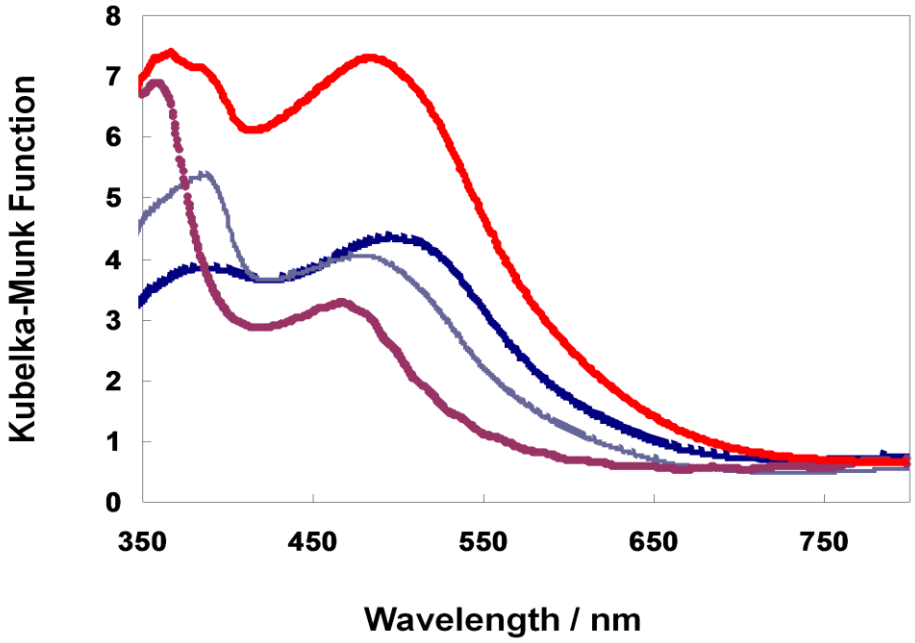

Figure 6.3. UV-Vis diffuse reflectance spectra of N719-Vis-TiO2 and N719-UV-TiO2 electrodes prepared under different sputtering times. (a) N719-Vis-TiO2(700), (b) N719-Vis-TiO2(300), (c) N719-UV-TiO2(700), (d) N719-UV-TiO2(300)

The maximum IPCE value of $DSSC_{Vis(700)}$ is around 88 % at 520 nm, which is considerably higher than that of $DSSC_{Vis(300)}$ (around 65 % at 520 nm). Furthermore, roughness factor (rf) of Vis-$TiO_{2\ (700)}$ was determined to be 764, which is considerably larger than that of Vis-$TiO_{2\ (300)}$ (rf = 377). These results show that the roughness factor of Vis-TiO_2 electrode increases with longer sputtering time, leading to the increase in the loading amount of N719 dye as well as the IPCE value of DSSCs. However, it should be noted that IPCE value decreases in the region of sputtering time above 700 min (data not shown). In fact, the maximum IPCE value of $DSSC_{Vis(1000)}$ (film thickness: 16 μm) was about 54 % at 520 nm, which is

considerably lower than that of $DSSC_{Vis(700)}$. The low IPCE value of $DSSC_{Vis(1000)}$ can be ascribed to the large TiO_2 film thickness, which decreases the efficiency of electron transfer from the photoexcited N719 dyes at the outer surface of TiO_2 film to the conductive ITO substrate.

Figure 3 also shows UV-Vis diffuse reflectance of N719-UV-$TiO_{2\ (700)}$. The intensity of the absorption band due to N719 dye is smaller for N719-UV-$TiO_{2\ (700)}$ than N719-Vis-$TiO_{2\ (700)}$, showing the lower loading amount of N719 dye on N719-UV-$TiO_{2(700)}$. It should be noted that the film thickness of UV-$TiO_{2(700)}$ (11 μm) is comparable to that of Vis-$TiO_{2(700)}$ (12 μm), while roughness factor of UV-$TiO_{2(700)}$ (rf = 2380) is much higher than that of Vis-$TiO_{2(700)}$ (rf = 764). These results indicate that UV-$TiO_{2\ (700)}$ has more porous structure than Vis-$TiO_{2\ (700)}$, although these porous structures cannot be directly observed by SEM investigations (Fig. 6.2). Thus, it can be concluded that the unique columnar structures of TiO_2 crystallites constituting Vis-$TiO_{2\ (700)}$ play more important role for the adsorption of N719 dye than the porous film structures of UV-$TiO_{2\ (700)}$, that is, the large interspace between columnar TiO_2 crystallites of Vis-$TiO_{2(700)}$ realize the facile diffusion of N719 dye and its adsorption throughout the Vis-$TiO_{2(700)}$ thin film. Photocurrent action spectra of $DSSC_{UV(700)}$ is also shown in Fig. 6.4. As expected by the low loading amount of N719 on $DSSC_{UV(700)}$, IPCE value of $DSSC_{UV(700)}$ (around 71 % at 520 nm) is lower than that of $DSSC_{Vis(700)}$ (around 88 % at 520 nm) .

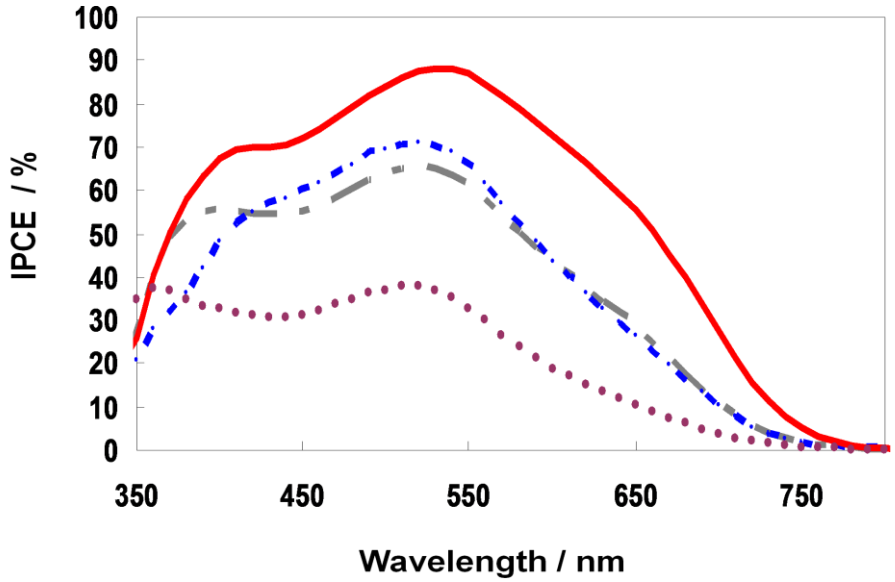

Figure 6.4. Photocurrent action spectra of various DSSCs measured under illumination with an AM-1.5 solar simulator lamp (100 mW cm^{-2}). (a) $DSSC_{Vis(700)}$, (b) $DSSC_{Vis(300)}$, (c) $DSSC_{UV(700)}$, (d) $DSSC_{UV(300)}$, Active area: 1.0cm^2.

UV-Vis diffuse reflectance as well as photocurrent action spectra of $DSSC_{UV(300)}$ (film thickness: 3.9 μm) are shown in Fig. 6.3 and Fig. 6.4, respectively. It can be seen that the loading amount of N719 as well as ICPE value of $DSSC_{UV(300)}$ are significantly lower than those of $DSSC_{UV(700)}$, although the roughness factor of UV-$TiO_{2(300)}$ (rf = 736) is comparable to that of Vis-$TiO_{2(700)}$ (rf = 764). These results also confirm that the porous film structure of UV-TiO_2 does not have remarkable advantage for the efficient adsorption of N719 dye, probably because the average pore diameter of UV-TiO_2 is not significantly larger than the molecular diameter of N719 dye.

Figure 5 illustrates the photocurrent-voltage curves of various DSSCs. The short circuit photocurrent density (J_{sc}), open circuit voltage (V_{oc}), fill factor (FF) and solar-to-electric energy conversion efficiency (η) were determined by the

photocurrent-voltage curves and summarized in Table 1. $DSSC_{Vis(700)}$ exhibited a highest photovoltaic performance and it is clearly demonstrated that N719-Vis-TiO_2 act as more efficient active electrode than N719-UV-TiO_2 when compared under the same sputtering time.

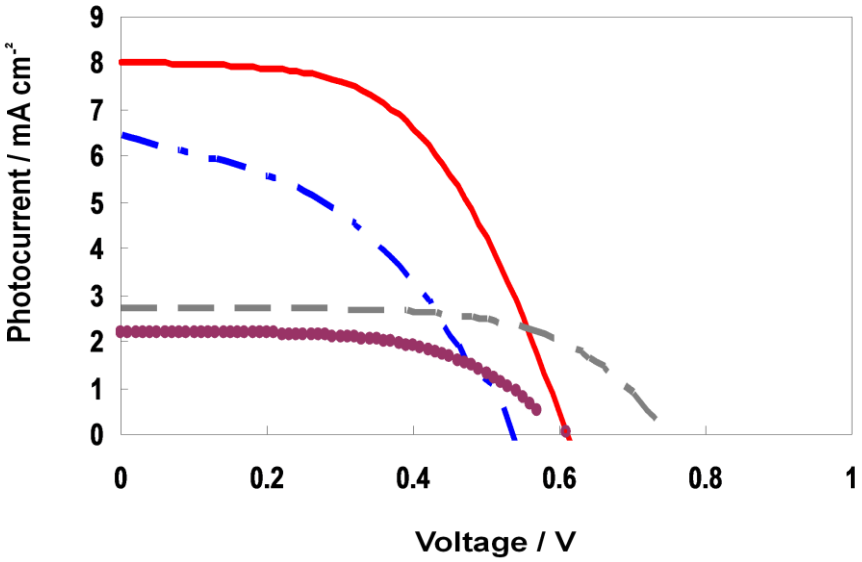

Figure 6.5. Photocurrent-voltage curves of various DSSCs measured under illumination with an AM-1.5 solar simulator lamp (100 mW cm^{-2}). (a) $DSSC_{Vis(700)}$, (b) $DSSC_{Vis(300)}$, (c) $DSSC_{UV(700)}$, (d) $DSSC_{UV(300)}$, Active area: 0.12cm^2.

The high photovoltaic performance of $DSSC_{Vis}$ could be explained by the unique morphology of the Vis-TiO_2 electrode consisting of well-defined columnar TiO_2 crystallites, which enables the efficient diffusion and adsorption of N719 dye within TiO_2 film, increasing the photoabsorption efficiency. Furthermore, unique columnar structure of the Vis-TiO_2 electrode can contribute to the facile diffusion of the electrolyte into the deep inside bulk of the TiO_2 film electrode, enhancing the electron transfer between I- ions and N719 dye. One of other important factors influencing the photovoltaic performance of DSSC can be the difference in the energy levels of

the conduction band edge (E_{CB}) of Vis-TiO_2 and UV-TiO_2. The conduction band edge (E_{CB}) of the Vis-TiO_2 (-1.02 V) shifts more positively than that of UV-TiO_2 (-1.11V).[10-12]

Table 6.1. Photovoltaic performance of various DSSCs.

	J_{sc} (mA cm^{-2})	V_{oc} (v)	FF	η%
$DSSC_{Vis(700)}$	8.0	0.61	0.54	2.6
$DSSC_{UV(700)}$	6.2	0.52	0.41	1.30
$DSSC_{Vis(300)}$	2.7	0.75	0.62	1.25
$DSSC_{UV(300)}$	2.2	0.61	0.56	0.76

Thus, the higher photovoltaic performance of $DSSC_{Vis}$ can also be ascribed to the lower energy level of E_{CB} of Vis-TiO_2 than that of UV-TiO_2, which realizes more efficient electron injections from the photo-excited N719 dye into the conduction band (CB) of Vis-TiO_2 than in the case of UV-TiO_2. Although $DSSC_{Vis}$ showed the high IPCE value, it does not show so high photovoltaic performance as expected by its high IPCE value. This indicates the significant losses of electron in the electrolyte

or at the counter-electrode. The further investigations on the relationship among the morphology and band structure of TiO_2 thin film electrode and photovoltaic performances of DSSC are now under way and will be reported elsewhere.

6.4 Conclusions

It was found that Vis-TiO_2 electrode prepared on ITO-glass plate by an RF-MS deposition method can be successfully applied as the working electrode for DSSCs, showing remarkably higher photovoltaic performance than UV-TiO_2 electrode. The solar-to-electric energy conversion efficiency (η) of $DSSC_{Vis(700)}$ fabricated using N719-Vis-$TiO_{2(700)}$ electrodes was determined to be 2.6 %, showing higher performance than $DSSC_{UV(700)}$ (1.3 %) under illumination with an AM-1.5 solar simulator lamp (100 mW cm^{-2}). The high performance of $DSSC_{Vis(700)}$ can be ascribed to the high loading amount of N719 dye as well as the facile diffusion of the electrolyte into the deep inside bulk of Vis-TiO_2 , which is realized by the unique film morphology of Vis-$TiO_{2(700)}$ consisting of well-defined columnar TiO_2 crystallites. Furthermore, photoelectrochemical investigations suggested that the high photovoltaic performance of $DSSC_{Vis(700)}$ can be also ascribed to the low energy level of conduction band of Vis-$TiO_{2(700)}$, which enables efficient electron injections from the photo-excited N719 dye to Vis-$TiO_{2(700)}$.

6.5 References

1. O'Regan B., Grätzel M., Nature, 353, 737 (1991).
2. Grätzel M., J. Photochem. Photobiol. A: Chem., 164, 3 (2004).
3. Islam A., Sugihara H., Singh L. P., Hara K., Katoh R., Nagawa Y., Yanagida

M., Takahashi Y., Murata S., Arakawa H., Inorg. Chim. Acta., 322, 7 (2001).

4. Pavasupree S., Ngamsinlapasathian S., Nakajima M., Suzuki Y., Yoshiokawa S., J. Photochem. Photobiol. A: Chem., 184, 163 (2006).
5. Anpo M., Bull. Chem. Soc. Jpn., 77, 1427 (2004).
6. Matsuoka M., Kitano M., Takeuchi M., Anpo M., Thomas J. M., Top. Catal., 35, 305 (2005).
7. Kikuchi H., Kitano M., Takeuchi M., Matsuoka M., Anpo M., Kamat P. V., J. Phys. Chem. B., 110, 5537 (2006).
8. Kitano M., Tsujimaru K., Anpo M., Appl. Catal. A: Gen., 314, 179 (2006).
9. Kitano M., Takeuchi M., Matsuoka M., Thomas J. M., Anpo M., Chem. Lett., 34, 616 (2005).
10. Matsumoto Y., J. Solid State Chem., 126, 227 (1996).
11. Kitano M., Takeuchi M., Matsuoka M., Thomas J. M., Anpo M., Catal. Today, 120, 133 (2006).
12. Fukumoto S., Kitano M., Takeuchi M., Matsuoka M., Anpo M., Catal. Lett., 127, 39 (2009).

Chapter 7

Investigation on Photocatalytic Hydrogen Evolution Using Different Concentration of Ammonia

7.1 Introduction

Fuel cells operate with hydrogen or hydrogen-rich chemicals. Hydrogen-rich fuels utilize for supplying of hydrogen for Fuel cells. The most common fuels include gases (i.e., hydrogen, natural gas, or ammonia), liquids (i.e., methanol, hydrocarbons, hydrazine). A preliminary conversion or reforming process is required for all fuels, except for direct utilizing of hydrogen.

Here a procedure for production of Hydrogen from aqueous solution ammonia (NH_3) is presented. This chapter presents some preliminary results showing the technology of photocatalytic hydrogen production from ammonia aqueous solution is so beneficial. Lately in-situ and on-demand chemical and photocatalytical production of energy carriers such as hydrogen is gaining increasing importance as new technologies such Fuel cell developing. Proton exchange membrane (PEM) fuel cells need a sustained source of hydrogen fuel to use. Hydrogen is the main fuel source for power generation with fuel cells, but its storage and transportation are still major issues. To overcome these problems, hydrogen has been stored and transported via other chemical compounds, such as alcohols, hydrocarbons, ammonia, etc. In many ways, ammonia is an excellent hydrogen carrier [1]; liquid ammonia represents a convenient way of storing supplies of hydrogen, boasting a specific energy density (kWh/l) 50% higher than liquefied hydrogen. Ammonia is also easily condensed at ambient temperature (under pressure of 8 bar), which makes it a good choice for transportation and storage. Even though ammonia is flammable within defined limits (16%-25% by volume in the air) and toxic (above 25 ppm) its presence can be detected by its characteristic odor (above 5 ppm). Ammonia is produced world-wide

in large quantities (more than 100 million ton/year), which allows the effect of economy of scale on the cost of production. Its decomposition by electro-oxidation in alkaline media at low overpotentials is NOx and COx free with nitrogen and water as products of reaction [2]. The production of smaller volumes of hydrogen and nitrogen mixtures used as protective gases for chemical products and for metal-working processes by decomposition of ammonia over iron- or nickel-based catalysts at 800-900 °C may be an economic alternative where production or purchase of pure hydrogen is too expensive.

The works presented here basically based on use of a clearly defined anode and cathode geometry as initially described by Fujishima and Honda [1] which uses semiconductor materials for photo-assisted water splitting. In such processes the hydrogen and oxygen areevolved separately in different vessels. While that described approach (Chapter 2) offers the fundamental advantages which the most important one is that no gas separation step is required there, but the photoconversion efficiency suffers from losses inherent in the transport of the photogenerated electrons and H^+ ions from the anode to the cathode.

In the other process that is so popular and much convenient in water-splitting theme,

TiO_2-based photocatalyst utilizes to carry out the photocatalytic decomposition of water in a reaction cell. In this kind of processes with the simultaneous co-generation of oxygen and hydrogen occur, resulting gases accumulate in one vessel. Many efforts investigated the use of various kinds of semiconductors such as doped TiO_2 for direct photocatalytic splitting of water in aqueous or vapor phase [2-5] with the mixed evolution of hydrogen and oxygen. The important advantage of this kinds of

processes is that any form of photocatalysts is usable, bulk to planar to particulate, is a dispersion of semiconductor "nano particles" of various geometry, e.g. sphere, tube, ribbon, or wire, throughout either liquid or vapor phase water resulting in the photocatalytic splitting thereof. The concept offers an appealing simplicity that has gained considerable academic interest.

Several modified TiO_2 catalysts in powder form or as thin films, including Pt-TiO_2, Pt-RuO_2-TiO_2, Pt-$SrTiO_3$, NiO-$SrTiO_3$,… suspended or dispersed in liquid water for solar hydrogen production have been studied [6-18]. To date no homogeneous or heterogeneous photocatalysts have been found suitable for stoichiometric water splitting, primarily due to the difficulty in oxygen formation and the rapid reverse reaction between products. Of the reported studies [6-18], efforts have focused on approaches such as metal loading, ion doping, composite formation, and the addition of electron donors or hole scavengers with an aim towards preventing the rapid recombination of photogenerated electron/hole pairs, and improving the visible light response of the semiconducting particles. As we will discuss further, these photocatalysts involve a two-step water splitting process for H_2 production and are comprised of a combination of either metal and/or two or more different oxide semiconductors. Modification of these nanoparticle photocatalysts has resulted in comparatively effective catalysts for H_2 evolution [19-26]. The high surface area of these nanoparticles, at least in principle, allow solution species to capture photogenerated electrons quickly and thereby significantly reduce the occurrence of charge recombination [25-27].

Over the past several years' considerable effort has been made to design, synthesize and fabricate metal oxide nanoparticle photocatalysts capable of using

visible light energy.

Several review articles [24-26, 31-33] consider the importance of semiconductor particulate systems for solar hydrogen production. About 45 million metric tons of hydrogen is produced globally each year from fossil fuel. Approximately half of this hydrogen goes to making ammonia (NH_3), which is a major component of fertilizer and a familiar ingredient in household cleaners.

Ammonia is potentially a good source of hydrogen for mobile fuel cells since it can be used in aqueous solution at ambient conditions, has high hydrogen ratio, and can be converted to hydrogen using Photocatalytic processes.

The ability to produce hydrogen for fuel cells from renewable sources would be a great benefit to the next generation of energy conversion technology. Additionally, developing a means to safely store hydrogen would solve a major obstacle to fuel cell commercialization. Light biomass solution such as methanol and also ethanol was under consideration for long time. Methanol as the smaller alcohol molecule can release H_2 through different processes such as Photocatalysis. It also can be produced from many sources, including renewable sources, and it allows hydrogen to be stored in the form of a higher energy density, less dangerous liquid.

Although it reported before that methanol can be converted to hydrogen with better efficiency than any other hydrocarbon being considered for on-board hydrogen production [34]. But evolution of CO_2 and CO in the hydrogen production process is a disadvantage of it. However, the use of fuel cells could potentially yield a 100% reduction of CO_2 emissions if a renewable source of H_2 were developed (i.e. ethanol or methanol produced from CO_2 consuming plants or biomass, or electrolysis of water with solar energy), and even if H_2 were produced onboard from ammonia, the

estimated energy

7.2 Experimentals:

It has been reported by many researchers that the rate of H_2 evolution from aqueous solution containing a sacrificial electron donor by a given photocatalyst is enhanced with increasing the amount of loaded Pt, while excess loading results in lowering the catalytic activity.[35-40] This is because an increase in Pt loading amount contributes to increasing the density of active sites for H2 evolution, while excess loading can hinder light absorption of the photocatalyst and/or cause enhanced recombination between photogenerated electrons and holes.[41]

In the case of the photodeposition method, Pt deposits are formed by the reduction of $PtCl_6^{2-}$ anions with photogenerated electrons that come from TiO_2, and tend to aggregate because photogenerated electrons migrate easily to the previously deposited Pt nanoparticles. The effect of platinisation on the photocatalytic activity of TiO_2has a great importance. The enhancement of the photocatalytic activity of TiO_2 by platinisation depend highly on the properties and amount of deposited Pt.

The Pt and also Ru metal deposition on TiO_2 particle surface was achieved by the room-temperature photodeposition of H_2PtCl_6 and $RuCl_3$.

7.2.1 Preparation of catalysts

For the synthesis of the platinised TiO_2-catalysts the basic commercially available TiO_2-catalysts, namely Degussa P25, were used. For each platinised sample, 1000 mg of TiO_2 were suspended ultrasonically in 65 mL of aqueous solution containing 4 mL of H_2PtCl_6 or $RuCl_3$ and 25 mL of methanol as the reducing agent for holes. The well-dispersed suspension was irradiated by a 500W Mercury lamp for 10 h in an agitated

vessel. It was then dried at an oven at 100°C overnight and pulverized by mortar manually, yielding a grayish Pt/TiO_2 powder. As the highest available commercial concentration of “Ammonium hydroxide" which is a solution of NH_3 in water is 28W%. Different amount of concentration of ammonia was used with utilizing this solution.

The TiO_2 used, Degussa P-25, was about 70% anatase. According to the manufacturer’s specification, the elementary particle in dry powder was approximately spherical in shape with a size of 20 nm. The commercial P25- TiO_2 has the ratio of anatase to rutile between 70-80% and 20-30%; average particle sizes between 20-30 nm; specific surface are between 35-65 m^2g^{-1} and more even size distribution. The literature information indicates that the anatase phase has a better photocatalytic activity than the rutile phase and that there is a certain anatase to rutile ratio for TiO_2 to exhibit the maximum photocatalytic activity.

As the highest available commercial concentration of "Ammonium hydroxide" which is a solution of NH_3 in water is 28W%. Different amount of concentration of ammonia was used.

For all of samples 100 mg of previously described catalyst plus 7.5 ml of different concentration of ammonia poured in a reaction cell with total volume about 50 or 200cc. The solution agitated with a small magnet and bare Mercury lamp irradiation was used.

Overall reaction:

$$2NH_3\ (aq) \xrightarrow{\text{Pho.Cat.+ UV}} N_2\ (g) + 3H_2\ (g)$$

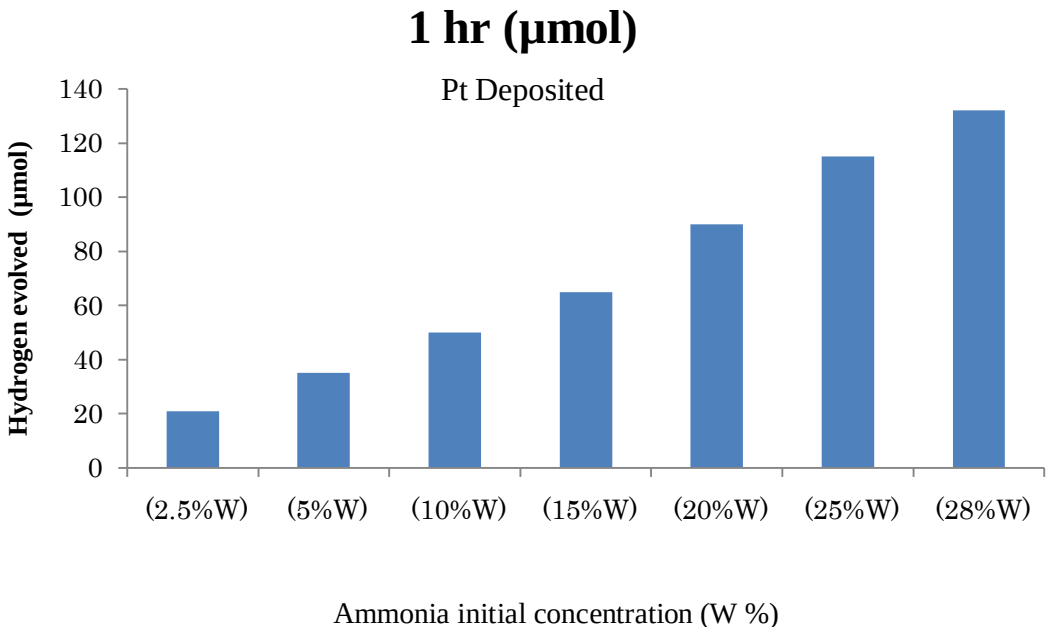

Fig. 7.1 Comparison of evolved H_2 based on different initial concentration of ammonia after 1 hr utilizing Pt deposited TiO_2

As illustrated in Fig. 7.1 the evolution of H_2 is increasing with the initial concentration of ammonia, the highest available ammonia concentration solution shows the best results.

Fig. 7.2 shows the evolution of hydrogen based on different initial concentration of ammonia after 1 hr utilizing Ru deposited TiO_2 and Fig. 7.3 is a comparison of evolution of hydrogen utilizing Ru deposited TiO_2 and Pt deposited TiO_2 in different initial concentration of ammonia after 1 hr, it shows that Ru deposited TiO_2 compare to Pt deposited TiO_2 has 10 times smaller activity.

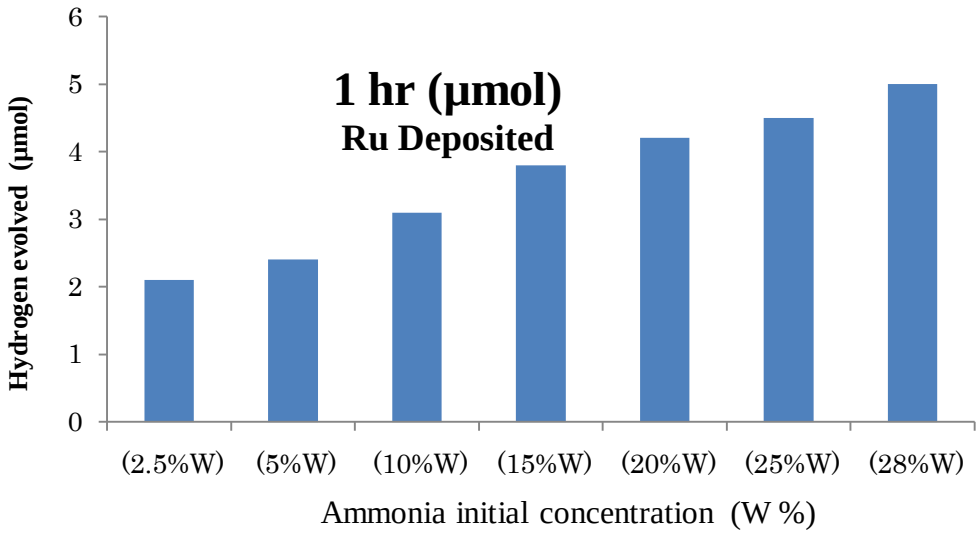

Fig. 7.2 Comparison of evolved H_2 based on different initial concentration of ammonia after 1 hr utilizing Ru deposited TiO_2

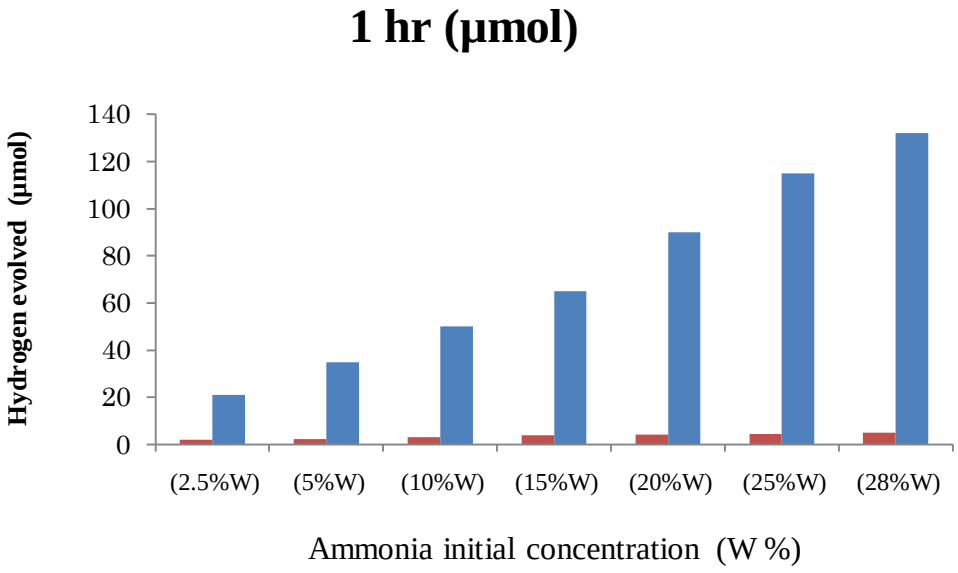

Fig. 7.3 Comparison of evolution of hydrogen utilizing Ru deposited TiO_2 and Pt deposited TiO_2 in different initial concentration of ammonia after 1 hr

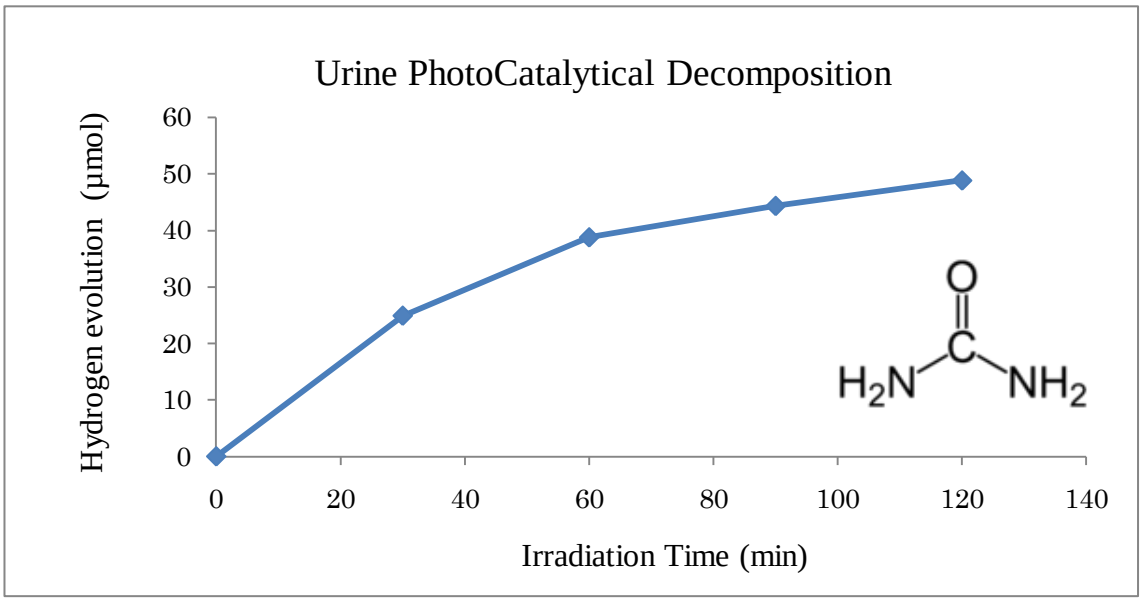

Fig. 7.4 Evolution of H_2 from Urine photocatalytic decomposition, utilizing Pt deposited TiO_2

Here we introduce an efficient way of producing hydrogen from urine, production of hydrogen from urine is win-win scenario that could not only fuel the cars of the future, but could also help clean up municipal wastewater. The same process we utilized for ammonia had been used here. As urine's major constituent is urea, which incorporates four hydrogen atoms per molecule - importantly, less tightly bonded than the hydrogen atoms in water molecules. As it can be seen in the fig. 7.4 the hydrogen evolution from urine is considerable and it might be a source of hydrogen in future. It may help to clean up sewage plants as a cheap and readily available waste

As it shows in the figure the rate of evolution decreases during the time that it might be because contamination of photocatalyst.

7.4 Conclusion:

Evolution of H_2 from an aqueous solution involving light hydrogen-rich compounds for evolution of hydrogen especially for using in novel PEM fuel cells investigated. The most common compounds include various alcohols, hydrocarbons, hydrazine and ammonia. As NH_3 contains no carbon, it is a promising source of hydrogen, then our novel, simple and cost-efficient process of utilizing Pt deposited TiO_2 photocatalyst would be a brilliant process for production of in-situ hydrogen. Storing hydrogen as NH_3 may solve the challenging problem of storing high-pressure hydrogen with an H_2 density of 136 Kg H_2/m3, which is the highest in chemical compounds and makes ammonia the most hydrogen-dense chemical in existence. Investigations on photocatalytic hydrogen evolution using different concentrations of ammonia led to the development of a procedure for the production of hydrogen from water soluble ammonia (NH_3). Our recent research shows that the technology of photocatalytic hydrogen production from ammonia aqueous solution is beneficial and that the photocatalytic decomposition of ammonia is a promising alternative process for low-cost, low-temperature, high-purity *in situ* hydrogen production. Using the highest concentration of ammonia in aqueous solution led to a reasonably good production of hydrogen and the best results related to higher amounts of ammonia in the solution (28%W).These results point to ammonia photocatalytic decomposition as a promising candidate for an alternative process for low-cost, low-temperature, high-purity in-situ hydrogen production.

7.5 References:

1. Fujishima A., Honda K., Nature, 238, 37 (1972).
2. Schrauzer G.N., Guth T.D., J. Am. Chem. Soc., 99, 7189 (1977).
3. Kawai T., Sakata T., Chem. Phys. Lett., 72:87(1980).
4. Van Damme H., Hall W.K., J. Am. Chem. Soc., 101, 4373 (1979).
5. Domen K., Naito S., Soma M., Onishi T., Tamaru K., Chem. Commun., 543 (1980).
6. Sato S., White J.M., Chem. Phys. Lett., 72, 83(1980).
7. Wagner F.T., Somerjai G.A., J. Am. Chem. Soc., 102, 5494 (1980).
8. Wagner F.T., Somerjai G.A., Nature, 285, 559 (1980).
9. Sato S., White J.M., J. Catal., 69, 128 (1981).
10. Duonghong D., Borgarello E., Grätzel M., J. Am. Chem. Soc., 103,4685 (1981).
11. Domen K., Naito S., Onishi T., Tamaru K., Chem. Phys. Lett., 92,433.(1982).
12. Lehn J.M., Sauvage J.P., Ziessel R., Hilaire L., Israel J. Chem., 22,168(1982).
13. Domen K., Kudo A., Onishi T., J. Catal., 102,92 (1986).
14. Kudo A., Domen K., Maurya K., Aika K., Onishi T., J. Catal. 111, 67 (1988),
15. Inoue Y., Kubokawa Y., Sato K., J. Phys. Chem., 95,4059 (1991)
16. Inoue Y., Asai Y., Sato K., J. Chem. Soc. Faraday. Trans., 90, 797 (1994).
17. Sayama K., Arakawa H., J. Photochem. Photobiol. A. Chem., 77,243 (1994).
18. Sayama K., Arakawa H., Res. Chem. Intermed., 26, 145 (2000).
19. Baba R., Nakabayashi S., Fujishima A., Honda K., J. Phys. Chem. 89, 1902 (1985).
20. Aspnes D.E., Heller A., J. Phys. Chem. 87, 4919 (1983).

21. Bard A.J., Fox M.A., Acc. Chem. Res., 28,141 (1995).
22. Ashok Kumar M., Int. J. Hydrogen Energy, 23, 427 (1998).
23. Kudo A., Kato H., Tsuji I., Chem. Lett., 33, 1534 (2004).
24. Takata T., Tanaka A., Hara M., Kondo J.N., Domen K., Catal. Today, 44, 17(1998).
25. Kamat P.V., Chem. Rev., 93, 267(1993).
26. Thompson T.L., Yates J. T., Top. Catal., 35, 197 (2005).
27. Hagfeldt A., Gratzel M., Chem. Rev., 95, 49 (1995)
28. Hara M., Kondo T., komoda M., Ikeda S., Shinohara K., Tanaka A., Kondo J.N., Domen K., Chem. Commun. 357 (1998).
29. Morikawa T., Asahi R., Ohwaki T., Aoki K., Taga Y., Jpn. J. Appl. Phys., 40, L561 (2001).
30. Wang H., Lewis J.P., J. Phys. Condens. Matter., 18, 421(2006).
31. Kudo A., Catal. Surv. Asia, 7, 31(2003).
32. Ni M., Leung M.K.H., Leung D.Y.C., Sumathy K., Renew. Sust. Energy Rev., 11, 401 (2007).
33. Kudo A., Int. J. Hygrogen Energy, 31, 197 (2006).
34. Ahmed S., Krumpelt M., Int. J. Hydrogen Energy, 26, 291(2001).
35. Hara M., Nunoshige J., Takata T., Kondo J. N., Domen K., Chem. Commun., 24, 3000 (2003).
36. Sakata T., Kawai T., Hashimoto K., *Chem. Phys. Lett.*, *88*, 50 (1982).
37. Pichat P., Mozzanega M. N., Disdier J., Herrmann J. M., NouV. J. Chim., 6, 559 (1982).
38. Reber J. F., Meier K. J., Phys. Chem., 90, 824 (1986).

39. Ohtani B., Iwai K., Nishimoto S., Sato S., J. Phys. Chem. B, 1997, 101, 3349 (1997).
40. Bao N., Shen L., Takata T., Domen K., Chem. Mater., 20, 110 (2008).
41. Hidalgo M.C., Maicu M., Navío J.A., Colón G., Catal. Today, 129, 43 (2007).

Chapter 8

General Conclusions

General Conclusions

Semiconductor photocatalysis has many potential applications for environmental problems. One of the most-studied semiconductors has been TiO_2, as it has the advantage of being cheap, nontoxic, and stable. Studies on the surface chemistry of TiO_2 help answer important questions such as the active species for photooxidation, the fate of charge carriers, and the mechanism for transfer of charge to species bound to the surface.

Hydrogen as a promising green energy

Today, hydrogen is truly the flexible energy carrier for our sustainable energy future. Hydrogen is primarily used as a chemical feedstock in the petrochemical, food, electronics, and metallurgical processing industries, but is rapidly emerging as a major component of clean sustainable energy systems. It is relevant to all of the energy sectors - transportation, buildings, utilities, and industry. Hydrogen can provide storage options for intermittent renewable technologies such as solar and wind, and, when combined with emerging decarbonization technologies, can reduce the climate impacts of continued fossil fuel utilization.

In the beginning of second decade of new millennium, concerns about global climate change and energy security create the forum for mainstream market penetration of hydrogen. Ultimately, hydrogen and electricity, our two major energy carriers, will come from sustainable energy sources, although, fossil fuel will likely remain a significant and transitional resource for many decades. Our vision for a hydrogen future is one of clean sustainable energy supply of global proportions that

plays a key role in all sectors of the economy. We will implement our vision with advanced technologies including direct solar production systems and low-temperature metal hydrides and room- temperature carbon nanostructures for storage.

Hydrogen can be produced directly from sunlight and water by photocatalytic reaction and some other processes. Hydrogen can also be produced indirectly via thermal processing of biomass or fossil fuels. Global environmental concerns are leading to the development of advanced processes to integrate such the environment friendly processes. These green production technologies have the potential to produce essentially unlimited quantities of hydrogen in a sustainable manner.

Artificial photosynthesis to produce renewable energy and other green energy materials is a major challenge to mankind. Efficient use of the freely available resource of solar energy by its conversion into electricity as well as clean chemical energy will be significant in reducing our dependence on fossil fuels. TiO_2 is one of the most popular oxide materials for its many applications and potential use in a variety of technologies where surface chemistry is critical, including photocatalysis. Recently, TiO_2 has been widely studied as a key component of photocatalysis in water splitting reactions. The main objective of this study is to modify and develop new TiO_2-based photocatalysts that allow the efficient absorption of visible light, thus, enabling such modified TiO_2 to initiate various desired reactions effectively even under visible or solar light irradiation.

Summary of Chapter 1

This chapter outlines the various studies detailed in this thesis.

Summary of Chapter 2

In Chapter 2, the preparation methods used to develop the TiO_2 thin films were discussed. Among these, sputtering methods have several advantages and, in this study, TiO_2 thin films were deposited by a radio-frequency magnetron sputtering (RF-MS). The films were deposited using a stoichiometric TiO_2 target sputtered in pure Ar at different pressures. The aim of this study was to investigate the effect of the deposition conditions on the structural and photocatalytic properties of the thin films before and after heat treatment. As is shown in the studies, the crystalline phase of the TiO_2 catalysts is an important factor that determines its activity. The influence of the substrate temperatures on the photocatalytic activity of the TiO_2 thin films was also investigated. The main influence of temperature was found to affect the crystallinity of TiO_2.

Reducing the pressure was found to decrease the total sputtering time for a specified thickness. In this Chapter, the design of optimized Vis-TiO_2 thin films for the separate production of H_2 and O_2 was also discussed. Optimizing of the photocatalytic activity of Vis-TiO_2 thin films prepared by a RF magnetron sputtering (RF-MS) method by controlling the various parameters such as sputtering pressure and target-to-substrate distance $D_{T\text{-}S}$ was investigated. It was shown through different characterization experiments that the optimal sputtering pressure was 2.0 Pa. At this pressure, the highest activity for the Vis-TiO_2 thin films could be attained. When the sputtering pressure was fixed at 2.0 Pa and the target-to-substrate distance was $D_{T\text{-}S}$=75 mm, the best results

were obtained.

It was also found that chemical etching of the Vis-TiO_2 thin films with HF solution remarkably enhanced their photocatalytic activity. Such optimized HF-Vis-TiO_2/Ti thin film electrodes exhibited a significant increase in their photocurrent under UV and visible light irradiation as compared to untreated Vis-TiO_2/Ti. SEM and BET surface measurements revealed that the surface roughness increased and the interspace between the columnar TiO_2 crystallites were extended by HF treatment, indicating that HF-Vis-TiO_2/Ti has a shorter diffusion length for the photoformed holes to reach the solid–liquid interfaces than untreated Vis-TiO_2/Ti. The donor densities of Vis-TiO_2/Ti were found to increase after HF treatment, indicating that the photogenerated electrons of HF (60)-Vis-TiO_2/Ti can reach the TiO_2 substrate interface more easily than Vis-TiO_2/Ti due to its higher conductivity. Moreover, the chemical etching of Vis-TiO_2 by HF solution was found to lead a remarkable increase in the separate evolution of H_2 and O_2 under visible light irradiation ($\lambda \geq 450$ nm). Thus, HF (60)-Vis-TiO_2/Ti/Pt thin film photocatalysts were found to be successful in realizing the stoichiometric separate evolution of H_2 and O_2.

Summary of Chapter 3

Chapter 3 dealt with the post heat treatment of visible light-responsive TiO_2 thin film photocatalysts (Vis-TiO_2) prepared on Ti metal foil (Vis-TiO_2/Ti) or ITO glass (Vis-TiO_2/ITO) substrates by the RF magnetron sputtering (RF-MS). The UV–Vis spectra as well as photoelectrochemical performance of Vis-TiO_2 were affected by various heat treatments such as calcination in air or ammonia. Calcination treatment

in NH_3 (1.0×10^4 Pa, 673 K) was found to be particularly effective in increasing the visible light absorption of Vis-TiO_2 as well as in enhancing its photoelectrochemical performance and photocatalytic activity. The Vis-TiO_2 thin film photocatalyst was prepared by the RF-MS method on one side and nanoparticles of Pt were deposited on the opposite side of a Ti metal foil substrate (Vis-TiO_2/Ti/Pt). The separate evolution of H_2 and O_2 from H_2O could be successfully achieved by using an H-shape glass cell consisting of two aqueous phases separated by Vis-TiO_2/Ti/Pt photocatalytic device and a proton-exchange membrane. It was found that the rate of the separate evolution of H_2 and O_2 was also dramatically enhanced by the calcination treatment of Vis-TiO_2 photocatalyst in ammonia.

Summary of Chapter 4

Chapter 4 dealt with the preparation of double-layered TiO_2 thin film in order to improve the reactivity of TiO_2 thin film photocatalyst. A double-layered visible light-responsive TiO_2 thin film photocatalyst was prepared on a Ti foil substrate by a RF-MS method. The produced DL-TiO_2/Ti consisted of a UV light-responsive TiO_2 thin film (UV-TiO_2) prepared on a Ti foil substrate which a visible light-responsive TiO_2 thin film (Vis-TiO_2) was prepared on it. DL-TiO_2/Ti exhibited higher photoelectrochemical and photocatalytic performance under both UV and visible light irradiation than a single-layered Vis-TiO_2 thin film photocatalyst prepared on a Ti foil substrate. The optimal thickness of the UV-TiO_2 thin film of DL-TiO_2/Ti was found to be about 100nm. Expanding on this work, a novel double-layered TiO_2 thin film device, DL-TiO_2/Ti/Pt, was also prepared by a RF-MS method where DL-TiO_2 was prepared on

one side and Pt was deposited on the other side of a Ti foil substrate. The separate evolution of H_2 and O_2 from H_2O was successfully achieved by using an H-type glass cell consisting of two aqueous phases separated by the DL-TiO_2/Ti/Pt and a proton-exchange membrane.

Summary of Chapter 5

In Chapter 5, two aspects, the production of visible light responsive TiO_2 thin films and their characterizations were focused. TiO_2 thin films were fabricated on quartz substrates under similar conditions. The main part of this Chapter dealt with the photocatalytic degradation of organic contaminants which were found in landfill leachate and methylene blue by utilizing the Vis-TiO_2 thin films. In this study, the changes in the concentrations of COD and TOC as well as UV absorbance of the water involving contaminants at a given wavelength were investigated. The results clearly showed that the novel Vis-TiO_2 thin film photocatalyst led to a remarkably decrease in the concentration of contaminants under solar light irradiation.

Summary of Chapter 6

In Chapter 6, the Vis-TiO_2 thin films developed in Chapter 2 were also applied in developing sandwich-type dye-sensitized solar cells (DSSC). Two kinds of sandwich-type dye-sensitized solar cells, $DSSC_{Vis}$ and $DSSC_{UV}$, were fabricated using Vis-TiO_2 ($DSSC_{Vis}$) and UV-TiO_2 electrodes ($DSSC_{UV}$), and their photovoltaic performances were investigated under illumination with an AM-1.5 solar simulator

lamp (100 $mWcm^{-2}$). $DSSC_{Vis}$ exhibited remarkably higher incident photon-to-electron conversion efficiency (IPCE) than $DSSC_{UV}$. Furthermore, it was found that the optimized solar-to-electric energy conversion efficiencies (η) reached 2.6 % for $DSSC_{Vis}$. UV-Vis, SEM and photoelectrochemical investigations on $DSSC_{Vis}$ and $DSSC_{UV}$ revealed that the unique film morphology as well as band structure of Vis-TiO_2 thin films play an important role in realizing the high photovoltaic performance of $DSSC_{Vis}$.

Summary of Chapter 7

Chapter 7 presented the results of the evolution of H_2 from an aqueous solution involving various light hydrogen-rich compounds such as various alcohols, hydrocarbons, hydrazine and ammonia. As NH_3 contains no carbon, it is a promising source of hydrogen. Investigations on photocatalytic H_2 evolution using different concentrations of NH_3 clearly showed that the production of hydrogen from ammonia aqueous solution. Thus the present research unveiled that the photocatalytic hydrogen production from ammonia aqueous solution is a promising process for low-cost, low-temperature, high-purity *in situ* hydrogen production. Using higher concentrations of ammonia in aqueous solution led to a reasonably high production of hydrogen, and the best result was obtained at 28%W of ammonia solution.

List of Publications

No.	Title of the Article	Author(s)	Journal	Corresponding Chapter
1	Recent Progress on Photocatalytic Decomposition of Water With a Separate Evolution of H_2 and O_2 Utilizing Novel Visible Light-responsive TiO_2 Thin Film Photocatalysts	A. Ebrahimi M. Matsuoka M. Moriyasu M.Takeuchi M. Kitano M. Anpo	submitted to Catal. Lett. (2010).	Chapter 2
2	New Trends in the Nanoscience and Nanotechnology of Titanium Oxide-based Photocatalysts as Environmentally-friendly Catalysts --Decomposition of H_2O into H_2 and O_2 with a Separate Evolution Using Visible Light-Responsive TiO_2 Thin Film Photocatalysts under Sunlight Irradiation as well as the Reduction of CO_2 with H_2O to Form CH_3OH and O_2 on Ti-oxide Single Site Heterogeneous Photocatalysts--	M. Anpo A. Ebrahimi M. Matsuoka	Proc. Solar Chem. Photocatal. (SPEA5), pp.5-12 (Palermo, Italy, 2008).	Chapter 2
3	A Survey on the Relationship Between the Surface Structure and Photocatalytic Reactivity of Newly Developed Visible Light-responsive TiO_2 Photocatalysts	A. Ebrahimi R. Tode M. Moriyasu M. Matsuoka M. Takeuchi M. Anpo	submitted to Curr. Org. Chem. (2010).	Chapter 2
4	Separate Evolution of H_2 and O_2 from H_2O on Visible Light-responsive TiO_2 Thin Film Photocatalysts Prepared by a RF Magnetron Sputtering Method --The Effect of Various Calcination Treatments on the Photocatalytic Reactivity--	M. Matsuoka A. Ebrahimi M.Nakagawa T.-H. Kim M. Kitano M. Takeuchi M. Anpo	Res. Chem. Intermed., Vol. 35, pp. 997-1004 (2009).	Chapter 3
5	Photocatalytic Decomposition of Water on Double-layered Visible Light-responsive TiO_2 Thin Films Prepared by a RF Magnetron Sputtering Deposition Method	R. Tode A. Ebrahimi S. Fukumoto K. Iyatani M. Takeuchi M. Matsuoka C. Hui L.C.-S. Jiang M. Anpo	Catal. Lett., in press (2010).	Chapter 4

6	Morphology, Structure and Photoelectrochemical Activity of TiO_2 Thin Films having different Thickness Prepared on Different Substrates by a RF Magnetron Sputtering Method	A. Ebrahimi M. Saito R. Tode M. Matsuoka M. Takeuchi M. Anpo	submitted to J. Catal. (2010).	Chapter 4
7	Purification of Polluted Water with Various Organic Compounds by Applying Newly Developed Visible Light-responsive TiO_2 Photocatalysts under Sunlight Irradiation --Features and Functionality of Vis-TiO_2 Photocatalyst--	A. Ebrahimi M. Matsuoka M. Minakata M. Takeuchi M. Anpo	submitted to J. Mater. Chem. (2010).	Chapter 5
8	Photovoltaic Performance of a Dye-Sensitized Solar Cell Using a Visible Light-responsive TiO_2 Thin Film Electrode Prepared by a RF Magnetron Sputtering Deposition Method	M. Minakata A. Ebrahimi C.-H. Lee C.-S. Jiang H.-C. Chen W.-T. Lin S. Fukumoto M. Matsuoka M. Anpo	submitted to Energ. Environ. Sci. (2010).	Chapter 6
9	Photoelectrochemical Investigations of Visible Light-responsive TiO_2 Thin Film Photocatalysts Supporting Ru and RuO_2 by the Photodeposition and Sputtering Methods.	A. Ebrahimi M.Nakagawa M. Matsuoka M. Takeuchi M. Anpo	submitted to Catal. Lett. (2010).	Chapter 6
10	Investigations on The Photocatalytic Evolution of Hydrogen from Ammonia Aqueous Solutions	A. Ebrahimi K. Iyatani M. Matsuoka M. Takeuchi M. Anpo	submitted to Res. Chem. Intermed. (2010).	Chapter 7

Other Publications

No.	Title of the Article	Authors(s)	Journal
1	Application of Highly Functional Ti-oxide-based Photocatalysts in Clean Technologies	M. Takeuchi S. Sakai A. Ebrahimi M. Matsuoka M. Anpo	Top. Catal., Vol. 52, pp. 1651-1659 (2009).
2	Construction of Solid State Thin Film Solar Cell Applying Visible Light-responsive TiO_2 Thin Film Materials	M. Matsuoka, M. Minakata A. Ebrahimi H.-C. Chen W.-T. Lin M. Anpo	Environmentally Benign Photocatalysts: --Applications of Titanium Oxide-Based Catalysts-- Eds. M. Anpo and P. Kamat, in press (2010).

ACKNOWLEDGEMENTS

First and foremost, I would like to thank my supervisor and advisor Professor Masakazu Anpo without whom I would never have made it this far. I am very grateful for the opportunity to have worked with Professor Anpo in his lab at Osaka Prefecture University. Six years ago on October, 2004, I met Prof. Anpo at "The Conference and Workshop on Nanotechnology" in Tehran, Iran, and at that time, I could not even imagine I would be working with him in Japan someday. My dreams came true with his great assistance and, since then, new doors have opened in my life. My goal was mainly to do research under his supervision, however, living in a country as Japan with a great cultural and historical background and unique lifestyle has also taught me many things so that not only my mind but also my lifestyle has been completely affected. I am deeply indebted to him for the rest of my life as a man would be to his parents.

It is largely in this context that I have written the following dissertation and it has been the overarching theme of all my research at OPU. In fact, I have no doubt that my future research in the field of Photocatalysis will never be far from this theme. It is with the outstanding training I have received from Professor Anpo, as a scientist in general and in the area of solar energy conversion in particular, that I hope to be able to make a meaningful contribution to solving the daunting problem of providing humanity with a clean, safe, low-cost, and abundant source of energy in the future.

I am also grateful to Professor Masahiro Tatsumisago and Professor Hiroshi Inoue from the Department of Applied Chemistry for their critical guidance, useful suggestions and kind advice during the preparation of this thesis.

I would also like to thank another mentor, Associate Prof. Masaya Matsuoka, who has been a prominent part of nearly every aspect of my research here. He spent countless hours working one-on-one with me, helping me to address any questions and problems I had, and always with seemingly infinite patience. Prof. Matsuoka is extremely knowledgeable, easy to learn from and a very tolerant supervisor. I am deeply grateful for the considerable contribution he has made, both to my research and to my growth as an individual.

The other lecturer of mine, Assistant Prof. Masato Takeuchi, also deserves special mention. Dr. Takeuchi is one of those people who has encouraged me to keep going ahead in my work and every interaction I have ever had with him has been a pleasure. I will never forget his kind and comprehensive answers to my many questions.

I do not think it is possible to acknowledge fully and completely all the people I have interacted with and learned from during my studies at OPU or give them the thanks they truly deserve. Their contribution has simply been too great to express in a few brief paragraphs. But that is what I shall attempt to do nonetheless.

Most important in my day-to-day experience at OPU has, of course, been the other members of the Prof. Anpo research group. I am specifically grateful to the graduate and undergraduate student members of this group. I owe a great deal of what I know about photocatalysis to Dr. Masaaki Kitano. I've been blessed to have such competent people help me expand my limited ideas into real working parts and instruments. Almost all of the members of this research group have helped me with my work and supported me in countless ways, particularly current and previous PhD course students, Mr. Kim Tae-Ho, Dr. Eddy Diana Rakhmawaty, Dr. Takashi Kamegawa, Dr. Haijun Chen, and Dr. Yun Hu.

I owe a special thanks to members of the Water Splitting subgroup, without whose contributions my research would not have worked at all: Kazushi Iyatani and Shohei Fukumoto both of whom helped get my work started; Masayuki Minakata, Masaki Nakagawa, Ryohei Tode and Mudoka Moriyasu who were not only terrific co-workers but very good friends. They always seemed to go out of their way to drop whatever they were doing to help me with whatever I asked of them.

Furthermore, I am grateful to graduate students Kazuhiro Uchihara, Masato Hozumi, Satoru Kuranari and Jun Morishima with whom I got a lot of inspiration and energy while working with them.

My research experience at OPU would have not been the same without the terrific staff of the OPU International office, who consistently exceeded my expectations in every interaction I had with them. I am especially indebted to Mrs. Keiko Mizobata and Mr. Takao Miyoshi for all of their valuable assistance during my studies.

I have also been lucky enough to have several friends not affiliated with OPU. In particular, Mr. Kazuo Iwasaki, Mr. Toru Nakachi and Mrs.Toshie Nakachi, Ms. Mayuko Kinoshita, Mr. Tadashi Yoshida and our kind host family Mr. Noboru and Mrs. Maki Matsuura. Our new life style in Japan couldn't be successful or stable without their constant help and encouragement.

I also wish to thank Mrs. Sumiyo Ono whose kind encouragements were so important to me and also for her assistance in the final editing of my writing which assured me that I could carry on in this work.

I also owe a great deal of thanks to Mrs. Fumiko Shibano and her kind family who freely provided much valuable assistance, spending a great deal of time and effort to help me and my family adapt smoothly to life in Osaka.

My heartfelt thanks are also extended to the volunteer members of the Sakai International Friendship Club, "KoKoC", supervised by Mrs. Machiko Fumoto and Mrs. Kayoko Ishikawa, for all of their precious help in familiarizing our family with Japanese culture and language. I am also grateful to the "Perape～ra" group members supervised by Mrs. Emiko

Katsuyama for their Japanese language classes and her other coworkers, Mrs. Meiko Tsuchiyama and Mrs. Kazuko Iihama for their great assistance to my family since our arrival here in Sakai City.

Special thanks are also due to the generous financial support of the "Ninety-nine Asian Student Scholarship Foundation" and the Japan Student Services Organization "JASSO" during my Doctorate course studies at OPU.

Finally, I would like to sincerely and with heartfelt thanks acknowledge the support of my family and parents who have been unflagging in their love, even when I have often put my work ahead of their requests. Without their kind understanding, it definitely would not have been possible to carry out my research work. Of course, none of this would have been possible at all without the love and bottomless support of my family. They have always been there for me no matter what and my mother, Parvaneh and my father, Mohammad are the best parents a person could hope for. They have not only provided moral support and love but also great financial support, sacrificing their own needs to help me reach my goals in life. Also, I appreciate my dear mother -in-law, Ashraf and father-in-law, Amrollah. I could not have completed this work without their great support. I would like to thank my sister, Anita, and my brother-in-law, Amin, who both have tried their best to take our place and make up for our absence with our families in Iran.

In remembrance of my late brother, Farzad, who has always been a guiding influence in my life, I pray for his soul to be in eternal peace.

Sincere thanks also go to my children, Shiva and Shervin, for bringing us great happiness and joy. Shervin joined us just a few weeks ago when I was involved in the final part of my research but his presence gave us more energy and hope to cope with the problems surrounding us. Their good fortune is my first aim and I would do anything for them in the future.

Finally, I have saved the most important person for last. My wife Nooshin has done as much for me as any person could ask for, and then done more. Her endless love and support has made all the difference. Giving me encouragement, or just being there for me, I can't imagine having completed this work without her and my other family members also. I can only say that I do know how lucky I am. Nooshin, I love you with all my heart.

Afshin Ebrahimi,
Sakai, Osaka, Japan
February 2010